UNIVERSITY OF CALIFORNIA SAN DIEGO

KLF3 Promotes Human Epidermal Differentiation Through the Epigenomic Writer CBP and the Epigenomic Reader BRD4

A dissertation submitted in partial satisfaction of the
requirements for the degree
Doctor of Philosophy

in

Biomedical Sciences

by

Jackson Jones

Committee in charge:

Professor George Sen, Chair
Professor Kelly Frazer
Professor Richard Gallo
Professor Alysson Muotri
Professor Jing Yang

2020

The Dissertation of Jackson Jones is approved, and it is acceptable in quality and form for publication on microfilm and electronically:

Chair

University of California San Diego

2020

DEDICATION

To my mother Monique and my father Steve. None of this would have been possible without their unwavering love and support.

TABLE OF CONTENTS

Signature Page iii
Dedication iv
Table of Contents v
List of Figures vi
List of Abbreviations vii
Acknowledgements ix
Vita xi
Abstract of the Dissertation xii
Chapter 1 : KLF3 Mediates Epidermal Differentiation Through the Epigenomic Writer CBP 1
Chapter 2 : BRD4 is Necessary for Differentiation Downstream of Epidermal Lineage-determining Transcription Factors 56
References 95

LIST OF FIGURES

Figure 1.1. KLF3 expression is increased during epidermal differentiation. 11
Figure 1.2. KLF3 is necessary for human epidermal differentiation 14
Figure 1.3. KLF3 binds to enhancers proximal to differentiation genes that it regulates. 20
Figure 1.4. CBP and KLF3 regulate a similar gene expression program. 23
Figure 1.5. CBP and KLF3 binds to similar sites in the genome. 26
Figure 1.6. KLF3 is necessary for CBP localization proximal to differentiation genes. 29
Supplementary Figure 1.1. Increase in KLF3 expression is necessary for differentiation. 38
Supplementary Figure 1.2. KLF3 and KLF4 are not redundant in the regulation of epidermal differentiation gene expression. 40
Supplementary Figure 1.3. KLF3 and epidermal lineage determining transcription factors bind to similar regions in the genome. 42
Supplementary Figure 1.4. CBP is necessary for human epidermal differentiation. 44
Supplementary Figure 1.5. CBP and KLF3 directly overlap at ~35% of their binding sites in the genome. 46
Supplementary Figure 1.6. KLF3 is necessary for CBP localization to genomic sites. 47
Figure 2.1. BRD4 is necessary for epidermal differentiation gene expression. 62
Figure 2.2. BRD4 shares similar genomic binding profiles with epidermal LDTFs 65
Figure 2.3. BRD4 and KLF3 transcriptional programs and genomic localization functionally overlap 71
Figure 2.4. KLF3 knockdown alters BRD4 localization during epidermal differentiation. 75
Supplementary Figure 2.1. BRD4 is necessary to promote epidermal differentiation. 81
Supplementary Figure 2.2. BRD4 is bound to active enhancers and promoters. 82
Supplementary Figure 2.3. BRD4 and KLF4 regulate a similar transcriptional program. 84
Supplementary Figure 2.4. BRD4 and KLF3 share transcriptional programs and genomic localization... 85

LIST OF ABBREVIATIONS

AP1: Activator protein 1

BRD4: Bromodomain-containing protein 4

BRD4i: BRD4 targeting siRNA knockdown

CBP: CREB-binding protein (CREBBP)

CBPi: CBP targeting siRNA knockdown

CEBP: CCAAT/enhancer-binding protein

CTBP: C-terminal-binding protein

CTLi: Control non-targeting siRNA knockdown

ETS: E26 transformation-specific transcription factor family

FLG: Filaggrin

GO: Gene ontology

GRHL: Grainyhead like transcription factor

H3K27ac: Acetylated histone H3 protein lysine 27

H3K4me: Methylated histone H3 protein lysine 4

H3K27me3: Tri-methylated histone H3 protein lysine 27

H3K9me3: Tri-methylated histone H3 protein lysine 9

H&E: Haemotoxylin and Eosin staining

IVL: Involucrin

KLF3: Krüppel-like factor 3

KLF3i: KLF3 targeting siRNA knockdown

KLF4: Krüppel-like factor 4

KLF4i: KLF4 targeting siRNA knockdown

KLK: Kallikrein

K/KRT: Keratin

LCE: Late cornified envelope protein

LDTF: Lineage-determining transcription factors

LOR: Loricrin

MAF/MAFB: MAF family transcription factor

P300: E1A-associated protein p300 (EP300)

P300i: P300 targeting siRNA knockdown

P63: Tumor protein p63 (TP63)

S100: Calcium-binding protein

SPRR: Small proline-rich protein

TF: Transcription factor

TGM: Transglutaminase

ZNF750: Zinc finger protein 750

ACKNOWLEDGEMENTS

I would like to acknowledge Professor George Sen for his mentorship as principal investigator and chair of my committee. His guidance and support have been phenomenal. I could not have asked for a better advisor and would not be the scientist I am today without him. In addition, I would like to thank Professors Kelly Frazer, Richard Gallo, Alysson Muotri, and Jing Yang for their service on my committee. I appreciate all their great contributions and discussions. I would also like to acknowledge Jingting Li, Nancy Ling, Yifang Chen, Ying Wang, and Manisha Tiwari for various training and assistance. Their advice and contributions were invaluable.

In addition, I want to acknowledge my family and friends who have made my journey to this point in life a great one. Thank you to my parents Monique and Steve, and my brother Forrest for being the best family a man can ask for. Thank you to my closest friends for always being there for me. Finally, I want to thank Alyssa Howe for all of the love and support that kept me going through graduate school. I could not have done it without you.

Chapter 1 is based on material currently in review: Jackson Jones, Yifang Chen, Manisha Tiwari, Jingting Li, Ji Ling, and George L. Sen. KLF3 mediates epidermal differentiation through the epigenomic writer CBP. *In Review: iScience.* 2020. I am the primary author and researcher for this manuscript. The co-authors listed above either supervised or provided support for the research and have given permission for the inclusion of the work in this dissertation.

Chapter 2 is based on material recently accepted for publication: Jackson Jones, Yifang Chen, Manisha Tiwari, Jingting Li, Ji Ling, and George L. Sen. BRD4 is necessary for

differentiation downstream of epidermal lineage determining transcription factors. *In Press: Journal of Investigative Dermatology.* 2020. I am the primary author and researcher for this manuscript. The co-authors listed above either supervised or provided support for the research and have given permission for the inclusion of the work in this dissertation.

VITA

2009-2013 Bachelor of Science: Molecular, Cellular, and Developmental Biology, Minor: Marine Biology, University of Washington

2014-2020 Doctor of Philosophy, Biomedical Sciences, University of California San Diego

PUBLICATIONS

First Author

KLF3 mediates epidermal differentiation through the epigenomic writer CBP. *In Review: iScience.* 2020

BRD4 is necessary for differentiation downstream of epidermal lineage determining transcription factors. *In Press: Journal of Investigative Dermatology.* 2020

Other Authorship

HNRNPK maintains epidermal progenitor function through transcription of proliferation genes and degrading differentiation promoting mRNAs. *Nature Communications. 2019*

The Cohesin Complex Is Necessary for Epidermal Progenitor Cell Function through Maintenance of Self-Renewal Genes. *Cell Reports.* 2017

Biochemical Screening of Five Protein Kinases from Plasmodium falciparum against 14,000 Cell-Active Compounds. *Plos One*. 2016

The Bacterial Sec Pathway of Protein Export: Screening and Follow-Up. *Journal of Biomolecular Screening.* 2015

ABSTRACT OF THE DISSERTATION

KLF3 Promotes Human Epidermal Differentiation Through the Epigenomic Writer CBP and the Epigenomic Reader BRD4

by

Jackson Jones

Doctor of Philosophy in Biomedical Sciences

University of California San Diego, 2020

Professor George Sen, Chair

Human epidermis acts as an essential barrier between the body and the outside environment. It is a stratified epithelium that requires a proper balance of cell proliferation and differentiation to maintain its homeostasis and integrity. Stem and progenitor cells in the basal layer of the epidermis maintain a population of proliferative cells while also giving rise to

differentiated progeny. Those cells entering the differentiation program undergo various stages of differentiation as they migrate outwards through the epidermis, where they will eventually form the protective outer layer known as the stratum corneum. As this process occurs, a variety of genes become expressed or repressed depending on the process of differentiation. Coordination of this differential gene expression between the stem/progenitor state and the differentiated state is a complex process that continues to undergo extensive investigation. Here, we identify and characterize KLF3 as a novel epidermal LDTF necessary for epidermal differentiation. In addition, we demonstrate that KLF3 promotes differentiation gene expression by promoting the localization of the epigenomic writer CBP and the epigenomic reader BRD4 at enhancers proximal to epidermal differentiation genes.

CHAPTER 1 : KLF3 MEDIATES EPIDERMAL DIFFERENTIATION THROUGH THE EPIGENOMIC WRITER CBP

Abstract

The differentiated layers of the epidermis protect the body from the outside environment. Impairments in the differentiation process can lead to skin diseases that can afflict ~20% of the population. Thus, it is of utmost importance to characterize and understand the factors that promote the differentiation process. Here we identify the transcription factor KLF3 as a novel regulator of epidermal differentiation. Knockdown of KLF3 results in reduced differentiation gene expression and increased cell cycle gene expression. Over 50% of KLF3's genomic binding sites occur at regions containing H3K4me/H3K27ac with the vast majority at active enhancers. KLF3 bound to active enhancers proximal to differentiation genes that are dependent upon KLF3 for expression. Based on this association, we sought to investigate KLF3's possible relationship with the enhancer associated proteins CBP and P300. Analysis of the transcriptome controlled by CBP and P300 showed that CBP and KLF3 control a similar gene expression program and are both essential for promoting differentiation. In addition, 35% of CBP's genomic binding sites overlap with KLF3 and knockdown of KLF3 results in reduced CBP localization at enhancers proximal to differentiation gene clusters. Our results suggest that KLF3 regulates differentiation gene expression by promoting CBP localization at enhancers.

Introduction

The human epidermis is a stratified epithelial tissue that serves as a protective interface between the body and the surrounding environment[1]. Not only does it act as a barrier against detrimental factors such as pathogen exposure and physical harm, it allows the body to retain water and prevent dehydration. These protective attributes rely on the proper homeostasis and differentiation of the tissue. There are four primary layers of the epidermis: the basal layer, the spinous layer, the granular layer, and the stratum corneum[2]. Each layer represents a different stage in the differentiation process of keratinocytes.

The epidermis is maintained by stem and progenitor cells that reside in the basal layer[3]. These cells are capable of generating new cells destined for differentiation, while also maintaining the proliferative population. Cells that leave the proliferative state and enter the differentiation program undergo various stages of differentiation as they migrate outward and ultimately form the cornified envelope (stratum corneum). When basal layer cells initially differentiate, they migrate upwards to form the spinous layer (stratum spinosum). Here, KRT5 and KRT14 expression is downregulated, while the expression of KRT1 and KRT10 increases substantially. The cells of this layer are connected by desmosomes and begin expressing involucrin (IVL), which is essential in the eventual development of the cornified cell envelope. They also begin to express transglutaminases (TGMs), which mediate the crosslinking of the proteins that form this envelope. However, this is just the beginning of the terminal barrier formation, which progresses in the granular layer of the epidermis[2,4].

As cells enter the granular layer (stratum granulosum), they undergo multiple changes. The defining feature of cells in this layer is the formation of keratohyalin granules. These granules can contain the early forms of Filaggrin (FLG), an important late differentiation protein, as well as Loricrin (LOR), which is essential for the formation of the cornified envelope. Transglutaminases begin to crosslink a variety of target proteins, such as LOR underneath the plasma membrane. In addition, cells of the granular layer produce lamellar bodies and other vesicles that mediate the deposition of lipids into the extracellular environment.

The differentiation process ends at the stratum corneum. In this layer, the cells lose their nuclei and the cornified envelope becomes fully formed due to the crosslinking of the proteins underneath the plasma membrane. Furthermore, the lipids from the lamellar bodies formed in the granular layer are extruded into the extracellular space. Thus, the stratum corneum layer is primarily composed of bundled keratin filaments, lipids, and crosslinked proteins. Together, these structures create a highly protective outer layer of the epidermis[2,4]. The outer cells of this layer are eventually shed into the environment, a process known as desquamation, through the action of Kallikrein proteins (KLKs), a group of serine proteases. Defects in differentiation and thus the formation of this barrier can lead to a variety of skin diseases such as ichthyosis, atopic dermatitis, and psoriasis which impact up to 20% of the population[5].

Here, we focus on Krüppel-like factor 3 (KLF3) and its role in epidermal differentiation. KLF3 is a member of the Krüppel-like factor family of transcription factors. These factors are characterized by three C2H2 (two cysteine, two histidine) zinc finger domains that facilitate their binding to DNA. These domains are highly conserved among the various KLF proteins, and

generally contact DNA at CACCC box motifs, as well as GC rich areas. In contrast, these factors can be distinguished by variations in their N-terminal domains, which allow them to have unique protein-protein interactions[6,7]. KLF family transcription factors have been implicated in epidermal differentiation previously. For example, KLF5 is highly expressed in the epidermis. It has been shown that the overexpression of Klf5 in the basal layer of the epidermis in mice disrupts the normal differentiation process during embryogenesis. Klf5 overexpression also causes issues in adult mice, such as epidermal erosions and reductions in certain epidermal stem cells[8]. Another Krüppel-like factor, KLF4, which is well known as one of the factors involved in the generation of iPSCs, has been shown to play an essential role in the epidermis[9]. It has been shown in mice that Klf4 has high levels of expression in the epidermis and it essential for barrier formation, an essential process for survival. This is supported by the death of $Klf4^{-/-}$ mice right after being born. This death is due to the compromised integrity of the barrier on the outermost layer of the epidermis, which can cause a variety of problems such as dehydration[10]. In addition to these findings, it has been shown in mice that ectopic expression of Klf4 via a tetracycline inducible promotor system results in more efficient terminal differentiation and barrier formation in the epidermis[11]. It has also been shown that during epidermal development, Klf4 regulates many of the same genes that therapeutic corticosteroids target (corticosteroids accelerate skin barrier formation, as well as epithelial differentiation, which is useful in treating babies who will be born prematurely)[12]. More recently, KLF4 has been shown to be a target of ZNF750, another transcription factor essential for epidermal differentiation. ZNF750 is activated by p63 (transcription factor, important in controlling epidermal homeostasis), and in turn binds at the

KLF4 promotor and regulates its level of expression[13]. Interestingly, a later study found that KLF4 also acts as a cofactor to ZNF750 at specific target genes during the differentiation process. It was shown that, at these sites, KLF4 is necessary for proper ZNF750 activation of differentiation genes. In contrast, KLF4 is replaced by the chromatin regulator KDM1A at progenitor genes, where the ZNF750 complex suppresses expression[14]. The importance of KLF4 in the differentiation process suggests that the related KLF3 could also play a role in this system.

KLF3 has been found to act as a transcriptional repressor in most previous studies. It has even been shown to contain a "repression domain" in its N-terminus. Data from yeast two-hybrid screens have shown that this domain is the interaction site of CTBP1/2 (C-terminal binding protein), which can act as a corepressor with KLF3. In addition, mutagenesis of this binding site can greatly reduce KLF3 repression activity[15]. It is worth noting that CtBP1/2 has been shown to interact with ZNF750 at its target sites during epidermal differentiation, including sites where it is activating transcription[13]. Thus, this repressive role may be context specific. It is suggested CTBP factors may not be the only activity enhancing factors of KLF3. In addition to this interaction, KLF3 can also be sumoylated at two different sites. In some cases, this sumoylation has been shown to enhance KLF3 repression activity, and simultaneous mutation of the sumoylation and CtBP binding sites can convert KLF3 into a transcriptional activator[16]. It is worth noting that some of these KLF3 activity studies are based on *in vitro* systems in other cell types, and the activity and interactions of KLF3 in the context of epidermal differentiation could be unique.

KLF3 has been demonstrated as an important factor in multiple differentiation contexts, making it a suitable candidate for study in epidermal differentiation. In the context of adipogenesis in mouse 3T3-L1 cells, Klf3 shows reduced expression as differentiation occurs. In addition, overexpression of Klf3 disrupts the differentiation process. Murine embryonic fibroblasts knocked out for KLF3 show a greater ability to differentiate into adipocytes upon stimulation with adipogenic factors, suggesting that KLF3 inhibits adipogenesis[17]. It was found that Klf3, along with Ctbp, bind the Cebpα promoter in these cells and repress its expression[17]. This gene is important in the generation of white adipose tissue. However, it is not involved in the generation of brown adipose tissue[18]. Interestingly, Klf3 knockout mice show reduced white adipose tissue, but not brown adipose tissue. It is possible that complete Klf3 knockout results in premature and uncontrolled Cebpα expression, which could cause improper differentiation. As a general takeaway from this study, it is suggested that Klf3 may inhibit adipogenesis[17].

In addition to adipogenesis, KLF3 has been associated with B cell development. In Klf3 knockout mice, B cell differentiation and development is disrupted, and the marginal zone of the spleen has compromised integrity. In addition, the peritoneal cavity of these mice has significantly less B1 B cells. When B cells from the Klf3 knockout mice are treated with LPS, the response is reduced compared to normal B cells[19,20].

In the context of erythropoiesis, KLF3 also has activity and is highly expressed[19,21]. It was found that KLF3 expression increases as erythroid cells differentiate and is most important in the late stages of this process. In addition, Klf3 knockout mice show increased anemia. They

also have increased levels of abnormal erythrocytes, and even increased levels of erythroid progenitor cells, substantiating the important role that KLF3 plays in erythropoiesis[22].

Lastly, KLF3 has been implicated in skeletal muscle cell development. This is one of the few systems in which KLF3 has been shown to activate gene transcription. KLF3 expression is upregulated in the myocytes as they differentiate. While there were multiple muscle cell related genes targeted by KLF3, the study focused on the Muscle Creatine Kinase (MCK) promoter. Here, KLF3 can act as a transcriptional activator when it interacts with the serum response factor (SRF) [23]. This is particularly interesting for studying KLF3 in the epidermis, as it could be possible that it both inhibits and activates genes based on the physiological context or its protein interactions, just like ZNF750 was shown to do[14].

Work from our lab as well as others have shown that epidermal differentiation gene expression is reliant on a variety of regulatory factors, including lineage determining transcription factors (LDTFs) such as KLF4, MAF/MAFB, CEBPA/B, ZNF750, and GRHL3[10,13,14,24-29]. While many of these important factors have been identified, the search continues for novel transcription factors that promote differentiation. LDTFs can recruit epigenetic writers and readers to remodel chromatin for gene activation or repression. For example, ZNF750 was found to promote differentiation and suppress proliferation gene expression through interactions with epigenetic factors such as CTBP1/2, RCOR1, and KDM1A[14]. Similarly, GRHL3 is able to recruit the Trithorax complex (including MLL2, a histone-lysine methyltransferase) through WDR5 to a variety of epidermal differentiation genes and activate their expression through H3K4 methylation[27]. While these studies have elucidated

how some LDTFs recruit epigenetic factors to regulate epidermal differentiation, it is not known whether epigenomic writers of active enhancers have any role in this process.

Enhancers are essential for cell type specific, developmental, and differentiation gene expression[30]. Two types of enhancers have been described namely primed and active which can be identified by associated histone modifications. Primed enhancers are marked by mono-methylation of H3K4 (H3K4me1) while active enhancers contain both H3K4me1 and acetylated H3K27 (H3K27ac)[31-33]. P300 and CBP are highly homologous histone acetyl transferases enriched at active enhancers and promote their activation through acetylation of H3K27[34,35]. Inhibition of these epigenomic writers lead to inactivation of enhancers and downregulation of target genes. CBP and P300 have been shown to be functionally redundant in many studies however there are studies where they have been found to have distinct and opposite roles[36-38]. CBP has been shown in hematopoietic stem cells to promote stem cell self-renewal while P300 is necessary for their differentiation[39]. Whether P300 or CBP plays any role in the skin and how they localize to active enhancers is a question of active investigation.

In this study we identify KLF3 as a novel LDTF that promotes epidermal differentiation. We show that KLF3 is expressed throughout the human epidermis but is upregulated in the differentiated layers. Functionally, KLF3 promotes differentiation gene expression and suppresses cell cycle associated genes. KLF3 does this independently and is not redundant with closely related transcription factor KLF4. Chromatin immunoprecipitation followed by high throughput sequencing (ChIP-Seq) of KLF3 revealed that the majority of KLF3 binding occurred at active enhancers. Based on this enhancer association, we sought to compare the transcriptional

programs of KLF3 to P300 and CBP by RNA-Seq. We found that KLF3's transcriptional regulation correlates closely with that of CBP, but not P300. ChIP-Seq of CBP binding sites shows substantial overlap with KLF3 at active enhancers. Loss of KLF3 prevented CBP binding to KLF3 bound active enhancers. Our results demonstrate that KLF3 promotes CBP's localization at active enhancers to drive epidermal differentiation gene expression.

Results

KLF3 Expression is Upregulated during Epidermal Differentiation

To identify potential regulators of epidermal differentiation, we searched for transcription factors whose mRNA levels were upregulated during this process. Analysis of a previously generated RNA sequencing (RNA-Seq) data set showed that *KLF3* transcripts were upregulated during differentiation. (Figure 1.1A, Supplementary Figure 1.1A)[40]. This increase in expression is similar to other known transcription factors involved in promoting epidermal differentiation including KLF4 and ZNF750 as well as differentiation structural genes FLG and LCE2C (Figure 1.1A). To validate KLF3 expression levels, primary human keratinocytes were induced to differentiate by seeding in full confluence and high calcium. Keratinocytes were differentiated for 1, 3, or 5 days and KLF3 expression levels were analyzed. Compared to the undifferentiated control (Day 0), KLF3 expression was elevated on both the mRNA and protein levels after just one day of differentiation (Figure 1.1B-C). In human skin, KLF3 protein localized to the nucleus and was found throughout the epidermis. However, KLF3 expression was highest in the

differentiated layers of the epidermis which co-expressed the differentiation protein keratin 10 (K10) (Figure 1.1D).

To confirm the specificity of the KLF3 antibody, primary human keratinocytes were transfected with control siRNA (CTLi) or KLF3 siRNA (KLF3i) and induced to differentiate for 3 days. Efficient KLF3 knockdown and the specificity of the antibody on the protein level was confirmed by Western blot (Supplementary Figure 1.1B). Control and knockdown cells were also used to regenerate human skin by seeding the cells on devitalized human dermis. This allows the cells to establish cell-cell and cell-basement membrane contact all in 3 dimensions, which allows the stratification of the tissue and the accurate representation of the gene expression program of human epidermis[41-43]. KLF3 protein expression was increased in the upper, more differentiated layers of the epidermis, which coincided with the expression of K10 and a lack of P63 staining in control tissue. In contrast, KLF3 knockdown samples showed complete loss of KLF3 staining, demonstrating the specificity of the KLF3 antibody (Supplementary Figure 1.1C-D). There was also a decrease in K10 staining, suggesting that KLF3 knockdown may negatively impact differentiation (Supplementary Figure 1.1C). Together, these data demonstrate that KLF3 is expressed throughout the human epidermis but is elevated in the differentiated layers.

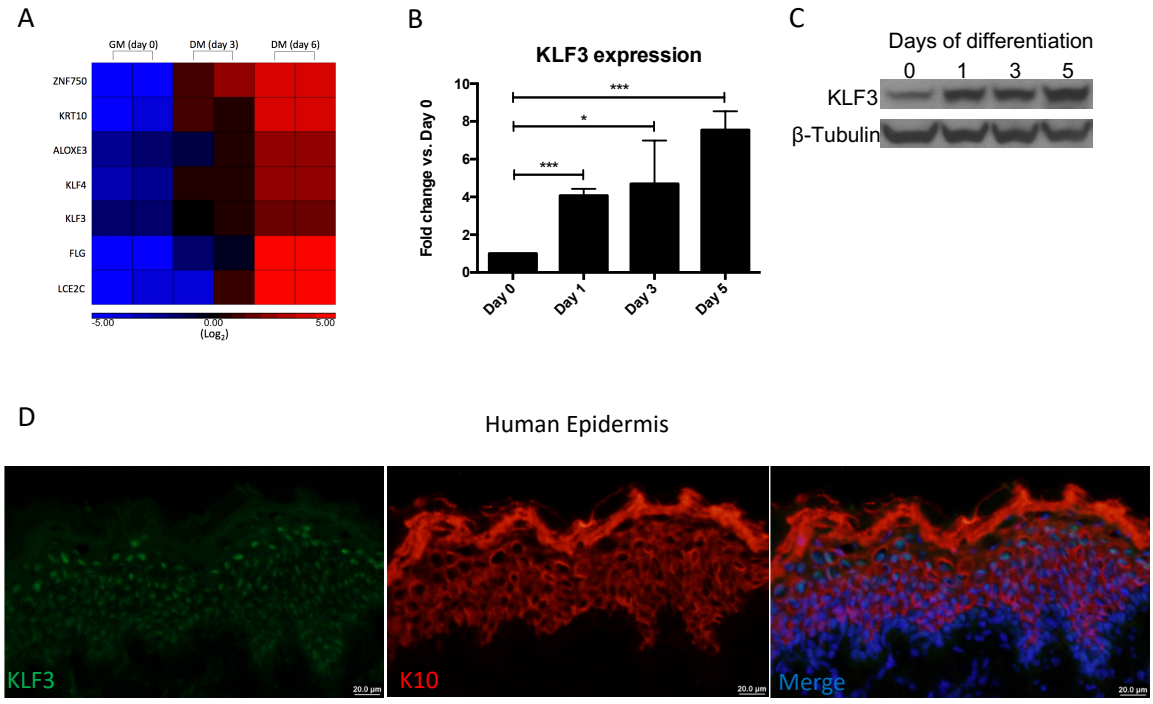

Figure 1.1. KLF3 expression is increased during epidermal differentiation.
(A) Heat map of replicate RPKM normalized, Log2 transformed RNA-sequencing data showing the relative expression of KLF3 and a panel of differentiation genes in keratinocytes cultured in growth media (GM) versus differentiation media (DM, day 3 differentiation). (B) RT-qPCR analysis of KLF3 mRNA levels in a time course of keratinocyte differentiation done in two-dimensions, with day 0 representing undifferentiated keratinocytes and day 1-5 representing progressively differentiated keratinocytes. n=3. Statistics: t-test, *$p < 0.05$, ** $p < 0.01$, ***$p < 0.001$. (C) Western blot of KLF3 protein levels in a time course of keratinocyte differentiation with B-Tubulin as a loading control. Representative image is shown. n=3. (D) Immunofluorescent staining of KLF3 (green) and KRT10 (red, a marker of the differentiated layers) in human skin biopsy. Merged image includes Hoechst staining of nuclei. n=3 Scale bar = 20μm.

KLF3 is Necessary for Epidermal Differentiation

Since KLF3 expression is increased during differentiation, we sought to determine if KLF3 plays a functional role in epidermal differentiation. Knockdown of KLF3 using 2 distinct siRNAs in primary human keratinocytes blocked differentiation gene expression (Figure 1.2A).

These include genes such as FLG, LOR, SPRR3, HOPX, and KRT23 many of which have been implicated in diseases of the skin (Figure 1.2A)[44,45]. To determine if KLF3 is necessary for differentiation in a tissue context, control and KLF3 depleted cells were seeded on devitalized human dermis to regenerate skin. Immunofluorescent staining and RT-QPCR from these samples show a dramatic reduction in the protein and mRNA levels for the late differentiation markers filaggrin (FLG) and loricrin (LOR) (Figure 1.2B-C).

To understand the genome wide gene expression changes associated with KLF3 depletion during differentiation, we performed RNA-Seq in replicates for control or KLF3 knockdown cells placed in differentiation conditions for 3 days. 563 genes were found to be decreased (>2 fold change (+/-) and a significant p-value with *FDR (*< 0.05), ANOVA) in KLF3 depleted samples (Figure 1.2D). Gene ontology (GO) analysis of these genes shows enrichment for terms related to epidermal differentiation, such as *formation of the cornified envelope, metabolism of lipids,* and *water homeostasis* (Figure 1.2E). This list of genes includes structural differentiation genes such as KRT, LCE, S100, and SPRR family proteins, as well as proteins associated with important differentiation processes like lipid metabolism (ALOX12B, ALOXE3) and desquamation (KLKs) (Figure 1.2F). 423 genes were increased in KLF3 knockdown cells and were enriched for GO terms primarily associated with cell division (Figure 1.2D-G). These

results suggest that KLF3 is necessary for promoting differentiation and suppressing proliferation.

Since KLF4 is critical for epidermal differentiation and related to KLF3, we wanted to determine the relationship between the two transcription factors. To do this, we performed RNA-Seq on KLF4 knockdown cells and compared it to the KLF3 gene expression profile. KLF4 knockdown resulted in 772 downregulated genes and 1,265 upregulated genes (Supplementary Figure 1.2A). Gene ontology for KLF4i decreased genes showed enrichment for genes related to epidermis development, while cell cycle genes are enriched in the upregulated gene set (Supplementary Figure 1.2B-C). Greater than half of KLF3 differentially regulated genes were also found in the KLF4 knockdown data with 298 co-downregulated ($p < 1.375e-313$) and 226 co-upregulated genes ($p < 1.243e-180$) (Supplementary Figure 1.2D-E). The KLF3i and KLF4i RNA-Seq datasets are also highly correlated with a Pearson Coefficient of ~0.86 (Supplementary Figure 1.2F). Due to their similar gene expression signatures, we wanted to determine if there are redundant genes that they co-regulate. RNA-Seq was performed on KLF3/KLF4 double knockdown cells with 741 genes downregulated while 958 were upregulated (Supplementary Figure 1.2G). Interestingly, only 95 downregulated (enriched for drug catabolic process) and 151 upregulated (enriched for interferon signaling) genes were uniquely identified in the double knockdown samples (Supplementary Figure 1.2H-K). Notably, there was no enrichment for differentiation or cell cycle GO terms in those genes (Supplementary Figure 1.2J-K). Thus, while KLF3 and KLF4 regulate many of the same differentiation and cell cycle genes, they cannot compensate for the loss of one another. Furthermore, KLF3 and KLF4 redundantly regulate a

Figure 1.2. KLF3 is necessary for human epidermal differentiation
(A) RT-qPCR quantifying the relative mRNA expression levels of a panel of epidermal differentiation genes in CTLi and KLF3i keratinocytes after three days of differentiation. Two separate siRNAs (siRNA 1 and siRNA 2) targeting different regions of KLF3 were used (n=6). Statistics: t-test, *p < 0.05, ** p < 0.01, ***p < 0.001. (B) Immunofluorescent staining of FLG, LOR, and P63 in day 5 regenerated human epidermis treated with control (CTLi) or KLF3 targeting (KLF3i) siRNA. Merged image includes Hoechst staining of nuclei. n=3. Scale bar = 20μm. (C) RT-qPCR quantifying the relative mRNA expression levels of LOR and FLG in CTLi and KLF3i day 5 regenerated human epidermis. n=4. (D) Heatmap generated for replicate (n=2) RPKM normalized RNA-Sequencing data from CTLi and KLF3i keratinocytes differentiated for 3 days. The expression of genes significantly increased (red) or decreased (blue), selected by a significant p-value with FDR (< 0.05) and fold change > 2 (+/-) vs. CTLi, are displayed (log2 scale). (E) Gene ontology (GO) term enrichment for the 563 genes significantly decreased upon KLF3 knockdown. (F) Heatmap showing the relative expression levels of a panel of differentiation-associated genes from the CTLi and KLF3i RNA sequencing data sets (log2 scale). n=2. (G) Gene ontology term enrichment for the 423 genes significantly increased in expression upon KLF3 knockdown.

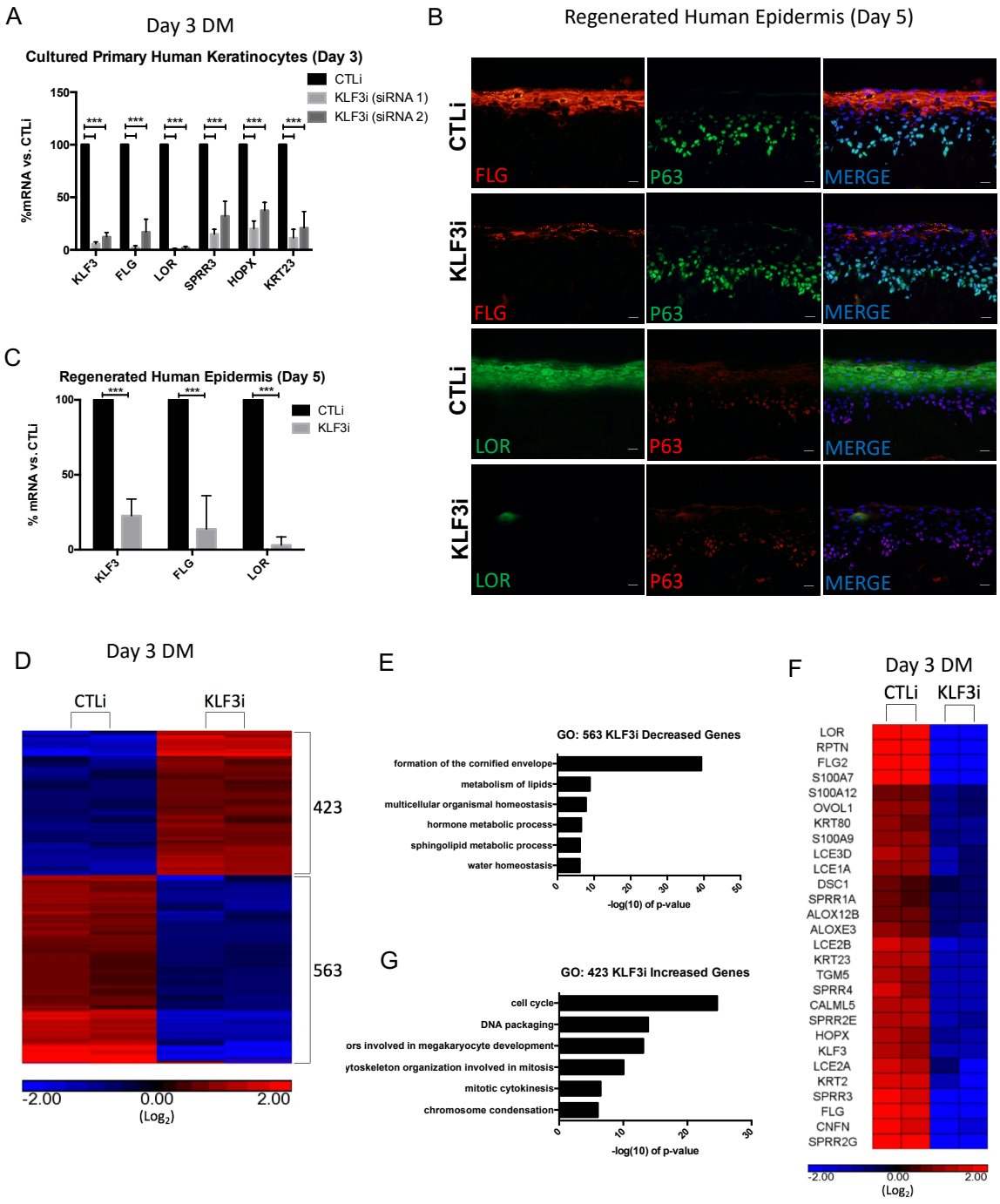
A
Day 3 DM
Cultured Primary Human Keratinocytes (Day 3)
CTLi
KLF3i (siRNA 1)
KLF3i (siRNA 2)
%mRNA vs. CTLi
KLF3
FLG
LOR
SPRR3
HOPX
KRT23
B
Regenerated Human Epidermis (Day 5)
CTLi
KLF3i
FLG
P63
MERGE
LOR
C
Regenerated Human Epidermis (Day 5)
% mRNA vs. CTLi
D
Day 3 DM
CTLi
KLF3i
423
563
-2.00
0.00
2.00
(Log2)
E
GO: 563 KLF3i Decreased Genes
formation of the cornified envelope
metabolism of lipids
multicellular organismal homeostasis
hormone metabolic process
sphingolipid metabolic process
water homeostasis
-log(10) of p-value
G
GO: 423 KLF3i Increased Genes
cell cycle
DNA packaging
ors involved in megakaryocyte development
ytoskeleton organization involved in mitosis
mitotic cytokinesis
chromosome condensation
-log(10) of p-value
F
Day 3 DM
CTLi
KLF3i
LOR
RPTN
FLG2
S100A7
S100A12
OVOL1
KRT80
S100A9
LCE3D
LCE1A
DSC1
SPRR1A
ALOX12B
ALOXE3
LCE2B
KRT23
TGM5
SPRR4
CALML5
SPRR2E
HOPX
KLF3
LCE2A
KRT2
SPRR3
FLG
CNFN
SPRR2G
-2.00
0.00
2.00
(Log2)

small subset of genes (246 unique genes that are differentially regulated only upon KLF3/KLF4 double knockdown) together which are not differentiation or cell cycle related. Together, these data suggest that KLF3 is essential for promoting epidermal differentiation and is non-redundant with KLF4 in regulating this process.

KLF3 Binds to Active Enhancers to Drive Epidermal Differentiation Gene Expression

To investigate how KLF3 may be regulating gene expression during differentiation, we determined the genomic binding sites for KLF3 by performing chromatin immunoprecipitation followed by high-throughput sequencing (ChIP-Seq). ChIP-Seq was performed on replicate KLF3 pulldowns from keratinocytes differentiated for 3 days. We identified 25,352 KLF3 peaks found in both replicate data sets (p-value < 0.0001, FDR < 0.001, 4x enrichment vs. input), which were primarily located at promoter (35%), intergenic (23%), and intronic (31%) regions (Figure 1.3A). A search for consensus binding motifs within KLF3 peak locations showed a significant enrichment for KLF family motifs, further confirming the specificity of the pulldown (Figure 1.3B). Interestingly, KLF3 peak locations were also enriched for AP1, CEBP, and ETS factor family motifs, which have all been implicated in epidermal differentiation (Figure 1.3B)[29,40,46]. This suggests that lineage determining transcription factors bind to similar sites in the genome.

Based on KLF3's enrichment for motifs related to other LDTFs, we compared the KLF3 ChIP-Seq data to previously published data sets for these factors in differentiation conditions. This included ChIP-Seq data for KLF4, ZNF750, GRHL3, MAF, and MAFB[14,26,27]. Pearson

correlation coefficients were generated comparing each of these data sets, revealing that the KLF3 sequencing data correlates well with these other transcription factors, with the most significant correlation being with KLF4 (replicate values of 0.77 and 0.80) (Supplementary Figure 1.3A). Based on the positive correlation with these LDTFs, we sought to quantify the shared binding between KLF3 and the various factors. KLF3 bound peaks were overlapped with each individual LDTFs bound peaks (Supplementary Figure 1.3B). The highest overlap was with MAFB where 45.4% of its peaks overlapped those of KLF3. It should be noted that there were very few MAFB peaks to begin with (6,489) which could account partially for the high overlap. 35.0% of KLF4 peaks directly overlapped with KLF3 and they co-occupy 15,203 common binding sites. Both factors have similar binding profiles near genes found on the epidermal differentiation complex (EDC), such as the S100 family (Supplementary Figure 1.3C). These results suggest that KLF3 binds to shared regions with KLF4 and other LDTFs, further demonstrating the importance of KLF3 to the differentiation process.

To further investigate how KLF3 regulates gene expression, we wanted to characterize the type of regions that KLF3 binds in the genome. Histone marks for open chromatin regions (H3K27ac and H3K4me) and closed chromatin regions (H3K27me3 and H3K9me3) obtained from the ENCODE data for primary human keratinocytes were plotted around KLF3 peak regions which revealed an association of KLF3 with open but not closed chromatin (Figure 1.3C)[47]. Since H3K27ac and H3K4me co-localization identifies active enhancers or promoters, we sought to investigate how many of these regions KLF3 binds[48]. We compared H3K4me data (representing primed regions), and H3K27ac data (representing active regions) from

differentiated keratinocytes [40,49]. Overlap of these datasets with KLF3 showed that over 53% (13,556/25,352) of KLF3 bound regions contained both H3K4me and H3K27ac peaks (Figure 1.3D). To determine the distribution of KLF3 at active enhancer versus promoter regions, KLF3 bound H3K4me/H3K27ac positive regions were mapped back to annotated promoters (HG19:REFSEQ transcription start sites). Promoter mapped regions were separated from the13,556 active regions, with the remaining regions being KLF3 bound active enhancers. KLF3 bound H3K4me/H3K27ac regions were found to be highly enriched for enhancers at 81%, while only 19% of these active regions mapped to promoters (Figure 1.3D). These KLF3 bound active enhancer and promoter regions were then mapped back to their nearest genes which identified 2,569 genes with KLF3 bound promoters and 8,329 genes with proximal KLF3 bound enhancers (with some genes having both). These gene lists were overlapped with the 563 genes significantly decreased in expression by KLF3 knockdown (Figure 1.3E-F). 42% (236/563) of the genes decreased upon KLF3 knockdown had proximal KLF3 bound enhancers ($p < 1.006e-5$). Importantly, the most significant GO term for the 236 genes decreased by KLF3 knockdown that have a proximal KLF3 enhancer binding is *skin development* (Figure 1.3G). In contrast only 8.7% (49/563) of the genes decreased upon KLF3 depletion had KLF3 bound at its promoter ($p < 0.119$). Those 49 genes do not have enrichment for epidermal differentiation associated GO terms but instead were enriched for *rhythmic process* (Figure 1.3H). This suggests that KLF3 regulation of differentiation genes is primarily enhancer dependent. To validate the binding of KLF3 to enhancer regions, KLF3 ChIP-qPCR was performed on control and KLF3 knockdown cells (Supplementary Figure 1.3D). Control samples show KLF3 enrichment at differentiation

relevant sites, such as enhancers proximal to PGLYRP3 and IVL as well as regions flanking the epidermal differentiation complex and keratin gene clusters (Supplementary Figure 1.3D). KLF3 knockdown ablated KLF3 binding to those genomic regions which demonstrates the robustness and specificity of the KLF3 bound regions (Supplementary Figure 1.3D).

CBP and KLF3 Control a Gene Expression Program that is Necessary for Epidermal Differentiation

Since a majority of KLF3 bound H3K27ac/H3K4me regions are active enhancers, we wanted to determine if epigenetic factors associated with enhancers are critical for epidermal differentiation. Enhancer regions are often bound by CBP/P300 which promote the acetylation of H3K27, which activates enhancers primed with H3K4me[34,35]. To determine whether these epigenetic factors have a role in epidermal differentiation and identify possible functional correlations with KLF3, RNA-Seq was performed on CBP and P300 knockdown cells.

CBP and P300 each regulated several thousand genes. 1,585 genes were upregulated and 1,138 genes were diminished in expression upon CBP knockdown (Figure 1.4A). Surprisingly, P300 knockdown resulted in twice as many upregulated (2,075) genes as downregulated (963) ones suggesting it may also function as a repressor (Figure 1.4B). GO term enrichments generated for downregulated genes revealed both factors regulate the epidermal differentiation gene expression program, with significant terms including formation of the cornified envelope and epidermis development for CBP and P300, respectively (Figure 1.4C-D). However, the significance of the CBP related term is much higher than that of P300 (Figure 4C-D). While

Figure 1.3. KLF3 binds to enhancers proximal to differentiation genes that it regulates. (A) Genomic localization of the 25,352 KLF3 bound peaks identified by HOMER. KLF3 ChIP Seq was performed in replicates (n=2) from day 3 differentiated keratinocytes. (B) *de novo* motif enrichments and their associated family of factors identified within the 25,352 KLF3 peaks. (C) Mean density profile displaying histone marks (H3K27ac:purple, H3K4me:green, H3K27me3:orange, and H3K9me3:red) centered around KLF3 peaks (blue). The 25,352 KLF3 peaks were used as the reference and the profiles are displayed +/- 5kb from the KLF3 peak centers. (D) Percent distribution of the 13,556 KLF3 bound peaks that overlapped with H3K27ac/H3K4me positive regions. These 13,556 regions with KLF3/H3K27ac/H3K4me binding were annotated using HOMER and all regions not mapped to promoters were considered enhancers. (E) Venn diagram showing the number of genes decreased in KLF3i that have a proximal KLF3 bound H3K27ac/H3K4me positive enhancer(s). Overlap significance in the Venn diagram was calculated using hypergeometric distribution p-values (F) Venn diagram showing the number of genes decreased in KLF3i that have a KLF3 bound H3K27ac/H3K4me positive promoter. (G) Gene ontology (GO) term enrichment for the 236 genes decreased in KLF3i that have a KLF3 bound H3K27ac/H3K4me positive, proximal enhancer(s). (H) Gene ontology term enrichment for the 49 genes decreased in KLF3i that have a KLF3 bound H3K27ac/H3K4me positive promoter.

A

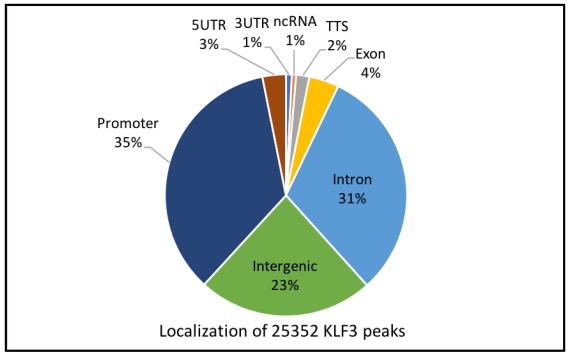

B

KLF3 de novo motif	Associated family	p-value
	KLF	1e-2617
	AP1	1e-634
	TEAD	1e-209
	CEBP	1e-149
	Zf (Zinc-finger)	1e-89
	ETS	1e-71

C

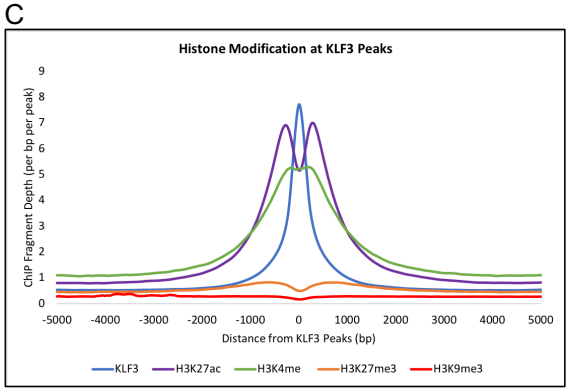

D

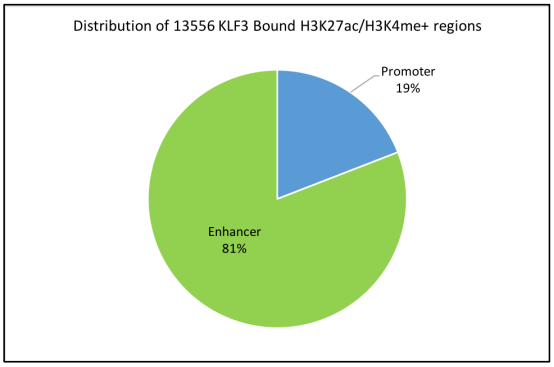

E

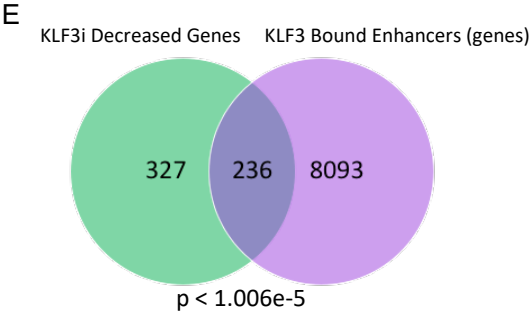

F

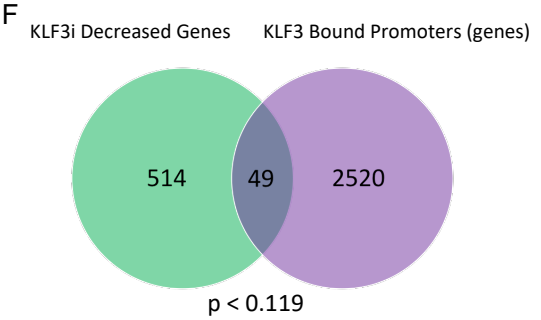

G

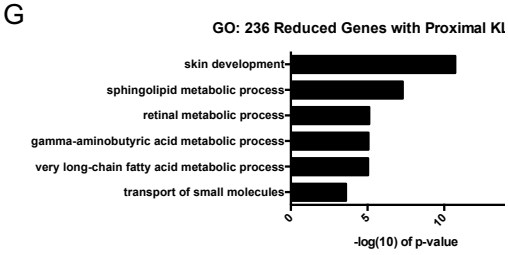

H

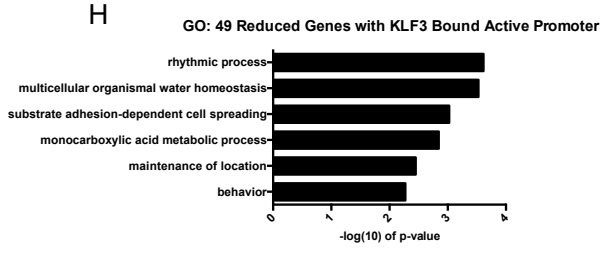

genes upregulated by CBP knockdown did not enrich for terms related to differentiation (Figure 1.4E), genes increased by P300 knockdown enriched for the terms *metabolism of lipids* and *cholesterol biosynthesis* which are both involved in the formation of the cornified envelope and critical for the differentiation process (Figure 1.4E-F). This suggests that P300 is involved in both the suppression and promotion of different parts of the differentiation program. This also suggests that P300 and CBP control non-redundant transcriptional programs in the skin, and CBP is more essential for promoting the differentiation program.

To determine whether KLF3 and the epigenetic factors regulated differentiation through the same genes, the downregulated genes were overlapped with each other. Over 50% (282/563) of the KLF3 knockdown reduced genes were also downregulated upon CBP knockdown ($p < 2.722e-231$), while only 133 were downregulated in the P300 knockdown ($p < 5.875e-67$), showing a more significant transcriptional overlap with CBP (Supplementary Figure 1.4A-B). Pearson correlations of the RPKM normalized RNA-Seq data sets also demonstrated that CBP (avg. = 0.70) correlated more with KLF3 than P300 (avg. = 0.48) (Figure 1.4G). Interestingly, CBP and P300 correlated with each other (avg.=0.52) less significantly than KLF3 with CBP (avg.=0.70) suggesting that CBP and P300 play non-redundant roles in the skin (Figure 4G). As an orthogonal confirmation of these relationships, a gene expression heatmap based on unsupervised hierarchical clustering was generated using KLF3 knockdown responsive genes as the reference (Figure 1.4H). KLF3 clustered with CBP while P300 clustered with the control samples. Validation of the RNA-Seq results by RT-qPCR also demonstrated that CBP knockdown blocked the expression of the same critical differentiation genes as KLF3 whereas

Figure 1.4. CBP and KLF3 regulate a similar gene expression program.
(A) Histogram summarizing the gene expression changes in CBP knockdown (CBPi) keratinocytes when compared to controls (CTLi) after three days of differentiation. RNA Seq was performed in replicates. Increased genes are displayed in red, while decreased genes are shown in blue. Differentially expressed genes were selected by a significant p-value with FDR (< 0.05) and fold change > 2 (+/-) vs. CTLi. (B) Histogram summarizing the gene expression changes identified by RNA sequencing in P300 knockdown (P300i) keratinocytes when compared to controls (CTLi) after three days of differentiation. RNA Seq was performed in replicates. (C) Gene ontology (GO) term enrichment for the 1,138 genes significantly decreased in expression upon CBP knockdown. (D) Gene ontology term enrichment for the 962 genes significantly decreased in expression upon P300 knockdown. (E) Gene ontology term enrichment for the 1,585 genes significantly increased in expression upon CBP depletion. (F) Gene ontology term enrichment for the 2,075 genes significantly increased in expression upon P300 depletion. (G) Heatmap plot of Pearson correlation coefficients comparing replicate KLF3i, CBPi, and P300i RNA sequencing data sets (RPKM normalized). (H) Unsupervised hierarchical clustering was performed on the RPKM normalized RNA-Sequencing data sets for CTLi, KLF3i, CBPi, and P300i keratinocytes differentiated for 3 days (log2 scale). Heatmap is focused on the KLF3 regulated genes. Increased genes are displayed in red, while decreased genes are shown in blue.

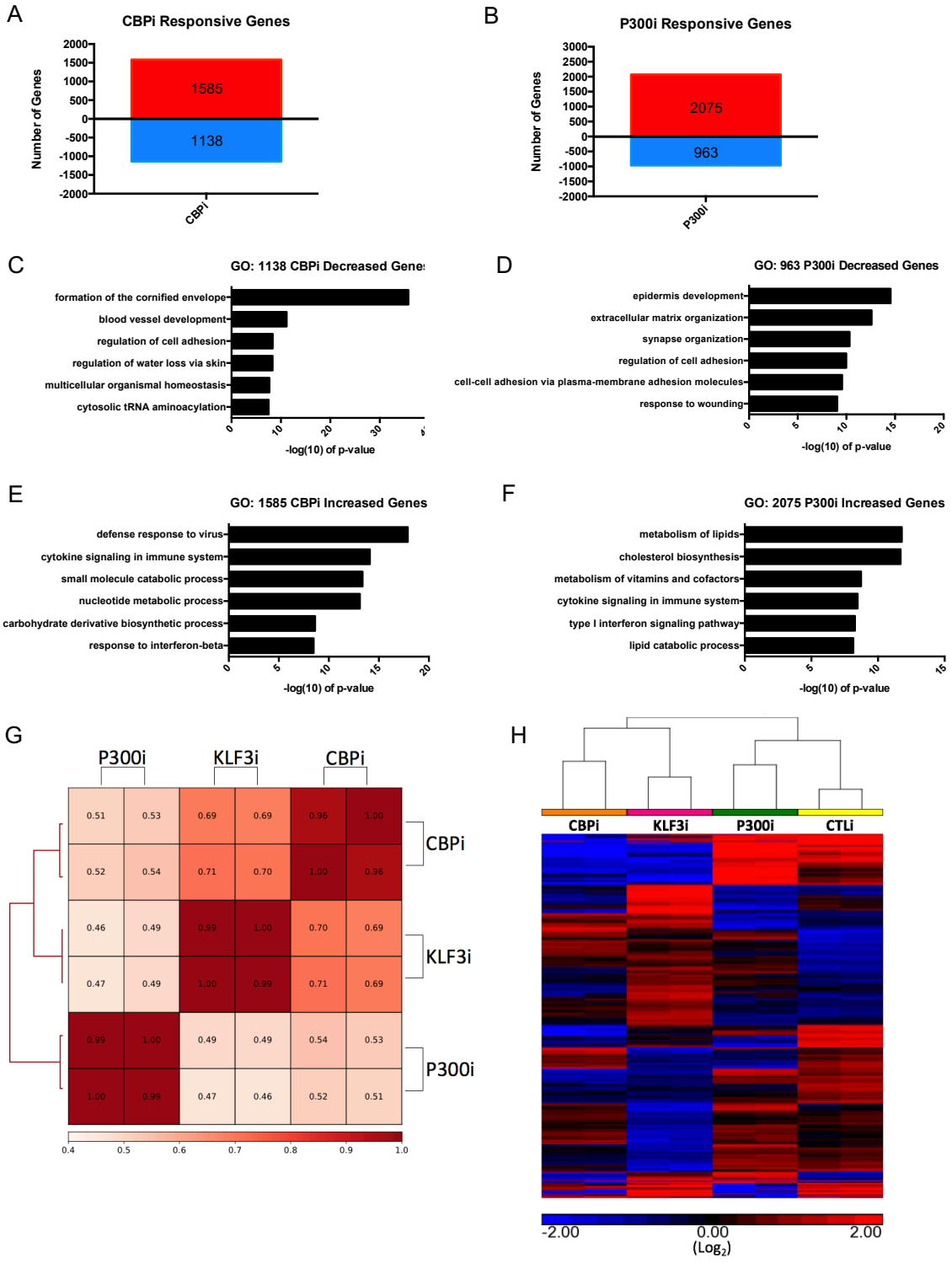
A
CBPi Responsive Genes
Number of Genes
2000
1500
1000
500
0
-500
-1000
-1500
-2000
1585
1138
CBPi
B
P300i Responsive Genes
Number of Genes
3000
2500
2000
1500
1000
500
0
-500
-1000
-1500
-2000
2075
963
P300i
C
GO: 1138 CBPi Decreased Gene
formation of the cornified envelope
blood vessel development
regulation of cell adhesion
regulation of water loss via skin
multicellular organismal homeostasis
cytosolic tRNA aminoacylation
0
10
20
30
-log(10) of p-value
D
GO: 963 P300i Decreased Genes
epidermis development
extracellular matrix organization
synapse organization
regulation of cell adhesion
cell-cell adhesion via plasma-membrane adhesion molecules
response to wounding
0
5
10
15
20
-log(10) of p-value
E
GO: 1585 CBPi Increased Genes
defense response to virus
cytokine signaling in immune system
small molecule catabolic process
nucleotide metabolic process
carbohydrate derivative biosynthetic process
response to interferon-beta
0
5
10
15
20
-log(10) of p-value
F
GO: 2075 P300i Increased Genes
metabolism of lipids
cholesterol biosynthesis
metabolism of vitamins and cofactors
cytokine signaling in immune system
type I interferon signaling pathway
lipid catabolic process
0
5
10
15
-log(10) of p-value
G
P300i
KLF3i
CBPi
0.51 0.53 0.69 0.69 0.96 1.00
0.52 0.54 0.71 0.70 1.00 0.96
0.46 0.49 0.99 1.00 0.70 0.69
0.47 0.49 1.00 0.99 0.71 0.69
0.99 1.00 0.49 0.49 0.54 0.53
1.00 0.99 0.47 0.46 0.52 0.51
CBPi
KLF3i
P300i
0.4
0.5
0.6
0.7
0.8
0.9
1.0
H
CBPi
KLF3i
P300i
CTLi
-2.00
0.00
2.00
(Log2)

P300 depletion had no impact (Supplementary Figure 1.4C-D and Figure 1.2A). In regenerated human skin, CBP knockdown phenocopied KLF3i with loss of expression of FLG and LOR on both the protein and mRNA levels (Supplementary Figure 1.4E-F). Together, this data shows that KLF3 shares a similar knockdown phenotype and transcriptional network with CBP.

CBP Genome Occupancy Correlates with KLF3

Due to the similarities between KLF3 and CBP transcriptional regulation during differentiation, we wanted to investigate how extensively these factors share genomic binding sites. ChIP-Seq was performed on replicate CBP pulldowns from day 3 differentiated keratinocytes. 24,357 replicate CBP peaks were identified, which primarily localized to intergenic (43%) and intronic (43%) genomic sites (Figure 1.5A). This is consistent with reports that CBP is primarily localized to enhancers[35]. To determine if CBP and KLF3 peaks can co-localize, signal from the CBP ChIP Seq dataset was plotted using KLF3 peak locations as a reference (Figure 1.5B). The summit of the CBP signal is found at the peak of KLF3 bound regions, suggesting that they bind to the same locations in the genome. To confirm this co-localization, CBP and KLF3 bound peak regions were overlapped with each other (Supplementary Figure 1.5A). This revealed 8461 shared peak locations between KLF3 and CBP. Thus ~35% (8,461/24,357) of the CBP bound peaks and ~33% (8,461/25,352) of the KLF3 bound peaks are shared with each other (Supplementary Figure 1.5A). *De novo* motif analysis of CBP bound regions also showed significant enrichment for KLF family binding motifs (Figure 1.5C). Motifs for AP1, CEBP, and ETS factors were also enriched in these data sets, as they

Figure 1.5. CBP and KLF3 binds to similar sites in the genome.
(A) Genomic localization of the 24,357 CBP bound peaks identified by HOMER. CBP ChIP Seq was performed in replicates from day 3 differentiated keratinocytes. (B) Mean density profile displaying CBP genomic binding centered around KFL3 peaks. The 25,352 KLF3 peaks were used as the reference and the profile of CBP binding is displayed +/- 5kb from the KLF3 peak centers. (C) *de novo* motif enrichments and their associated family of factors identified within the 24,357 CBP peaks. (D) Heatmap plot of Pearson correlation coefficients between replicate KLF3 and CBP ChIP sequencing data sets and histone marks data (H3K27ac, H3K4me, H3K27me3 and H3K9me3) (RPKM normalized). (E) UCSC genome browser tracks displaying KLF3 (red) and CBP (blue) ChIP sequencing profiles near a cluster of keratin genes. H3K27ac (maroon) and H3K4me (green) are included to represent open and active chromatin.

A

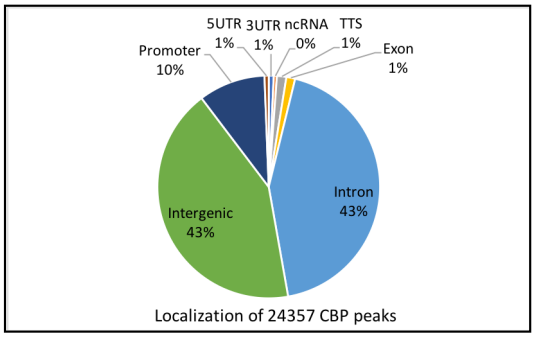

B

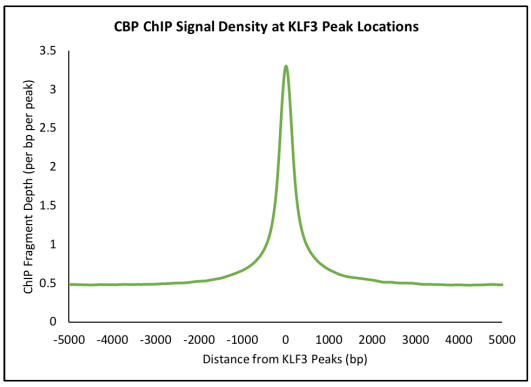

C

CBP de novo motif	Associated family	p-value
	AP-1	1e-4563
	CEBP	1e-958
	KLF	1e-911
	TEAD	1e-746
	GRHL	1e-375
	ETS	1e-271
	PAX	1e-226

D

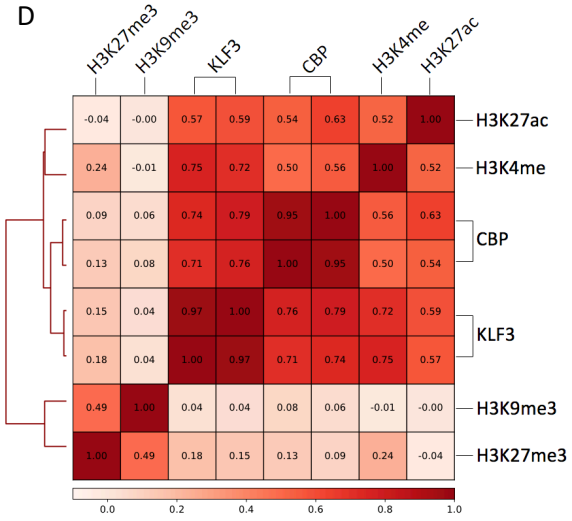

E

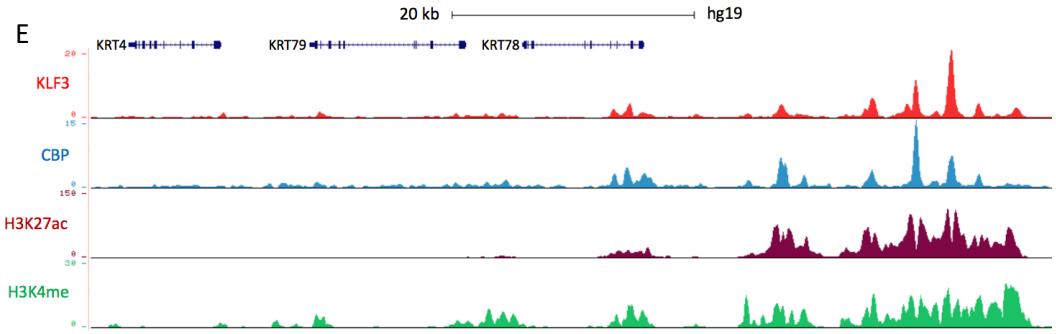

KLF3

were for KLF3 binding, suggesting that these important factors may co-localize and regulate similar regions (Figure 1.5C, 1.3B). Pearson correlations comparing these ChIP-Seq datasets also demonstrated strong positive correlation between KLF3 and CBP (avg. = 0.75) (Figure 1.5D). Importantly, there was also strong positive correlation between KLF3 and CBP with the chromatin marks of active enhancers, H3K4me and H3K27ac (Figure 1.5D). In contrast, there was no correlation with the marks H3K27me3 or H3K9me3, which represent inactive regions (Figure 1.5D). Visualization of the ChIP-seq profiles for KLF3 and CBP show co-localization at active enhancer regions (marked by H3K27ac and H3K4me) proximal to critical epidermal differentiation genes such as the keratin (KRT) family, SPRR4, and IVL (Figure 1.5E, Supplementary Figure 1.5B). This suggests that KLF3 and CBP co-localize at genomic regions that may regulate epidermal differentiation.

KLF3 Promotes CBP Localization at Active Enhancers Proximal to Differentiation Gene Loci

Since LDTFs can recruit epigenetic factors to promote gene expression changes, we sought to investigate whether KLF3 can promote the localization of CBP at active enhancer regions in differentiated keratinocytes. First, we knocked down KLF3 in differentiated keratinocytes and performed ChIP-Seq on CBP to determine if its localization to KLF3 bound active enhancers is affected. *DiffReps* was used to detect the loss or gain of CBP binding upon KLF3 depletion[50]. KLF3 knockdown resulted in 1,602 regions of significantly reduced CBP binding, while 2186 regions gained CBP binding (Figure 1.6A, Supplementary Figure 1.6A).

Figure 1.6. KLF3 is necessary for CBP localization proximal to differentiation genes. (A) Summary of significant CBP ChIP signal reduction events in day 3 differentiated keratinocytes knocked down for KLF3. The orange circle represents the total number of regions in the genome that lose CBP binding upon KLF3 knockdown. The green circle represents the number of regions that lose CBP binding that occur at a KLF3 peak upon KLF3 depletion. The blue circle represents the regions that lose CBP binding which also contain KLF3, H3K4me, and H3K27ac binding upon KLF3 knockdown. CBP ChIP Seq was performed in replicates in CTLi and KLF3i cells. Significant signal changes were identified by Diffreps. (B) Mean density profile displaying CBP binding centered around KLF3/H3K4me/H3K27ac peaks. The CBP mean density is plotted around the 612 regions identified in (1.6A:blue circle). The profile of CBP binding is shown +/- 10kb from the centers of the 612 regions in CTLi (blue) and KLF3i (red) cells. (C) Percent distribution of the 612 H3K27ac/H3K4me positive regions containing KLF3 peaks with significant CBP depletion upon KLF3 knockdown. These 612 regions were annotated using HOMER and all regions not mapped to promoters were considered enhancers. (D) Gene ontology (GO) term enrichment for the 49 genes that lose CBP binding at their active promoter (H3K4me/H3K27ac positive) containing a KLF3 peak. (E) Gene ontology term enrichment for the 527 genes that lose CBP binding at a proximal enhancer (H3K27ac/H3K4me positive) containing a KLF3 peak. (F) UCSC genome browser tracks displaying CBP binding (CBP ChIP Seq profiles) from CTLi (blue) and KLF3i (orange) cells, near differentiation genes LOR and PGLYRP3. KLF3 (red), H3K27ac (maroon), and H3K4me (green) binding are also shown. (G) UCSC genome browser tracks displaying CBP binding (CBP ChIP Seq profiles) from CTLi (blue) and KLF3i (orange) cells, near differentiation gene IVL. KLF3 (red), H3K27ac (maroon), and H3K4me (green) binding are also shown.

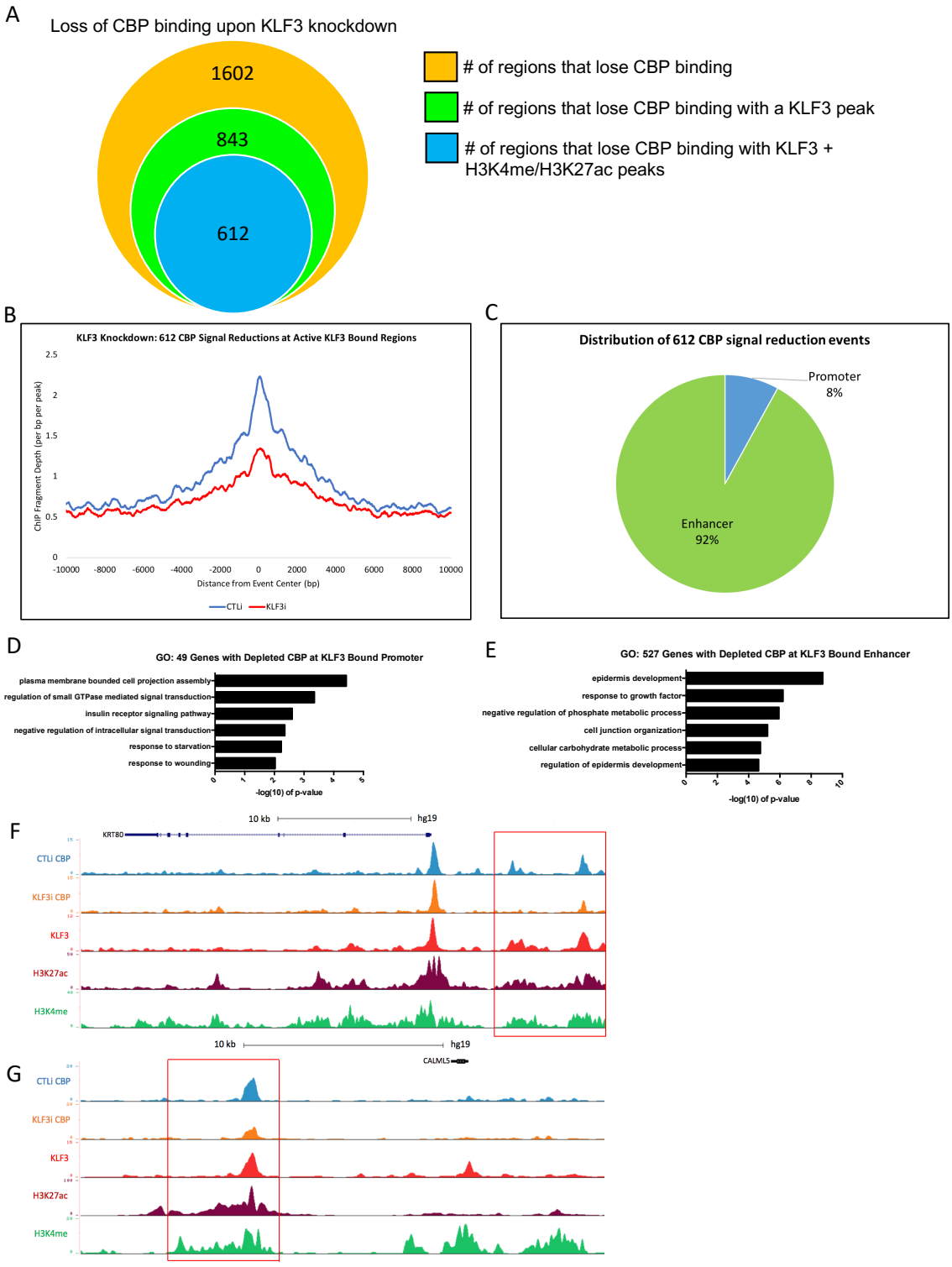
A
Loss of CBP binding upon KLF3 knockdown
1602
843
612
# of regions that lose CBP binding
# of regions that lose CBP binding with a KLF3 peak
# of regions that lose CBP binding with KLF3 + H3K4me/H3K27ac peaks
B
KLF3 Knockdown: 612 CBP Signal Reductions at Active KLF3 Bound Regions
ChIP Fragment Depth (per bp per peak)
Distance from Event Center (bp)
CTLi
KLF3i
C
Distribution of 612 CBP signal reduction events
Promoter 8%
Enhancer 92%
D
GO: 49 Genes with Depleted CBP at KLF3 Bound Promoter
plasma membrane bounded cell projection assembly
regulation of small GTPase mediated signal transduction
insulin receptor signaling pathway
negative regulation of intracellular signal transduction
response to starvation
response to wounding
-log(10) of p-value
E
GO: 527 Genes with Depleted CBP at KLF3 Bound Enhancer
epidermis development
response to growth factor
negative regulation of phosphate metabolic process
cell junction organization
cellular carbohydrate metabolic process
regulation of epidermis development
-log(10) of p-value
F
10 kb
hg19
KRT80
CTLi CBP
KLF3i CBP
KLF3
H3K27ac
H3K4me
G
10 kb
hg19
CALML5
CTLi CBP
KLF3i CBP
KLF3
H3K27ac
H3K4me

Next,

Next, we compared whether the losses in CBP binding occurred within KLF3 bound regions. 52.6% (843/1602) of the CBP reduced binding occurred within KLF3 peaks regions (Figure 1.6A). In addition, the vast majority of the reductions in CBP (72.6%, 612/843) signal at KLF3 peaks occur in active regions of chromatin (H3K4me/H3K27ac positive, promoters included) (Figure 1.6A). Plotting of the CBP signal density at the 612 sites of KLF3 bound active regions (H3K4me/H3K27ac positive) showed a dramatic reduction in CBP binding upon KLF3 knockdown (Figure 1.6B). The loss of CBP binding was also not due to global loss of CBP protein levels, as KFL3 depletion did not significantly impact its expression (Supplementary Figure 1.6B). We also tested whether KLF3 knockdown led to gains in CBP binding at KLF3 bound regions. Only 15% (328/2,186) of the KLF3 bound regions gained CBP binding upon KLF3 knockdown (Supplementary Figure 1.6A). These results suggest that KLF3 is necessary for the localization of CBP to its binding sites.

Based on this loss of CBP at KLF3 bound active chromatin regions, we wanted to explore whether these reductions are primarily occurring at enhancer or promoter regions. The 612 KLF3/H3K27ac/H3K4me bound regions that lost CBP binding upon KLF3 knockdown was mapped back to annotated promoters. This revealed that a small portion (8%) of these events occurred at promoters while 92% occurred at enhancers (Figure 1.6C). This suggests that the KLF3 dependent localization of CBP occurs primarily at active enhancer regions. Mapping these regions to proximal genes revealed only 49 genes associated with promoter reductions, while 527 genes have proximal enhancer reductions. Gene ontology analysis was performed for both sets of genes (Figure 1.6D-E). While CBP reductions at the 49 active promoters did not enrich for

differentiation genes, the 527 enhancer associated genes had *epidermis development* as the most significant term (Figure 1.6D-E). Validation of these results by ChIP-qPCR demonstrate that KLF3 is necessary for CBP to localize to enhancers proximal to differentiation genes such as *LOR*, *IVL*, *HOPX*, *CALML5*, and *KRT80* (Supplemental Figure 1.6C). Visualization of these enhancer sites that are proximal to important epidermal differentiation genes confirms the reduction of CBP signal (Figure 1.6F-G, Supplementary Figure 1.6D-E). This suggests that KLF3 dependent CBP localization occurs primarily at active enhancer, and that these regions are found proximal to epidermal differentiation genes. To determine if KLF3 directly recruited CBP to enhancers, co-immunoprecipitation (co-IP) experiments were performed. KLF3 did not co-IP out CBP suggesting that KLF3 may not directly recruit CBP to enhancer regions and may instead be necessary to set up the local enhancer region to allow for CBP to localize to KLF3 bound enhancers (Supplementary Figure 1.6F).

Discussion

Here, we sought to identify novel factors that are involved in regulating epidermal differentiation. Through the analysis of a previously generated RNA-seq data set comparing undifferentiated to differentiated keratinocytes, we identified the transcription factor KLF3 as being upregulated during epidermal differentiation. KLF3 expression was expressed throughout the epidermis but increased in the upper differentiated layers suggesting a possible role in regulating differentiation.

Next, we characterized the KLF3 knockdown phenotype and found that depletion of KLF3 blocked differentiation gene expression in both two-dimensional cultures and three-dimensional regenerated human skin. Global gene expression profiling of KLF3 knockdown cells showed 563 genes downregulated that were important for terminal differentiation including formation of the cornified envelope. In addition, 423 genes were upregulated upon KLF3 depletion which were genes involved in proliferation. This suggests that KLF3's normal function is to activate differentiation gene expression while suppressing proliferation. Since KLF3 is a related transcription factor to KLF4 which is a well characterized transcription factor necessary for epidermal differentiation, we decided to test functional redundancies between them[10,51]. Comparison of KLF3 knockdown to that of KLF4 knockdown revealed that over half of the KLF3 gene signature overlapped with that of KLF4 with significant shared regulation of differentiation genes. However, the double-knockdown of these factors revealed non-redundant functions in this regulation, as knockdown of either factor alone can impact the expression of differentiation genes, but genes only impacted by the double-knockdown do not enrich for functions related to differentiation. Instead there were only 95 and 151 genes uniquely downregulated and upregulated respectively in the KLF3/KLF4 double knockdown cells. These differentially regulated genes were not enriched for differentiation genes but rather genes involved in drug catabolic process or interferon response. This suggests that these factors cannot compensate for one another to promote differentiation gene expression as loss of either factor results in a blockade of differentiation. It has been previously shown that KLF factors can utilize

unique binding sites to regulate the same genes, as well as compete for common binding sites to balance transcriptional activity[52]. However, this competitive activity was shown in murine erythroid cells, where KLF3 acts primarily as a repressor competing for binding sites with the activator KLF1 to limit KLF1 induced gene expression. It is unclear if KLF3 and KLF4 are competing for common sites in human keratinocytes, as they do not have opposing roles but instead similar roles in promoting differentiation and suppressing cell cycle genes. It is possible that they simultaneously occupy binding sites to promote similar gene expression programs but provide unique functional activities at these genomic loci. Thus, while KLF3 and KLF4 share many genomic binding sites and regulation of transcription, their functions at these sites may not be redundant.

While KLF3 genome occupancy has been studied, the previous methods used for ChIP-Seq analysis primarily involved pulling down overexpressed exogenous KLF3 and these experiments were predominantly performed using murine cell lines[52-54]. Endogenous KLF3 has been pulled down in human primary erythroblasts, however sequencing was not performed on those samples[55]. To our knowledge, this study presents the first ChIP-seq of endogenous KLF3 in primary human cells. Genome-wide profiling of KLF3 binding sites through ChIP-seq revealed that KLF3 shares many binding sites with other epidermal LDTFs including KLF4, ZNF750, MAF, and MAFB. For example, 35% of KLF4 and 45.4% of MAFB peaks directly overlapped with KLF3 peaks suggesting that epidermal LDTFs regulate similar regions of the genome to control differentiation. Surprisingly, the majority of KLF3 bound peaks are enriched for H3K4me and H3K27ac signal (histone marks of open and active chromatin regions). This

suggests that in differentiating keratinocytes, KLF3 may be performing activities that contribute to the promotion of differentiation gene activation and transcription. This is in contrast to previous studies classifying KLF3 as a transcriptional repressor (primarily in murine cells), which showed KLF3's binding and repressive activity primarily through EMSA and luciferase reporter assays focused on single gene targets in addition to the regulation of gene expression identified through RT-qPCR and microarray[19,22,54-57]. KLF3 has also been proposed to be a repressor based on interactions with CTBP proteins, which can promote downstream chromatin modifying activity to repress gene expression[58,59]. However, it has recently been demonstrated that CTBP proteins can act as activators when forming complexes with epidermal transcription factors such as KLF4 and ZNF750 to promote differentiation gene expression[14]. Thus, while it is possible that KLF3 has this repressive activity at certain genes (i.e. cell cycle genes) in keratinocytes, we sought to further investigate its association with open and active chromatin regions throughout the genome since over 53% (13,556/25,352) of KLF3 binding occurs there. We found that 81% of KLF3 bound H3K4me/H3K27ac positive regions were enhancers, while only 19% were promoters. When these regions were mapped to proximal genes and compared to the KLF3 knockdown, we found that there were only 49 genes with KLF3 bound, active promoters that have decreased expression upon KLF3 knockdown. These 49 genes were also not enriched for GO terms such as epidermal differentiation but instead were enriched for rhythmic process and multicellular organismal water homeostasis. However, 42% (236/563) of the genes that decreased in expression upon KLF3 knockdown had proximal KLF3 bound enhancers. Furthermore these genes were highly enriched for GO terms related to skin development. This

suggests that KLF3 dependent differentiation gene expression may be due to KLF3 activity at nearby enhancers and not by KLF3 activity at their promoters.

Due to this enhancer association, we sought to investigate the functional relationship between KLF3 and the enhancer associated epigenomic writers CBP and P300. CBP and P300 are well known chromatin modifying proteins that have been shown to be necessary for enhancer activity and the recruitment of the transcriptional machinery necessary to promote gene expression[60]. However, their roles in epidermal differentiation remain unclear. These factors are often considered redundant in their functions due to their largely overlapping genomic binding sites as well as redundant functions in promoting stem cell self-renewal such as in embryonic stem cells[36,61]. However, there is also evidence these epigenetic factors are non-redundant. Knockout of either gene leads to embryonic lethality in mice which precluded further analysis in adults[62,63]. Conditional knockout in murine hematopoietic stem cells (HSC) have shown that CBP is necessary for HSC self-renewal whereas p300 is important for HSC differentiation[39]. We show here that CBP and P300 do not play redundant roles in epidermal differentiation. While knockdown of P300 blocked the expression of a subset of differentiation genes, it also induced the expression of terminal differentiation genes involved in lipid metabolism and cholesterol biosynthesis which are critical to the formation of the epidermal barrier. In contrast, knockdown of CBP blocked epidermal differentiation in 2D and regenerated human skin and shared a similar transcriptional program as KLF3. Based on this, we sought to explore the relationship between CBP and KLF3.

We found that CBP bound to 24,357 sites in the genome with 86% of those localized to intergenic or intronic regions which are indicative of enhancers. In contrast, only a small minority (10%) mapped back to promoter regions. CBP bound sites were enriched for transcription factor motifs such as the CEBP, KLF, GRHL, and ETS family. Importantly ~35% (8,461/24,357) of CBP bound sites directly overlapped with KLF3 bound regions. It has been shown that CBP/P300 localization and activity at enhancer regions can be dependent on LDTFs[64]. Due to this relationship, we investigated whether KLF3 is necessary for CBP localization at KLF3 bound enhancer regions. Remarkably, 53% (843/1,602) of the regions where CBP lost binding upon KLF3 knockdown occurred at KLF3 bound sites. Of these 843 regions, 73% (612/843) of the regions were also bound with H3K4me/H3K27ac, (with 92% being in active enhancers). Mapping these regions back to their most proximal genes showed that there was significant enrichment for epidermal differentiation genes. Since KLF3 is necessary for CBP localization to KLF3 bound enhancers, we asked whether KLF3 directly recruited CBP to enhancers. Interestingly, KLF3 and CBP do not directly associate with each other through endogenous co-IP experiments. It is possible that the KLF3 and CBP interaction is extremely transient or weak. Another possibility is that KLF3 is needed to set up the chromatin structure with associated proteins at the KLF3 bound enhancers which then allows CBP to localize. Together these data suggest that KLF3 regulates differentiation gene expression by promoting the proper localization of CBP to enhancers proximal to differentiation gene clusters.

In summary, we have identified KLF3 as a novel regulator of epidermal differentiation that is necessary for CBP localization at differentiation associated enhancers.

Chapter 1 Supplementary Figures

Supplementary Figure 1.1. Increase in KLF3 expression is necessary for differentiation. (A) UCSC Genome Browser tracks displaying representative RNA-sequencing data of KLF3 expression in growth media (GM, orange track) and differentiation media (DM, day 3, blue track). (B) Western blot of KLF3 protein levels in day 3 differentiated keratinocytes treated with control (CTLi) or KLF3 targeting (KLF3i) siRNA. Representative image is shown, n=3. (C) Immunofluorescent staining of KLF3 (green) and KRT10 (red, a marker of the differentiated layers) in day 5 regenerated human epidermis treated with control (CTLi) or KLF3 targeting (KLF3i) siRNAs. Merged image includes Hoechst staining of nuclei. n=3. Scale bar =20μm. (D) Immunofluorescent staining of KLF3 (green) and P63 (red, a marker of the basal layer) in day 5 regenerated human epidermis treated with control (CTLi) or KLF3 targeting (KLF3i) siRNAs. Merged image includes Hoechst staining of nuclei. n=3. Scale bar =20μm.

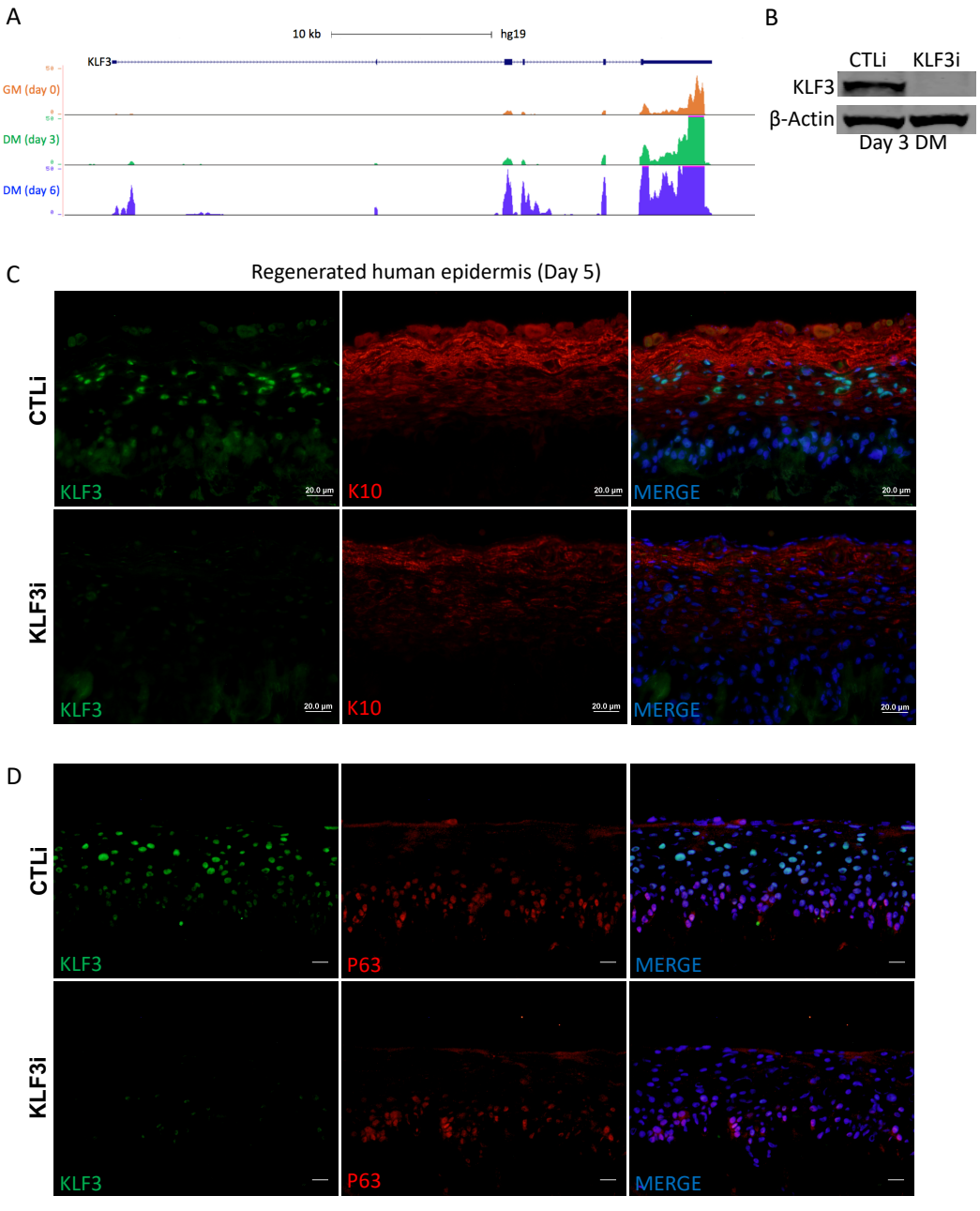
A
10 kb
hg19
KLF3
GM (day 0)
DM (day 3)
DM (day 6)
B
CTLi
KLF3i
KLF3
β-Actin
Day 3 DM
C
Regenerated human epidermis (Day 5)
CTLi
KLF3i
KLF3
K10
MERGE
20.0 µm
D
CTLi
KLF3i
KLF3
P63
MERGE

Supplementary Figure 1.2. KLF3 and KLF4 are not redundant in the regulation of epidermal differentiation gene expression.
(A) Histogram summarizing the gene expression changes identified by RNA Seq in KLF4 knockdown (KLF4i) keratinocytes when compared to controls (CTLi) after three days of differentiation. Increased genes are displayed in red, while decreased genes are shown in blue. Differentially expressed genes were selected by a significant p-value with FDR (< 0.05) and fold change > 2 (+/-) vs. CTLi, n=2. (B) Gene ontology (GO) term enrichment for the 772 genes significantly decreased in expression upon KLF4 knockdown. (C) Gene ontology term enrichment for the 1265 genes significantly increased in expression upon KLF4 knockdown. (D) Venn diagram showing the number of shared and uniquely decreased genes in the KLF3i and KLF4i gene signatures. Overlap significance in the Venn diagram was calculated using hypergeometric distribution p-values. (E) Venn diagram showing the number of shared and uniquely increased genes in the KLF3i and KLF4i gene signatures. (F) Heatmap plot of Pearson correlation coefficients between replicate KLF3i and KLF4i RNA sequencing data sets (RPKM normalized). (G) Histogram summarizing the gene expression changes identified by RNA Seq in KLF3/KLF4 double knockdown (DKD) keratinocytes when compared to controls (CTLi) after three days of differentiation. Increased gene counts are displayed in red, while decreased genes are shown in blue. n=2. (H) Venn diagram showing the number of unique and shared decreased genes in the KLF3i/KLF4i double knockdown versus the KLF3i and KLF4i gene signatures. (I) Venn diagram showing the number of unique and shared increased genes in the KLF3i/KLF4i double knockdown versus the KLF3i and KLF4i gene signatures. (J) Gene ontology term enrichment for the 95 genes uniquely decreased in the KLF3i/KLF4i double knockdown condition. (K) Gene ontology term enrichment for the 151 genes uniquely increased in the KLF3i/KLF4i double knockdown condition.

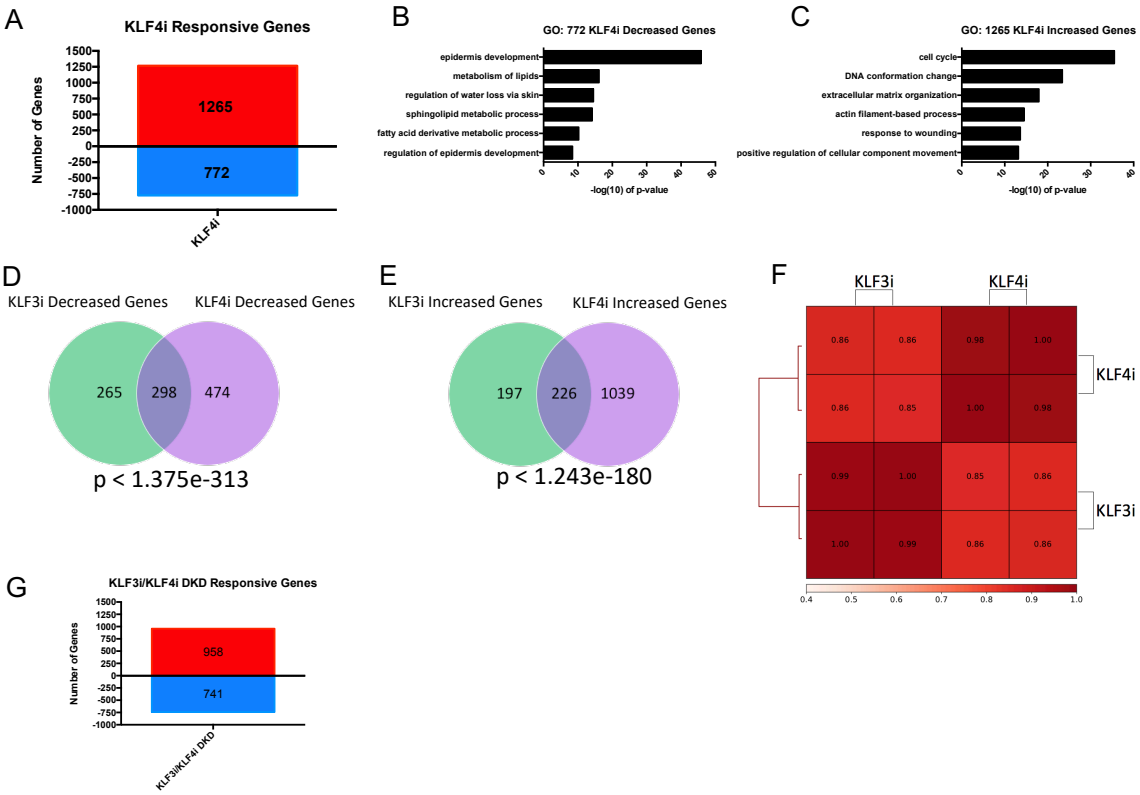
A
KLF4i Responsive Genes
Number of Genes
1265
772
KLF4i
B
GO: 772 KLF4i Decreased Genes
epidermis development
metabolism of lipids
regulation of water loss via skin
sphingolipid metabolic process
fatty acid derivative metabolic process
regulation of epidermis development
-log(10) of p-value
C
GO: 1265 KLF4i Increased Genes
cell cycle
DNA conformation change
extracellular matrix organization
actin filament-based process
response to wounding
positive regulation of cellular component movement
-log(10) of p-value
D
KLF3i Decreased Genes
KLF4i Decreased Genes
265
298
474
p < 1.375e-313
E
KLF3i Increased Genes
KLF4i Increased Genes
197
226
1039
p < 1.243e-180
F
KLF3i
KLF4i
0.86
0.86
0.98
1.00
0.86
0.85
1.00
0.98
0.99
1.00
0.85
0.86
1.00
0.99
0.86
0.86
KLF4i
KLF3i
0.4
0.5
0.6
0.7
0.8
0.9
1.0
G
KLF3i/KLF4i DKD Responsive Genes
Number of Genes
958
741
KLF3i/KLF4i DKD
H
KLF3i/KLF4i DKD Decreased Genes
95
106
257
283
159
15
217
KLF3i Decreased Genes
KLF4i Decreased Genes
I
KLF3i/KLF4i DKD Increased Genes
151
95
496
216
102
10
543
KLF3i Increased Genes
KLF4i Increased Genes
J
GO: 95 genes uniquely decreased in KLF3/KLF4 double knockdown
drug catabolic process
carbohydrate derivative transport
Rho protein signal transduction
-log(10) of p-value
K
GO: 151 genes uniquely increased in KLF3/KLF4 double knockdown
interferon alpha/beta signaling
riboflavin metabolic process
regulation of cell adhesion
antiviral mechanism by IFN-stimulated genes
Rho GTPase cycle
response to interferon-gamma
-log(10) of p-value

Supplementary Figure 1.3. KLF3 and epidermal lineage determining transcription factors bind to similar regions in the genome.
(A) Heatmap plot of Pearson correlation coefficients between KLF3 ChIP Seq data and ChIP Seq data for the epidermal LDTFs KLF4, ZNF750, MAF, MAFB, and GRHL3 (RPKM normalized). (B) Table displaying the peak overlap between KLF3 and each epidermal LDTFs. Each LDTFs total bound peak numbers identified by HOMER are shown with the number and percentage of overlap with KLF3 peaks. (C) UCSC genome browser track displaying KLF3 (red) and KLF4 (blue) ChIP Seq profiles near a cluster of differentiation associated S100 genes. H3K27ac (maroon) is included to represent open chromatin. (D) ChIP qPCR showing KLF3 pulldown at differentiation sites in both control (CTLi) and KLF3 knockdown (KLF3i) keratinocytes differentiated for 3 days. Enrichment is represented as the percent of input. n=2.

A

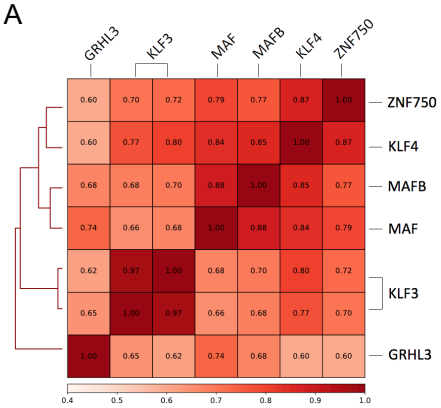

B

ChIP	Total Peaks	Shared Peaks with KLF3	% of peaks
KLF4	43408	15203	35.0
ZNF750	53922	10552	19.6
MAF	3521	856	24.3
MAFB	6489	2946	45.4
GRHL3	4383	357	8.2

C

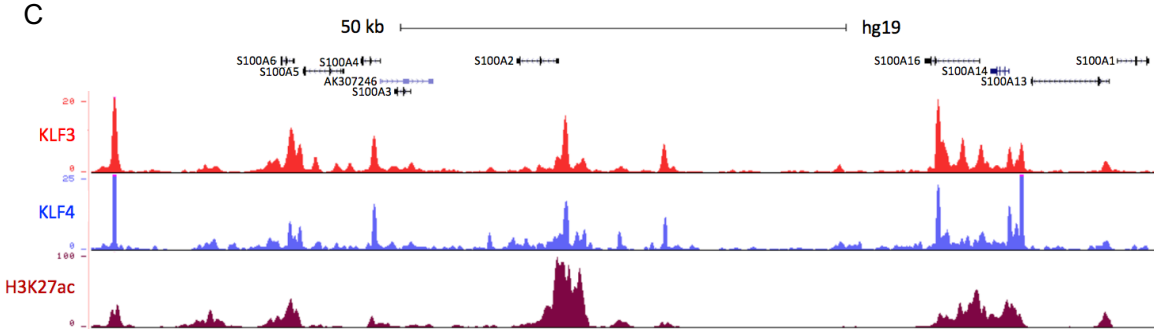

D

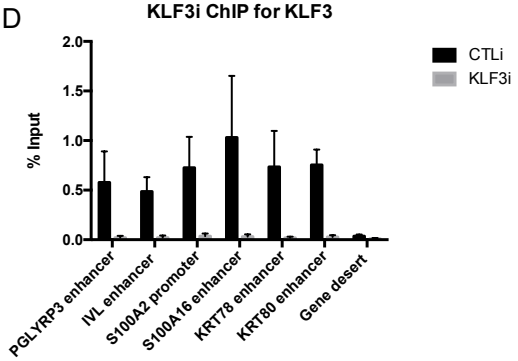

Supplementary Figure 1.4. CBP is necessary for human epidermal differentiation.
(A) Venn diagram showing the number of shared and uniquely decreased genes in the KLF3i and CBPi gene signatures. Overlap significance in the Venn diagram was calculated using hypergeometric distribution p-values. (B) Venn diagram showing the number of common and uniquely decreased genes in the KLF3i and P300i gene signatures. (C) RT-qPCR quantifying the relative mRNA levels of a panel of epidermal differentiation genes in CTLi and CBPi keratinocytes after three days of differentiation, n=4. Statistics: t-test, *$p < 0.05$, ** $p < 0.01$, ***$p < 0.001$. (D) RT-qPCR quantifying the relative mRNA levels of a panel of epidermal differentiation genes in CTLi and P300i keratinocytes after three days of differentiation, n=4. (E) Immunofluorescent staining of late differentiation markers LOR (green) and FLG (red) in day 5 regenerated human epidermis treated with control (CTLi) or CBP targeting (CBPi) siRNAs. Merged image includes Hoechst staining of nuclei, n=3. Scale bar = 20μm. (F) RT-qPCR quantifying the relative mRNA expression levels of LOR and FLG in CTLi and CBPi day 5 regenerated human epidermis, n=3.

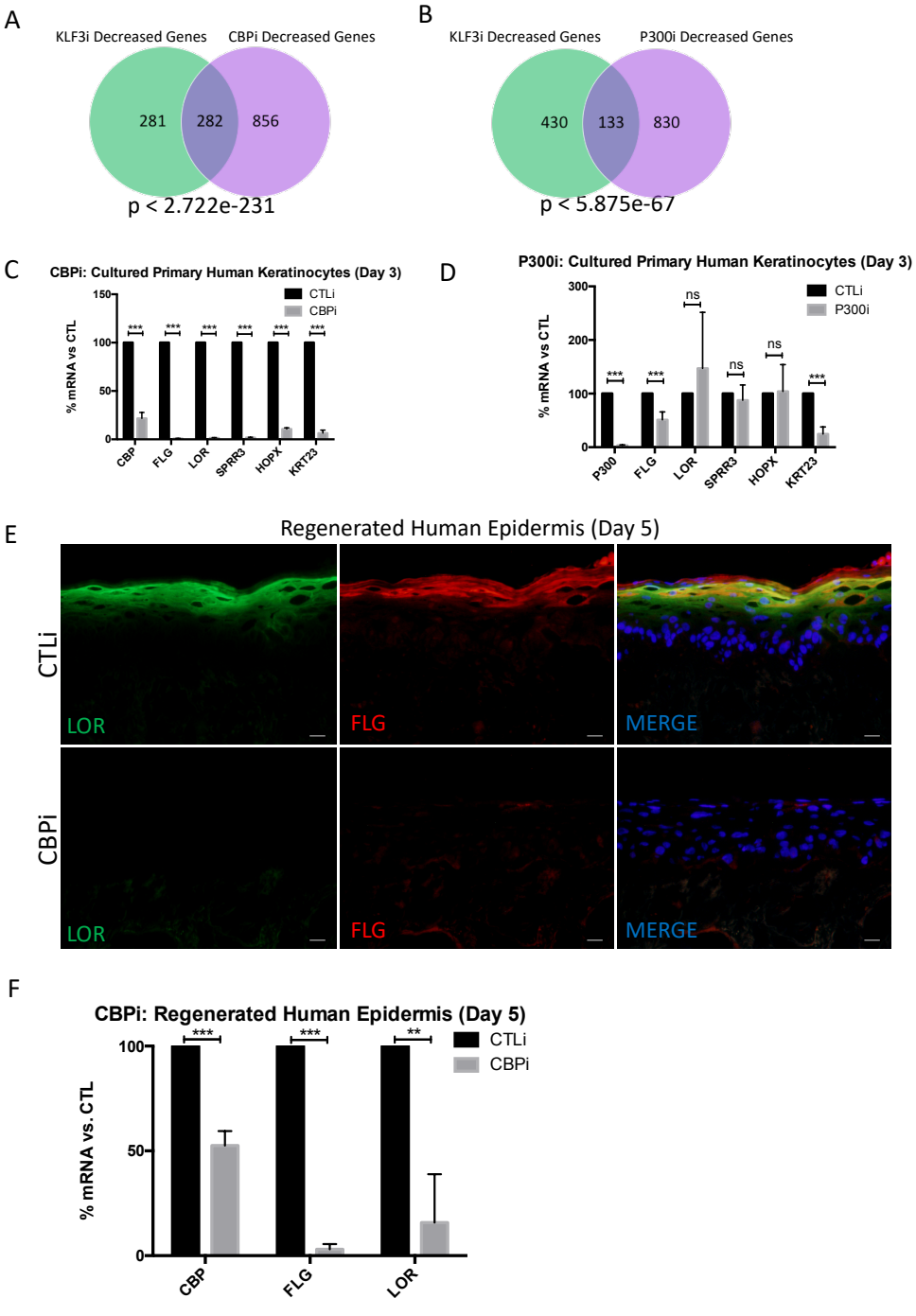
A
KLF3i Decreased Genes
CBPi Decreased Genes
281
282
856
p < 2.722e-231
B
KLF3i Decreased Genes
P300i Decreased Genes
430
133
830
p < 5.875e-67
C
CBPi: Cultured Primary Human Keratinocytes (Day 3)
CTLi
CBPi
% mRNA vs CTL
CBP
FLG
LOR
SPRR3
HOPX
KRT23
D
P300i: Cultured Primary Human Keratinocytes (Day 3)
CTLi
P300i
% mRNA vs CTL
ns
P300
FLG
LOR
SPRR3
HOPX
KRT23
E
Regenerated Human Epidermis (Day 5)
CTLi
CBPi
LOR
FLG
MERGE
F
CBPi: Regenerated Human Epidermis (Day 5)
CTLi
CBPi
% mRNA vs. CTL
CBP
FLG
LOR

A

ChIP	Total Peaks	Shared Peaks with KLF3	% of peaks
CBP	24357	8461	34.74

B

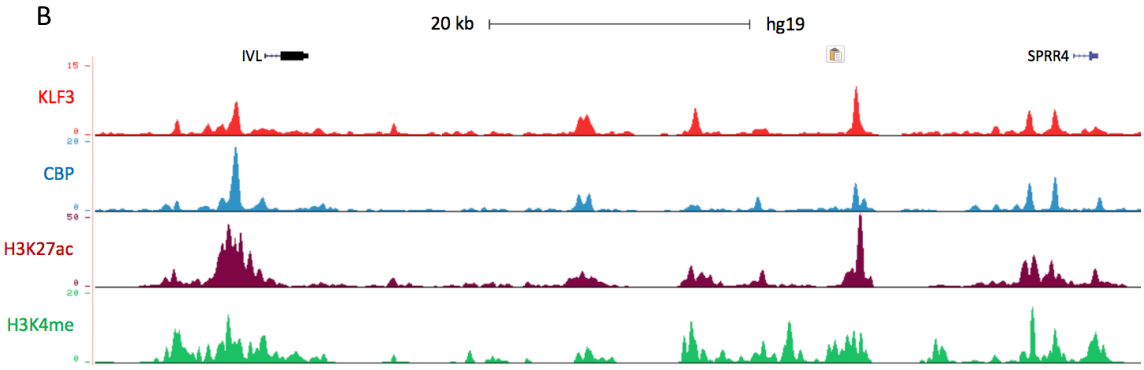

Supplementary Figure 1.5. CBP and KLF3 directly overlap at ~35% of their binding sites in the genome.
(A) Table displaying the peak overlap between KLF3 and CBP. The total CBP bound peak numbers identified by HOMER are shown with the number and percentage of overlap with KLF3 peaks. (B) UCSC genome browser tracks displaying KLF3 (red) and CBP (blue) ChIP Seq profiles near the differentiation genes IVL and SPRR4. H3K27ac (maroon) and H3K4me (green) are included to represent open and active chromatin.

Supplementary Figure 1.6. KLF3 is necessary for CBP localization to genomic sites.
(A) Summary of significant CBP ChIP signal enrichment events in day 3 differentiated keratinocytes knocked down for KLF3. The orange circle represents the total number of regions in the genome that gain CBP binding upon KLF3 knockdown. The green circle represents the number of regions that gain CBP binding that occur at a KLF3 peak upon KLF3 depletion. The blue circle represents the regions that gain CBP binding which also contain KLF3, H3K4me, and H3K27ac binding upon KLF3 knockdown. CBP ChIP Seq was performed in replicates in CTLi and KLF3i cells. Significant signal changes were identified by Diffreps. (B) Western blot of CBP protein levels in CTLi and KLF3i keratinocytes (day 3 differentiation) with B-Actin as a loading control. n=3 (C) ChIP-qPCR of CBP pulldown in CTLi and KLF3i keratinocytes (day 3 differentiation). The percent of input for each sample was used to calculate the efficiency of CBP pulldown. The percent input of CBP pulldown in the CTLi condition was then normalized to 100%, and the proportion of CBP pulldown in KLF3i cells was plotted as a percent of the controls. n=2. (D) UCSC genome browser tracks displaying CBP binding (CBP ChIP Seq profiles) from CTLi (blue) and KLF3i (orange) cells, near CALML5. KLF3 (red), H3K27ac (maroon), and H3K4me (green) binding are also shown. (E) UCSC genome browser tracks displaying CBP binding (CBP ChIP Seq profiles) from CTLi (blue) and KLF3i (orange) cells, near KRT80. KLF3 (red), H3K27ac (maroon), and H3K4me (green) binding are also shown. Statistics: t-test, *$p < 0.05$, ** $p < 0.01$, ***$p < 0.001$.

A

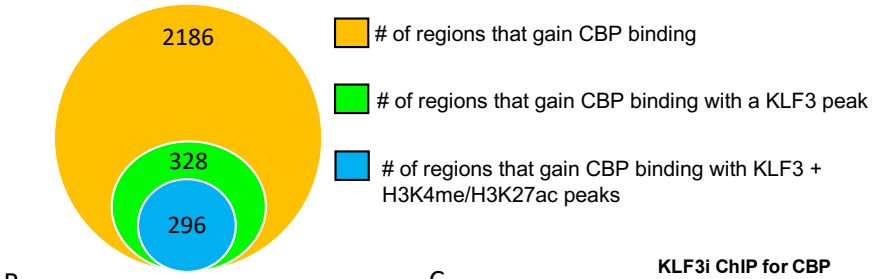
Gained regions of CBP binding upon KLF3 knockdown
2186
328
296
# of regions that gain CBP binding
# of regions that gain CBP binding with a KLF3 peak
# of regions that gain CBP binding with KLF3 + H3K4me/H3K27ac peaks

B

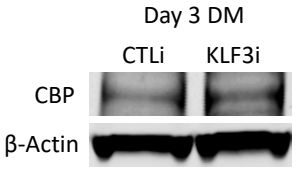
Day 3 DM
CTLi
KLF3i
CBP
β-Actin

C

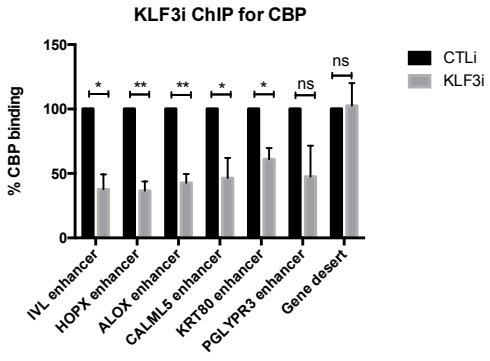
KLF3i ChIP for CBP
% CBP binding
150
100
50
0
*
**
**
*
*
ns
ns
CTLi
KLF3i
IVL enhancer
HOPX enhancer
ALOX enhancer
CALML5 enhancer
KRT80 enhancer
PGLYPR3 enhancer
Gene desert

D

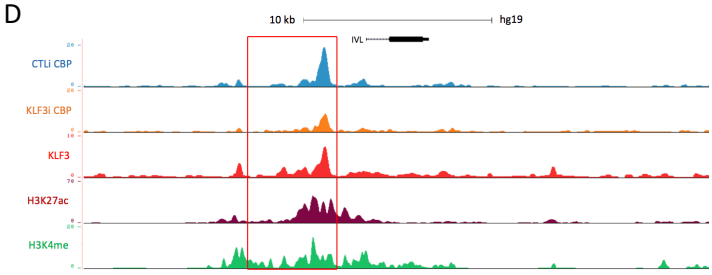
10 kb
hg19
IVL
CTLi CBP
KLF3i CBP
KLF3
H3K27ac
H3K4me

E

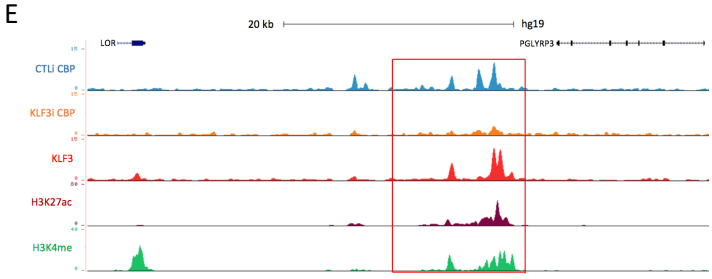
20 kb
hg19
LOR
PGLYRP3
CTLi CBP
KLF3i CBP
KLF3
H3K27ac
H3K4me

F

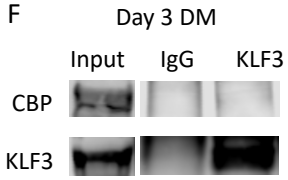
Day 3 DM
Input
IgG
KLF3
CBP
KLF3

Methods

Cell Culture

Primary human epidermal keratinocytes (derived from neonatal foreskin) were cultured in EpiLife medium (ThermoFisher MEPI500CA). This media was supplemented with Penicillin/streptomycin (HyClone SV30010) and human keratinocyte growth supplement (HKGS, ThermoFisher S0015). Keratinocytes were differentiated by seeding to full confluence and subsequently adding 1.2 mM calcium for 3 days as previously described [13].

Gene knockdown

siRNAs were placed into EpiLife media with the transfection reagent Lipofectamine RNAiMAX (25ul for 10cm plate transfection, 50 ul for 15cm plate transfection) (ThermoFisher 13778) and incubated for 5 minutes. This siRNA media was then diluted 1:10 and added to sub-confluent keratinocytes, with the siRNA at a final concentration of 10nM. The keratinocytes were then incubated in this media for a minimum of 18 hours to carry out siRNA knockdown. The siRNAs used in this study are as follows: Control siRNA (Ambion Silencer Select negative control 4390844), KLF3 siRNA1 (Ambion Silencer Select s229899), KLF3 siRNA 2 (Ambion Silencer Select s229898), KLF4 siRNA (Dharmacon:custom sequence), CBP siRNA (Dharmacon D-003477-21), P300 siRNA (Dharmacon D-003486-02). siRNA sequences can be found in the supplemental materials.

Regenerated human epidermis

Human dermis obtained from the New York Firefighters skin bank was devitalized, cut, and placed upon a cassette. The bottom of the dermis was coated in matrigel and the cassette was placed in KGM media, with the bottom of the dermis contacting the media and the top at the air interface. One million keratinocytes were then seeded on the top of the dermis and allowed to regenerate and stratify for five days. The constructs were then harvested for RNA or embedded in OCT for sectioning and staining. Additional details for regenerating human epidermis have been previously described [24,41,43].

Immunofluorescent staining

Sectioned tissue derived from human skin biopsies or regenerated human epidermis was fixed with 10% formalin solution (Sigma HT5012) for 12 minutes. Sections were blocked (PBS, 2% bovine serum albumin, 2.5% normal goat serum, and 0.3% triton X-100) for 30 minutes. Primary antibodies were then added to blocking buffer and put onto sections for 1 hour. The following antibodies were used at the following concentrations: KLF3 at 1:300 (Sigma HPA049512), KRT10 at 1:400 (ThermoFisher MS-611-P0), P63(Rb) at 1:600 (Abcam ab124762), P63(ms) at 1:600 (Biolegend 687204), FLG at 1:200 (Abcam ab3137), and LOR at 1:400 (Abcam ab198994). Secondary antibodies were used at 1:500 for 30 minutes and included Alexa Fluor 555 goat anti-mouse IgG (ThermoFisher: A21424) and Alexa Fluor 488 donkey anti-rabbit IgG (ThermoFisher: A21206). Hoechst 33342 (ThermoFisher H3570) was used at 1:1000 to stain nuclei.

RNA extraction and analysis by RT-qPCR

The GeneJET RNA purification kit (Thermo Scientific K0732) was used to extract RNA from cultured keratinocytes. RNA concentration for each sample was measured by nanodrop and 1μg of RNA was used for generating cDNA. This cDNA was generated using the Maxima cDNA synthesis kit (Thermo Fisher: K1642). qPCR was performed using this cDNA on the Roche 480 Light Cycler. The house-keeping genes L32 or GAPDH were used for normalization of signal. Primer sequences for all genes tested are listed in the supplementary materials.

Western blotting

IP samples or 20-80ug of cell lysates were loaded into 4-12% Bis-Tris (ThermoFisher NW04122BOX) or 3-8% Tris-acetate (ThermoFisher EA03752BOX) and transferred to PVDF membranes. Membranes were blocked in 5% BSA in TBS. Membranes were exposed to primary antibodies in blocking buffer overnight at 4 degrees. The following primary antibodies were used: KLF3 at 1:1000 (Sigma HPA049512), CBP at 1:1000 (Cell Signaling D6C5 #7389). The loading controls Beta-Actin (Santa Cruz sc-47778) and Beta-Tubulin (Santa Cruz sc-9104) were used at 1:5000. The secondary antibodies used were donkey anti-rabbit IRDye 680RD (Li-Cor 926-68073) and donkey anti-mouse IRDye 800CW (Li-Cor 926-32212) at 1:5000.

RNA sequencing and bioinformatic analysis

RNA isolated from day 3 differentiated keratinocytes was used for sequencing. Samples were sequenced by the Institute of Genomic Medicine core facility at UCSD on the Illumina Hi Seq

4000. Reads were aligned to the hg19 genome build using STAR with default settings. Identification of differential gene expression and downstream analysis was carried out using Partek Genomic Suite (Partek Incorporated, http://www. partek.com/partek-genomics-suite). Differential expression between control and knockdown samples was analyzed using ANOVA. Genes with fewer than ten reads among all samples were filtered out before analysis to avoid genes with low expression. Differentially expressed genes were selected by > 2-fold change (+/-) compared to controls and a significant p-value with FDR (< 0.05). Heatmaps representing RNA sequencing data were generated in Partek Genomic Suite. GO terms for selected gene lists were generated using Metascape [65]. DeepTools was used to RPKM normalize sequencing files and generate Pearson correlations and the representative heatmaps of these values [66,67]. Nemates.org was used to calculate the p-value of gene list overlaps: (http://nemates.org/MA/progs/overlap_stats.html). The number of refence genes used was 25000.

ChIP sequencing and bioinformatic analysis

For each pulldown, 20 million keratinocytes were differentiated for 3 days and subsequently crosslinked. These cells were crosslinked using 2mM DSG (disuccinimidyl glutarate, Thermo Fisher 20593) and 1% formaldehyde (ThermoFisher 28908). Cells were placed in Farnham lysis buffer (5 mM PIPES pH 8.0, 85 mM KCl, 0.5% IGEPAL CA-630) and sheared with a syringe. The cells were then pelleted and resuspended in SDS-Lysis Buffer (1% SDS, 10 mM EDTA, 50 mM Tris, pH 8.0) and sonicated in a water bath sonicator. Sonicated lysate was then centrifuged, and the supernatant was diluted 1:10 in low ionic strength ChIP dilution buffer (50mM NaCl,

10mM HEPES, pH 7.4, 1% IGEPAL CA-630, 10% Glycerol) and used for ChIP. 5ug of KLF3 antibody (Sigma HPA049512) was used for each pulldown and 20ul of CBP antibody (Cell Signaling D6C5 #7389) was used per pulldown. Antibody/lysate incubation was carried out at 4 degrees overnight. 50ul of Protein-G dynabeads were added to each solution of antibody/lysate the following day and incubated for 4 hours at 4 degrees. The beads were then washed twice with low ionic strength buffer, once with high salt wash buffer (500 mM NaCl, 0.1% SDS, 1% IGEPAL CA-630, 2 mM EDTA, 20 mM Tris, pH 8.0), once with LiCl wash (0.25 M LiCl, 1% IGEPAL CA-630, 1% Sodium Deoxycholate, 1 mM EDTA 10 mM Tris-Hcl, pH 8.0), and twice with TE (10 mM Tris-Cl, pH 7.5, 1 mM EDTA). Samples were then eluted at 65 degrees in elution buffer (0.09 M $NaHCO_3$, 1% SDS, 0.1 M $NaHCO_3$) and de-crosslinking mixture (0.2 M NaCl, 0.1M EDTA,0.4 M Tris-HCl, pH6.8, 0.4 mg/ml proteinase K) and treated with RNAse A to prevent RNA contamination during sequencing [43,51]. Samples were sequenced in replicate by the Institute of Genomic Medicine core facility at UCSD on the Illumina Hi Seq 4000. Sequenced reads were trimmed and aligned to the genome build hg19 using BowTie 2 [68]. Duplicate and low-quality reads were removed. To identify peaks, HOMER's findPeaks was used with default statistical settings (p-value < 0.0001, FDR < 0.001, 4x enrichment vs. input) and the following options: for KLF3, CBP, KLF4, ZNF750, MAF, MAFB, and GRHL3: style=factor, minDist 200; for H3K27ac and H3K4me: style=region, size=1000, minDist=2500) to identify significant peaks[69]. Input sample was used as background in peak calling. Genomic localization was annotated using HOMER's annotatePeaks (Refseq hg19 transcription start sites)[69]. HOMER was also used to identify motifs (findMotifsGenome), create UCSC tracks

(makeUCSCfile) to be visualized on the UCSC genome browser, and generate normalized mean density plots (annotatePeaks). mergePeaks was used to identify directly overlapping (d=given) peaks between samples. DeepTools was used to RPKM normalize sequencing files and generate Pearson correlations and the representative heatmaps of these values[66,67]. Diffreps 1.55.4 was used to identify differential enrichment between control and knockdown sequencing samples (negative binomial test, scanning window size of 1000 bp, step size of 100 bp, and a cutoff p-value of 0.0001)[50]. GO terms for selected gene lists were generated using Metascape [65]. Nemates.org was used to calculate the p-value of gene list overlaps: (http://nemates.org/MA/progs/overlap_stats.html). The number of reference genes used was 25000.

Co-immunoprecipitation

Differentiated keratinocytes were harvested in IP lysis buffer (25 mM Tris-HCl pH 7.4, 150 mM NaCl, 1 mM EDTA, 1% NP-40 and 5% glycerol) and sheared with a syringe. 5ug of KLF3 antibody (Sigma HPA049512) or control rabbit IgG (Millipore 12-370) was conjugated to 50ul of Protein G dynabeads (Life Technologies 10004D) for 30 minutes at room temperature. Lysis buffer was diluted to 1ml per sample and was added to the antibody conjugated beads and incubated overnight at 4 degrees. The following day the beads were washed with IP lysis buffer and boiled in RIPA buffer (25 mM Tris-HCl (pH 7.6), 150 mM NaCl, 1% NP-40, 1% sodium deoxycholate, 0.1% SDS) supplemented with NuPAGE LDS Sample Buffer (Life Technologies: NP0008) to elute. Samples were then loaded for western blotting.

Statistics

Statistical analyses were performed using GraphPad Prism. Histogram data are presented as the mean ± SD and the significance of differences between samples was determined by student's t tests.

Acknowledgments

Chapter 1 is based on material currently in review: Jackson Jones, Yifang Chen, Manisha Tiwari, Jingting Li, Ji Ling, and George L. Sen. KLF3 mediates epidermal differentiation through the epigenomic writer CBP. *In Review: iScience.* 2020. I am the primary author and researcher for this manuscript. The co-authors listed above either supervised or provided support for the research and have given permission for the inclusion of the work in this dissertation.

Conflicts of Interest

The authors have no conflicts of interest.

CHAPTER 2 : BRD4 IS NECESSARY FOR DIFFERENTIATION DOWNSTREAM OF EPIDERMAL LINEAGE-DETERMINING TRANSCRIPTION FACTORS

Abstract

Bromodomain-containing protein 4 (BRD4) is an epigenomic reader that has been implicated in the regulation of multiple cell differentiation processes. Through its bromodomains, BRD4 has an affinity for binding acetylated lysine groups on both histones and other proteins such as transcription factors. Due to this affinity, BRD4 can localize to active chromatin regions rich in H3K27ac, and subsequently recruit the transcriptional machinery necessary for differentiation gene transcription. Lineage-determining transcription factors, as well as epigenomic writers, such as CBP, have been implicated in the recruitment of BRD4 to enhancer and promoter regions to allow for downstream transcription mediated by BRD4, thus making BRD4 necessary for the transcriptional output associated with these factors. While this model has been demonstrated in other cell differentiation contexts, the role of BRD4 in epidermal differentiation and its relationship with skin LDTFs and epigenomic writers remains unclear. Here, we show that BRD4 is necessary for epidermal differentiation and functionally overlaps with epidermal LDTFs such as KLF3 and KLF4. In addition, BRD4's transcriptional regulation program is more closely related to that of CBP than P300, further suggesting CBP's importance during epidermal differentiation. KLF3 knockdown is able to destabilize BRD4 localization at active enhancers proximal to epidermal differentiation genes, and these destabilization events often occurred in regions where CBP was also reduced. Together, this data

suggests that BRD4 acts downstream of epidermal LDTFs such as KLF3 to allow for proper differentiation gene expression.

Introduction

It has been previously demonstrated in multiple differentiation contexts that LDTFs can contribute to the recruitment of epigenomic writers such as CBP and P300 to enhancer and promoter regions and subsequently epigenomic readers that recruit transcriptional machinery to promote differentiation gene expression [70,71]. Our work in Chapter 1 demonstrated that KLF3 is a novel LDTF of the epidermis that is required for differentiation, and this transcriptional control is in part reliant on the recruitment of the epigenomic writer CBP to active enhancer regions near differentiation genes. Based on this model, we sought to identify an epigenomic reader that works downstream of epidermal LDTFs, including KLF3, allowing for the functional output of their transcriptional control.

BRD4 (Bromodomain-containing protein 4) belongs to the bromodomain and extra-terminal domain (BET) family and utilizes its bromodomains to bind to acetylated lysine groups on both histones (i.e. H3K27ac) and transcription factors. However, it can also bind to TFs in a bromodomain-independent fashion. BRD4 has been shown to bind active promoters and enhancers to promote gene transcription at the initiation and elongation steps by recruiting transcription associated proteins such as P-TEFb [70-72]. It has recently been shown in acute myeloid leukemia cells that BRD4 works downstream of hematopoietic LDTFs to promote their transcriptional programs [71]. It was demonstrated that BRD4 genomic localization correlates with

that of hematopoietic transcription factors at active chromatin regions. In addition, BRD4 localization at these sites was found to be dependent on these transcription factors, as well as the epigenomic writers CBP and P300, which provide acetylation activity at H3K4me positive regions. Inhibition of BET protein bromodomain activity by the chemical inhibitor JQ1 was found to suppress the functional output of hematopoietic transcription factors, demonstrating the need for BET protein activity, such as that of BRD4, downstream of TFs.

A more recent study in murine cells demonstrated that Brd4 is necessary for Pol II binding at active enhancers and thus differentiation gene induction during adipogenesis and myogenesis [70]. Similarly, in these cellular contexts the authors demonstrate that LDTFs and epigenomic writers (such as the methyltransferases MLL3/MLL4 as well as CBP and P300) coordinate to promote Brd4 localization at active enhancers associated with cell identity genes. In cells knocked-out for Brd4, cell differentiation is impaired and enhancer RNA production is inhibited. Together these studies propose a model where LDTFs and epigenomic writers facilitate BRD4 localization at active chromatin regions, and BRD4 subsequently recruits the transcriptional machinery necessary to induce differentiation gene expression.

Based on these findings, we hypothesized that BRD4 functions similarly downstream of epidermal LDTFs at active chromatin regions during epidermal differentiation, allowing for the functional control of differentiation gene expression by these LDTFs, including KLF3. Indeed, we found that BRD4 is necessary for epidermal differentiation and its genomic localization correlates with active chromatin regions as well as epidermal LDTFs. In addition, BRD4 transcriptional control correlates with the epidermal LDTFs KLF3 and KLF4. Knockdown of

KLF3 results in the reduction of BRD4 binding at active chromatin regions, and in particular active enhancers, proximally to epidermal differentiation genes. Furthermore, many of these reductions coincided with regions of CBP signal reduction. Together, this data provides a model where epidermal LDTFs such as KLF3 rely on BRD4 activity at active enhancers to promote differentiation gene expression.

Results

BRD4 is necessary for keratinocyte differentiation

To determine if BRD4 is necessary for differentiation gene expression, keratinocytes were treated with scrambled control (CTLi) or BRD4 targeting (BRD4i) siRNA and cultured in differentiation conditions for three days. Two distinct siRNAs targeting different regions of BRD4 were used to ensure the phenotype seen was not the result of off-target siRNA effects. Knockdown of BRD4 resulted in a significant reduction in critical differentiation genes such as *K1*, *K10*, *LOR*, *FLG*, and *SPRR3* (Figure 2.1A). In regenerated human epidermis, BRD4 depletion resulted in the loss of K10 protein expression but did not impact K5 levels (Supplementary Figure 2.1A). Knockdown of BRD4 blocked terminal epidermal differentiation as evidenced by the reduction in stratum corneum formation and loss of structural proteins such as FLG and LOR on the mRNA and protein level (Figure 2.1B-C, Supplementary Figure 2.1B). To characterize the BRD4 knockdown phenotype on a genome wide transcriptional level, RNA sequencing (RNA-Seq) was performed on replicate control and BRD4 knockdown samples cultured in differentiation conditions for three days. Analysis of BRD4 knockdown associated

differential gene expression (≥2 fold change vs. CTLi and *FDR* ≤ 0.05) revealed 1,791 genes with decreased expression and 840 genes with increased expression (Figure 2.1D). More than twice the number of genes was downregulated upon BRD4 depletion than upregulated which supports the role of BRD4 as a transcriptional activator. Gene ontology (GO) analysis of the 1,791 decreased genes revealed a significant enrichment for differentiation related terms, such as *skin development* and *metabolism of lipids* (Figure 2.1E). Analysis of the 840 increased genes revealed terms related to *cell division*, as well as immune system functions (Figure 2.1F). Together, these data suggest that BRD4 is necessary for promoting epidermal differentiation gene expression while suppressing cell cycle and immune response genes.

Characterization of BRD4's genomic localization

To characterize the genomic localization of BRD4, we performed chromatin immunoprecipitation followed by high throughput sequencing (ChIP-Seq) for BRD4 in differentiated keratinocytes (day 3). ChIP-Seq was performed on replicate BRD4 pulldowns and analysis was done using HOMER [69]. 17,569 BRD4 peaks were identified which were primarily located in intronic (32%), intergenic (26%), and promoter (29%) regions (Figure 2.2A). Validation of these results by BRD4 ChIP followed by QPCR showed high enrichment for BRD4 at the bound sites whereas no binding was seen with IgG control pulldowns (Supplementary Figure 2.2A). Since BRD4 is primarily known as a transcriptional activator that binds to enhancers and promoters, we wanted to explore which genes are dependent upon BRD4 for expression[70,71]. Thus, we mapped back the 17,569 BRD4 peaks to its nearest genes which

resulted in the identification of 11,280 genes (Figure 2.2B). We overlapped the genes that BRD4 are bound with those genes decreased in expression upon BRD4 knockdown (Figure 2.2B). Importantly, ~70% (1,053/1,791) of the genes downregulated upon BRD4 knockdown were found to have a proximal BRD4 peak, and these genes were enriched for GO terms related to differentiation such as *epidermis development* and *metabolism of lipids* (Figure 2.2B-C). To gain insight into the types of genomic regions BRD4 is binding, we used the ENCODE ChIP-Seq data set as well as previously published data for human keratinocytes for a variety of histone marks [27,40,73]. These marks included repressive marks H3K27me3 and H3K9me3 (undifferentiated keratinocytes), as well as H3K4me (day 1 of differentiation, representing primed regions of DNA upon differentiation) and H3K27ac (day 3 differentiation, marking open chromatin in the differentiated state) [27,40,73]. Mapping of these histone marks to the 17,569 BRD4 bound peaks showed high enrichment for H3K27ac, as well as H3K4me (Supplementary Figure 2.2B). This correlates with the binding affinity of BRD4 to acetylated lysines and its activity as a transcriptional activator. In contrast, the repressive marks of H3K27me3/H3K9me3 had no enrichment at BRD4 regions (Supplementary Figure 2.2B). This relationship between BRD4 and the various histone marks was confirmed by generating Pearson correlation coefficients between the various sequencing experiments, with H3K27ac having the highest correlation with BRD4 (avg=0.74) (Supplementary Figure 2.2C). Due to the high enrichment of H3K27ac and H3K4me at BRD4 bound sites, we wanted to characterize how many of these regions were active enhancers or active promoters.

Figure 2.1. BRD4 is necessary for epidermal differentiation gene expression.
(A) RT-qPCR quantifying the relative mRNA expression levels of a panel of epidermal differentiation genes in scrambled control (CTLi) and BRD4 (BRD4i) siRNA treated keratinocytes after three days of differentiation. Two separate siRNAs (siRNA 1 and siRNA 2) targeting different regions of BRD4 mRNA were used (siRNA 1 n=4, siRNA 2 n=3). Statistics: t-test, ***$p < 0.001$. (B) RT-qPCR quantifying the relative mRNA expression levels of *LOR, BRD4,* and *FLG* in CTLi and BRD4i day 5 regenerated human epidermis. n=5 (C) Immunofluorescent staining of late differentiation markers LOR (green) and FLG (red) in CTLi and BRD4i day 5 regenerated human epidermis. Merged image includes Hoechst staining of nuclei. n=3. White Scale bar = 20μm. (D) Heatmap generated for replicate (n=2) RPKM normalized RNA-Sequencing data from CTLi and BRD4i keratinocytes differentiated for 3 days. The expression of genes significantly increased (red) or decreased (blue) is shown. Differential expression was determined with FDR ≤ 0.05 and fold change ≥ 2 vs. CTLi. Graphs are displayed in log2 scale. (E) Gene ontology (GO) term enrichment for the 1,791 genes significantly decreased in BRD4 knockdown cells. (F) Gene ontology (GO) term enrichment for the 840 genes significantly increased in expression in BRD4 knockdown cells.

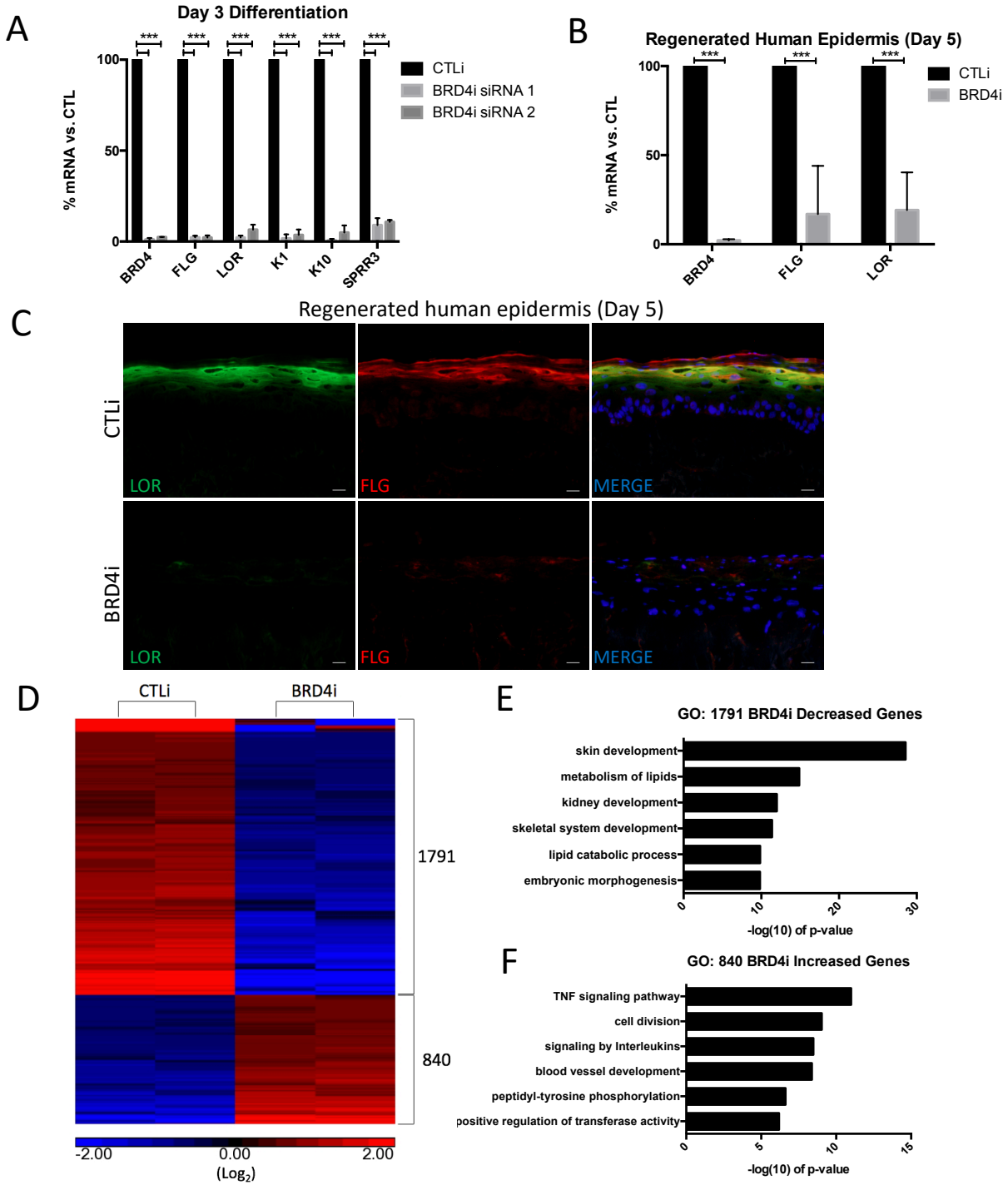
A
Day 3 Differentiation
% mRNA vs. CTL
100
50
0
***
BRD4
FLG
LOR
K1
K10
SPRR3
CTLi
BRD4i siRNA 1
BRD4i siRNA 2
B
Regenerated Human Epidermis (Day 5)
% mRNA vs. CTL
BRD4
FLG
LOR
CTLi
BRD4i
C
Regenerated human epidermis (Day 5)
CTLi
BRD4i
LOR
FLG
MERGE
D
CTLi
BRD4i
1791
840
-2.00
0.00
2.00
(Log2)
E
GO: 1791 BRD4i Decreased Genes
skin development
metabolism of lipids
kidney development
skeletal system development
lipid catabolic process
embryonic morphogenesis
0
10
20
30
-log(10) of p-value
F
GO: 840 BRD4i Increased Genes
TNF signaling pathway
cell division
signaling by Interleukins
blood vessel development
peptidyl-tyrosine phosphorylation
positive regulation of transferase activity
0
5
10
15
-log(10) of p-value

We found 11,832 regions of BRD4 co-localization with both H3K27ac and H3K4me (Supplementary Figure 2.2D). Most of these regions are active enhancers (82%) while a smaller portion are active promoters (18%) (Supplementary Figure 2.2D). These co-bound regions were mapped to the nearest genes and compared to genes decreased in the BRD4 knockdown. 42.2% (756/1,791) of BRD4i decreased genes were found to have proximal BRD4 bound active enhancer(s) which were highly enriched for the GO term *epidermis development* (Supplementary Figure 2.2E). 11.2% (200/1,791) of the genes decreased in the BRD4i cells had an active promoter bound by BRD4 and were enriched for the GO terms *metabolism of lipids* and *regulation of epidermis development* (Supplementary Figure 2.2F). This suggests that BRD4 may be regulating differentiation through both active enhancers and promoters.

BRD4 co-localizes with epidermal LDTFs

Next, we sought to investigate the relationship between BRD4 and LDTFs of the skin. Motif enrichment analysis of the 17,569 BRD4 peaks revealed an association with families of transcription factors known to regulate epidermal differentiation, such as AP1, ETS, CEBP, and KLF, suggesting that BRD4 may share binding regions with these factors (Figure 2.2D). Based on this data, we used previously generated ChIP-Seq data sets for LDTFs of the skin including KLF4, ZNF750, MAF, MAFB, and GRHL3 to compare to BRD4 [14,26,27]. All of these factors were found to have signal enrichment at BRD4 binding sites, with KLF4, ZNF750, and MAFB having the most enrichment (Figure 2.2E).

Figure 2.2. BRD4 shares similar genomic binding profiles with epidermal LDTFs
(A) Genomic localization of the 17,569 BRD4 peaks identified by HOMER. BRD4 ChIP sequencing was performed in replicates (n=2) from day 3 differentiated keratinocytes. (B) Venn diagram showing the number of genes (1,053) decreased in the BRD4 knockdown that also have an associated BRD4 peak. (C) Gene ontology (GO) term enrichment for the 1,053 genes that are decreased in the BRD4 knockdown and have an associated BRD4 peak. (D) *de novo* motif enrichments and the associated family of transcription factors identified within the 17,569 BRD4 peaks. (E) Mean density profile displaying epidermal LDTF ChIP-Seq profiles (KLF4: red, ZNF750: green, MAFB: orange, MAF: yellow, GRHL3: purple) centered around BRD4 peaks (blue). The 17,569 BRD4 peaks were used as the reference coordinates and the profiles are displayed +/- 5kb from the BRD4 peak centers. (F) Heatmap plot of Pearson correlation coefficients between replicate BRD4 ChIP-Seq data sets and epidermal LDTF ChIP-Seq data sets (RPKM normalized). (G) Table displaying the peak overlap statistics between BRD4 and epidermal LDTFs. Each LDTFs total bound peak numbers identified by HOMER are shown with the number and percentage of overlap with BRD4 peaks. (H) UCSC genome browser track displaying BRD4 (blue), KLF4 (red), ZNF750 (pink), H3K27ac (maroon), and H3K4me (green) ChIP-Seq profiles near IVL and a cluster of SPRR differentiation genes.

A

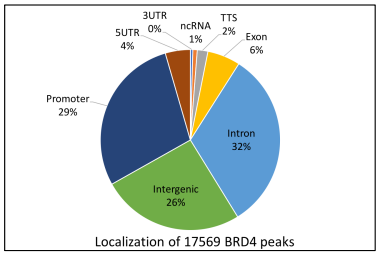

B

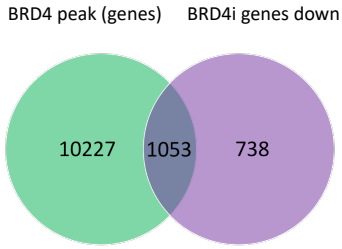

C

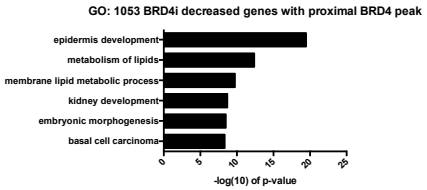

D

BRD4 de novo motif	Associated family	p-value
	AP-1	1e-124
	ETS	1e-107
	YY1	1e-75
	CEBP	1e-68
	TEAD	1e-38
	ATF	1e-37
	KLF	1e-26

E

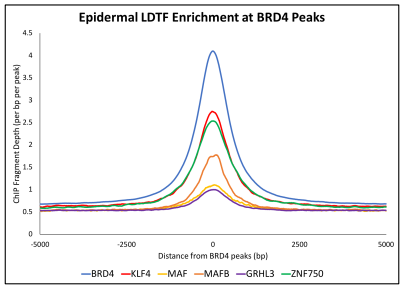

F

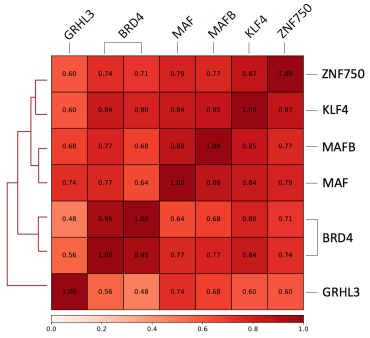

G

ChIP	Total Peaks	Shared Regions with BRD4	% of TF peaks	% of BRD4 peaks
KLF4	43408	11002	25.3	62.6
ZNF750	53922	9808	18.2	55.8
MAFB	6489	3965	60.2	22.6
MAF	3521	1152	32.8	6.6
GRHL3	4383	452	10.3	2.6

H

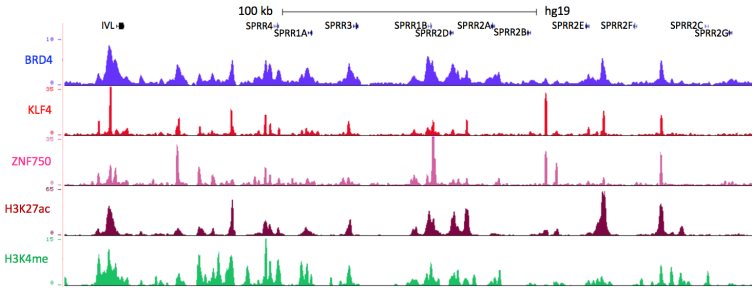

Analysis of the total peak overlap between BRD4 and the LDTFs also revealed a substantial overlap with KLF4 and ZNF750 (62.6% and 55.8% of BRD4 peaks, respectively) (Figure 2.2G). Visualization of BRD4 with KLF4 and ZNF750 showed substantial co-localization at active enhancer and promoter regions proximal to *IVL*, *DSG1*, *DSC1*, and the *SPRR* and keratin family of epidermal differentiation genes (Figure 2.2H, Supplementary Figure 2.2G-H).

BRD4 functionally overlaps with the epidermal LDTF KLF4

Since the genomic binding of KLF4 and BRD4 were the most similar to each other, we decided to knockdown KLF4 and perform RNA-Seq. 772 genes were downregulated upon KLF4 depletion which were enriched for epidermal differentiation related GO terms (Supplementary Figure 2.3A-B). 1,265 genes were increased upon KLF4 knockdown which were cell cycle and proliferation related (Supplementary Figure 2.3A,C). Comparison of the transcriptome between BRD4 and KLF4 showed positive Pearson correlation (avg=0.70) (Supplementary Figure 2.3D). ~60% (461/772) of the genes downregulated upon KLF4 depletion was also decreased in BRD4i cells (Supplementary Figure 2.3E). These genes are enriched for a variety of terms related to skin differentiation (Supplementary Figure 2.3F). 16.4% (208/1,265) of genes increased in the KLF4i cells were also upregulated in the BRD4i dataset which were enriched for proliferation related GO terms (Supplemental Figure 2.3G-H). It is also worth noting that the number of genes dependent on BRD4 (1,791) for expression is much greater than KLF4 (772). This could possibly be due to BRD4 being necessary to activate the genes of other epidermal LDTFs such as

ZNF750, MAFB, and MAF. Thus, loss of BRD4 may be similar to loss of multiple epidermal LDTFs simultaneously.

BRD4 and KLF3 have shared transcriptional control and genomic localization

As we have demonstrated that BRD4 and KLF4 have shared transcriptional regulation and genomic localization, we sought to determine if KLF3 also has these associations with BRD4. Pearson correlations of the BRD4i RNA-Seq data set was compared with KLF3i, KLF4i, CBPi, and P300i data sets. While BRD4i data sets had positive correlations with all of the other data sets, it had the highest correlation with the KLF3i and KLF4i data sets, while also being more similar to CBPi than P300i. P300i correlated with the other factors the least (Figure 2.3A). To confirm the similarity between the BRD4i and KLF3i data sets, a gene expression heatmap based on unsupervised hierarchical clustering was generated using KLF3 knockdown responsive genes as a reference. While the KLF3 knockdown once again clustered most closely with the KLF4 and CBP knockdowns, these datasets all clustered and showed similarity with the BRD4 knockdown (Figure 2.3B). Interestingly, BRD4 knockdown correlated more closely with CBP knockdown than P300 knockdown, suggesting that BRD4 activity may be more dependent on CBP in this system. To determine the number and types of genes commonly regulated by KLF3 and BRD4, both the downregulated and upregulated genes from both data sets were overlapped with each other. While BRD4i had many uniquely downregulated genes, likely due to its importance for transcriptional output downstream of a large group of epidermal LDTFs, more than half (355/563, or 63.1%) of the KLF3i downregulated genes were also downregulated in the

BRD4i dataset (Figure 2.3C). These 355 genes were highly enriched for GO terms related to skin differentiation, such as formation of the *cornified envelope*, *water homeostasis*, and *metabolism of lipids* (Figure 2.3D). This substantial co-regulation of a large group of epidermal differentiation genes suggests that BRD4 may act in coordination with KLF3 to promote differentiation gene transcription, as it seems to with KLF4. On the other hand, when comparing the genes that are upregulated in the KLF3i and BRD4i datasets, a much smaller percentage (74/423, or 17.5%) of the KLF3i genes overlap with the BRD4i dataset and primarily enrich for terms related to the cell cycle (Supplemental Figure 2.4A-B). This suggests that KLF3's suppression of gene expression is primarily independent of BRD4.

Due to the similarities between KLF3 and BRD4 transcriptional regulation during differentiation, we wanted to investigate how extensively these factors share genomic binding sites. Thus, ChIP sequencing from both KLF3 and BRD4 pulldowns were compared. To visualize if BRD4 may co-localize at KLF3 peak locations, signal from the BRD4 ChIP dataset was plotted using KLF3 peak locations as a reference (Figure 2.3E). This revealed substantial read densities for BRD4 concentrated at KLF3 bound regions. To confirm this co-localization, called peak locations for these data sets were compared and the number of shared regions was reported. In total, 10468 (59.6%) of BRD4 bound regions directly overlapped with a KLF3 bound region, confirming a high rate of genomic co-localization between KLF3 and BRD4. Visualization of the KLF3, CBP, and BRD4 ChIP-sequencing profiles show common binding to enhancer elements, such as those proximal to KRT80, IVL, and SPRR4 (Figure 2.3F,

Supplemental Figure 2.4D). Together, these data show that KLF3 and BRD4 share a significant transcriptional regulation of differentiation genes as well as a variety of genomic binding sites.

KLF3 knockdown alters BRD4 localization during epidermal differentiation

We previously showed that KLF3 knockdown can de-stabilized CBP localization to differentiation-relevant sites. As it has been shown that LDTFs can promote the localization of CBP and subsequently BRD4 at active chromatin regions to promote differentiation gene expression, we sought to investigate whether KLF3 knockdown can alter BRD4 localization during epidermal differentiation[70,71].

We knocked keratinocytes down for KLF3, differentiated them for 3 days, and performed ChIP sequencing experiments BRD4 to see if its localization at active chromatin regions is affected. In order to rule out that ChIP signal differences in the knockdown samples could be due to changes in BRD4 protein levels, we performed a western blot for BRD4 in control and KLF3 knockdown samples demonstrating that the protein levels are unchanged (Supplemental Figure 2.5A). Analysis of differential ChIP signal enrichment between CTLi and KLF3i BRD4 pulldowns revealed 2691 regions of significant BRD4 signal reduction in the KLF3 knockdown condition (Figure 2.4A). A total of 1056 (39.2%) of these events occurred at KLF3 peak locations, and 881 (32.7%) occurred at KLF3 bound, active (H3K27ac/H3K4me+) chromatin regions. Conversely, KLF3 knockdown resulted in 2036 BRD4 signal enrichment events (Supplemental Figure 2.5B). Unlike what is seen with areas of CBP enrichment, a high percentage of BRD4 enrichment sites overlap KLF3 peaks (899/2036, or 44.2%).

Figure 2.3. BRD4 and KLF3 transcriptional programs and genomic localization functionally overlap

(A) Heatmap plot of Pearson correlation coefficients comparing replicate KLF3i, KLF4i, CBPi, P300i and BRD4i RNA sequencing data sets (RPKM normalized). (B) Unsupervised hierarchical clustering was performed on the RPKM normalized RNA-Sequencing data sets for CTLi, KLF3i, KLF4i, BRD4i, CBPi, and P300i keratinocytes differentiated for 3 days (log2 scale). Heatmap is focused on KLF3 regulated genes. Increased genes are displayed in red, while decreased genes are shown in blue. (C-D) Venn diagram showing the number of genes (355) decreased in both the BRD4 and KLF3 knockdowns and the associated GO term enrichments for the 355 genes. (E) Mean density profile displaying BRD4 genomic binding centered around KFL3 peaks. The 25,352 KLF3 peaks were used as the reference and the profile of BRD4 binding is displayed +/- 5kb from the KLF3 peak centers. (F) UCSC genome browser tracks displaying KLF3 (red), CBP (gray), and BRD4 (blue) ChIP Seq profiles near KRT80. H3K27ac (maroon) and H3K4me (green) are included to represent open and active chromatin.

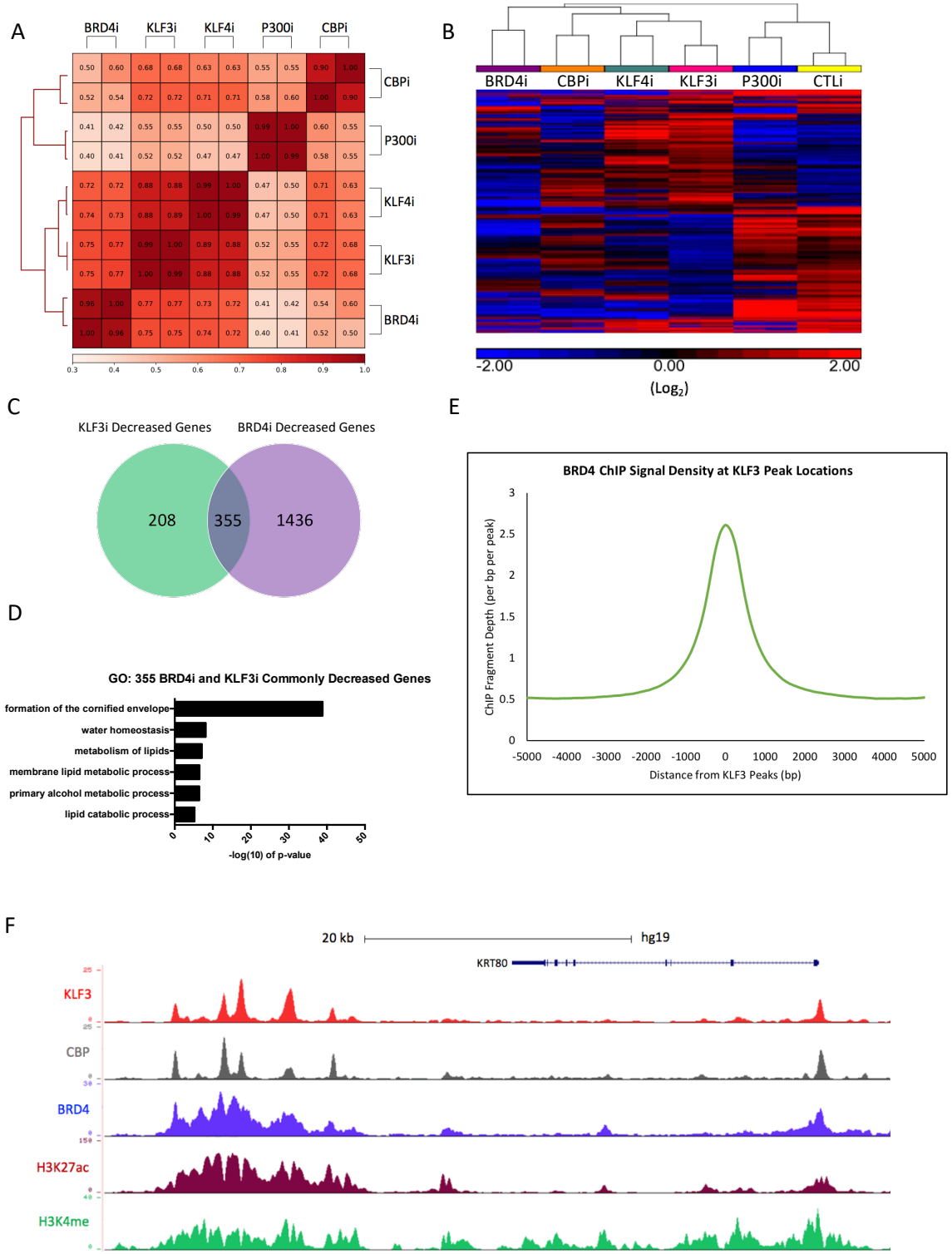
A
BRD4i
KLF3i
KLF4i
P300i
CBPi
B
BRD4i
CBPi
KLF4i
KLF3i
P300i
CTLi
-2.00
0.00
2.00
(Log2)
C
KLF3i Decreased Genes
BRD4i Decreased Genes
208
355
1436
D
GO: 355 BRD4i and KLF3i Commonly Decreased Genes
formation of the cornified envelope
water homeostasis
metabolism of lipids
membrane lipid metabolic process
primary alcohol metabolic process
lipid catabolic process
-log(10) of p-value
E
BRD4 ChIP Signal Density at KLF3 Peak Locations
ChIP Fragment Depth (per bp per peak)
Distance from KLF3 Peaks (bp)
F
20 kb
hg19
KRT80
KLF3
CBP
BRD4
H3K27ac
H3K4me

This suggests that while KLF3 is necessary for BRD4 localization at many sites, it may also inhibit BRD4 localization at others, performing a dual function of promoting/inhibiting gene expression based on context.

As KLF3 and BRD4 primarily share a transcriptional program related to the promotion of gene expression, we sought to further explore the regions of BRD4 signal reduction upon KLF3 knockdown. First, we confirmed BRD4 signal reduction at the 881 KLF3 bound active chromatin regions by using the 881 sites as reference loci to plot BRD4 ChIP read densities from both CTLi and KLF3i conditions (Figure 2.4B). Indeed, the average BRD4 signal was reduced at these regions in the KLF3 knockdown condition. Based on this loss of BRD4 at KLF3 bound active chromatin regions, we wanted to explore whether these reductions are primarily occurring at enhancer or promoter regions. The 881 KLF3/H3K27ac/H3K4me bound regions that lost BRD4 signal in the KLF3 knockdown condition were mapped to the most proximal genes and the localization of these events was determined (Figure 2.4C). We found that a low percentage of BRD4 reduction events occur at promoter regions (13%), while the majority of events occurred in enhancer regions (87%). This suggests that the KLF3 dependent localization of BRD4 occurs primarily at active enhancer regions, and less so at active promoters, following a similar trend as KLF3i associated CBP signal reduction events. Mapping the 881 regions of BRD4 reduction to proximal genes revealed 112 genes with associated BRD4 reductions at promoters, while 692 genes have proximal enhancer reductions of BRD4. Gene ontology analysis was performed on both these sets of genes and revealed that the enhancer associated data set is enriched for terms related to terminal differentiation and barrier formation, such as *endomembrane system*

organization, *plasma membrane organization*, and *metabolism of lipids*, while the genes with promoter associated BRD4 reductions do not enrich for such terms (Figure 2.4D-E). This suggests that similarly to CBP, KLF3 is primarily necessary for BRD4 localization at active enhancers, and these enhancers occur proximally to epidermal differentiation genes. As both LDTFs and CBP have been shown to be involved in promoting BRD4 localization, we wanted to investigate if both CBP and BRD4 reductions associated with KLF3 knockdown occur in common genomic loci. Comparison of the 612 CBP and 881 BRD4 binding reduction events at KLF3 bound active regions revealed 284 common regions of reduction (46.4% of CBP events, 32.2% of BRD4 events) (Figure 2.4F). Analysis of the distribution of these events revealed that 91% of CBP and BRD4 co-reductions associated with KLF3 knockdown occur at enhancer regions, while only 9% occur at promoter regions, once again suggesting that KLF3's role in CBP and BRD4 recruitment is primarily enhancer associated (Figure 2.4G). Gene ontology analysis of this gene list revealed terms related to epidermal differentiation, such as *epidermis development* and *plasma membrane organization* (Supplemental Figure 2.5C). Visualization of the CBP and BRD4 ChIP sequencing profiles in CTLi and KLF3i conditions confirmed a common reduction in both CBP and BRD4 signal at enhancers proximal to differentiation genes such as IVL and LOR (Figure 2.4H, Supplemental Figure 2.5D). Together, these data show that KLF3 is necessary for both CBP and BRD4 localization at a variety of enhancers proximal to epidermal differentiation genes. While KLF3 may directly regulate some genes, this suggests that the functional overlap of KLF3's transcriptional regulation of differentiation genes with that

Figure 2.4. KLF3 knockdown alters BRD4 localization during epidermal differentiation. (A) Summary of significant BRD4 ChIP signal reduction events in day 3 differentiated keratinocytes knocked down for KLF3. The orange circle represents the total number of regions in the genome that lose BRD4 binding upon KLF3 knockdown. The green circle represents the number of regions that lose BRD4 binding that occur at a KLF3 peak upon KLF3 depletion. The blue circle represents the regions that lose BRD4 binding and also contain KLF3, H3K4me, and H3K27ac binding. BRD4 ChIP Seq was performed in replicates in CTLi and KLF3i cells. Significant signal changes were identified by Diffreps. (B) Mean density profile displaying BRD4 binding centered around KLF3/H3K4me/H3K27ac peaks. The BRD4 mean density is plotted around the 881regions identified in (2.4A:blue circle). The profile of BRD4 binding is shown +/- 10kb from the centers of the 881 regions in CTLi (blue) and KLF3i (red) cells. (C) Percent distribution of the 881 H3K27ac/H3K4me positive regions containing KLF3 peaks with significant BRD4 depletion upon KLF3 knockdown. These 881 regions were annotated using HOMER and all regions not mapped to promoters were considered enhancers. (D) Gene ontology (GO) term enrichment for the 112 genes that lose BRD4 binding at their active promoter (H3K4me/H3K27ac positive) containing a KLF3 peak. (E) Gene ontology term enrichment for the 692 genes that lose BRD4 binding at a proximal enhancer (H3K27ac/H3K4me positive) containing a KLF3 peak. (F) Venn diagram showing the number of KLF3 bound, active regions that lose both CBP and BRD4 enrichment in the KLF3 knockdown condition. (G) Percent distribution of the 284 H3K27ac/H3K4me positive regions containing KLF3 peaks with significant CBP and BRD4 depletion upon KLF3 knockdown. (H) UCSC genome browser tracks displaying CBP and BRD4 binding (CBP ChIP Seq profiles) from CTLi and KLF3i cells, near LOR. KLF3 (red), H3K27ac (maroon), and H3K4me (green) profiles are also shown.

A

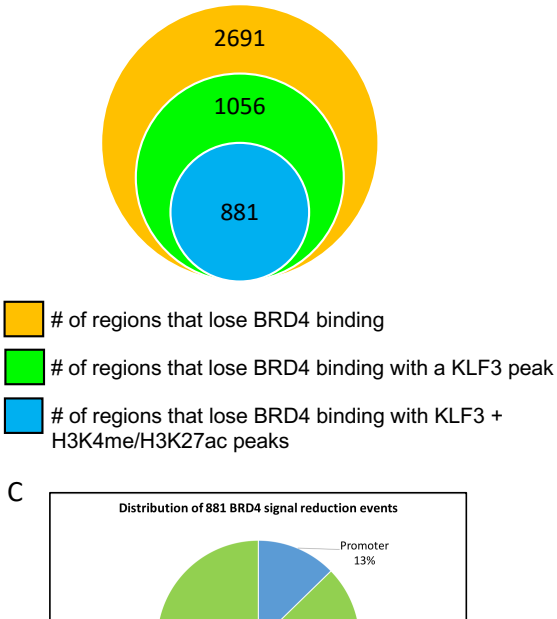
Loss of BRD4 binding upon KLF3 knockdown
2691
1056
881
# of regions that lose BRD4 binding
# of regions that lose BRD4 binding with a KLF3 peak
# of regions that lose BRD4 binding with KLF3 + H3K4me/H3K27ac peaks

B

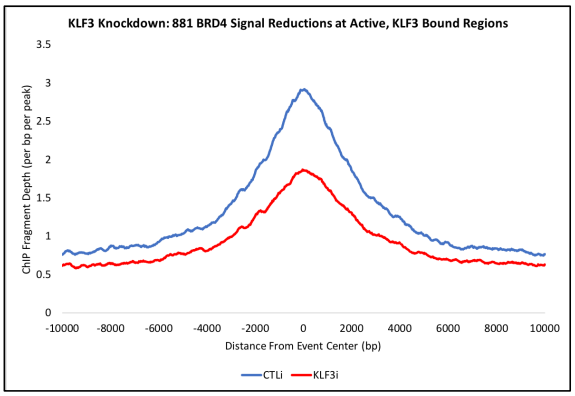
KLF3 Knockdown: 881 BRD4 Signal Reductions at Active, KLF3 Bound Regions
ChIP Fragment Depth (per bp per peak)
Distance From Event Center (bp)
CTLi
KLF3i

C

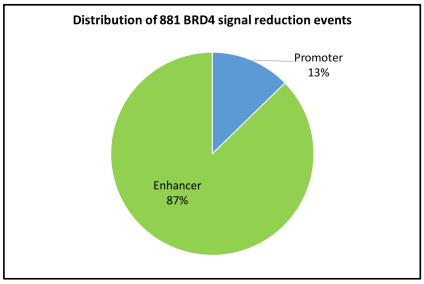
Distribution of 881 BRD4 signal reduction events
Promoter 13%
Enhancer 87%

D

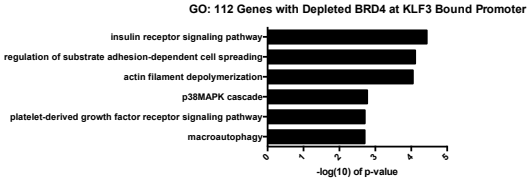
GO: 112 Genes with Depleted BRD4 at KLF3 Bound Promoter
insulin receptor signaling pathway
regulation of substrate adhesion-dependent cell spreading
actin filament depolymerization
p38MAPK cascade
platelet-derived growth factor receptor signaling pathway
macroautophagy
-log(10) of p-value

E

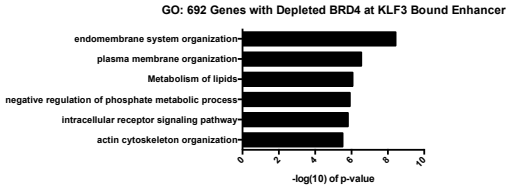
GO: 692 Genes with Depleted BRD4 at KLF3 Bound Enhancer
endomembrane system organization
plasma membrane organization
Metabolism of lipids
negative regulation of phosphate metabolic process
intracellular receptor signaling pathway
actin cytoskeleton organization
-log(10) of p-value

F

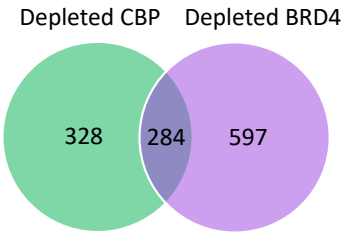
Depleted CBP
Depleted BRD4
328
284
597

G

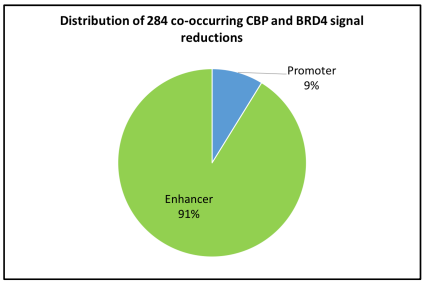
Distribution of 284 co-occurring CBP and BRD4 signal reductions
Promoter 9%
Enhancer 91%

H

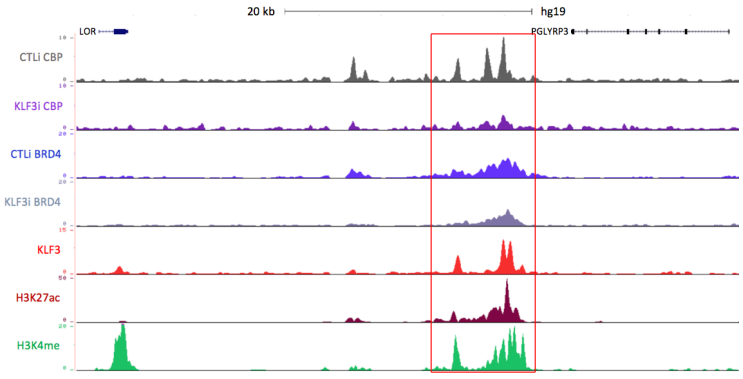
20 kb
hg19
LOR
PGLYRP3
CTLi CBP
KLF3i CBP
CTLi BRD4
KLF3i BRD4
KLF3
H3K27ac
H3K4me

of CBP and BRD4 is also based on KLF3's role in recruiting CBP and BRD4 to enhancers, allowing for the downstream promotion of differentiation gene transcription.

Discussion

BRD4 has previously been identified as necessary for differentiation in other cellular contexts, however little is known about the role of BRD4 in the keratinocytes and the epidermis. Here, we describe BRD4 as novel regulator of epidermal differentiation. In addition, we show that BRD4 shares a substantial transcriptional regulation and genomic localization with epidermal LDTFs, including KLF3.

We first characterized the BRD4 knockdown phenotype in both two-dimensional differentiation cultures and three-dimensional regenerated human epidermis. Knockdown of BRD4 resulted in a dramatic reduction in the differentiation gene signature as detected by RNA-sequencing. In addition, BRD4 knockdown reduced the mRNA and protein levels of the differentiation genes FLG and LOR in three-dimensional regenerated epidermis. In addition, H&E staining revealed reduced stratum corneum formation in BRD4 knockdown samples compared to controls, showing that BRD4 is necessary for proper barrier formation. Together, this demonstrates that BRD4 is necessary for human epidermal differentiation.

Next, we demonstrated that BRD4 binds at genomic loci proximal to a majority of the genes that are reduced in the BRD4 knockdown, and these genes are enriched for epidermal differentiation genes. As expected, BRD4 binding regions were generally enriched for the histone marks H3K27ac and H3K4me, but not the repressive marks H3K27me3 and H3K9me3.

This is consistent with BRD4's ability to bind active enhancers and promotes. BRD4 bound active regions (H3K4me/H3K27ac+) were mapped and divided into active enhancer and active promoter regions and compared to the genes reduced in the BRD4 knockdown condition. While the list of reduced genes with BRD4-bound active promoters did have enrichment for terms related to epidermal differentiation, there was a much more significant enrichment of these genes in the list associated with BRD4-bound active enhancers. This suggests that while BRD4 may promote differentiation gene expression directly at some promoters, the main source of its regulation of differentiation is derived from enhancer elements.

As this pattern is consistent with previous studies of BRD4 in regulating differentiation, we sought to determine the relationship between BRD4 and epidermal LDTFs. We found that BRD4 bound genomic loci are enriched in motifs associated with a variety of skin LDTFs, such as AP-1, ETS, CEBP, and KLF factors. In addition to the enrichment of these motifs, we also found epidermal LDTF (KLF4, ZNF750, MAF, MAFB, and GRHL3) ChIP-sequencing data sets had substantial signal enrichment at BRD4 bound regions and correlated well with the BRD4 data set. Peak overlapping confirmed this relationship, with BRD4 and epidermal LDTFs sharing many binding regions. This relationship between BRD4 and epidermal LDTFs suggests that, as in previously studied differentiation contexts, BRD4 may be acting as a downstream effector of LDTFs, recruiting the necessary transcriptional machinery to active regions to promote differentiation gene expression.

In order to elucidate whether this may be the case, we compared BRD4 knockdown RNA-sequencing data sets to KLF4 knockdown data sets, as KLF4 had the most shared binding

regions and the highest signal enrichment at BRD4 bound sites. We found that 461/772 (59.7%) of genes reduced in the KLF4 knockdown were also reduced in the BRD4 knockdown. In addition, this set of co-regulated genes was highly enriched for genes related to epidermis development. This suggests that BRD4 and KLF4 are both necessary for the expression of these differentiation genes, further suggesting that BRD4 may be acting downstream of epidermal LDTFs.

Lastly, due to the relationship demonstrated between BRD4 and KLF4, we wanted to explore the relationship between BRD4 and the novel epidermal LDTF KLF3. Comparison of BRD4i RNA-sequencing with that of the KLF3 knockdown revealed a substantial overlap of differentiation gene regulation, with 355/563 (63.1%) of downregulated genes in KLF3i also downregulated in BRD4i, and this set of genes is highly enriched for genes related to epidermal differentiation. This suggests that KLF3's promotion of differentiation gene expression may rely on the downstream activity of BRD4. Alternatively, far less upregulated genes were co-regulated by KLF3 and BRD4 (74/423, or 17.5%), suggesting that KLF3 gene suppression is primarily independent of BRD4. It is also worth noting that BRD4 shares a more similar transcriptional program with CBP than P300, suggesting that BRD4 is more reliant on CBP activity for differentiation gene promotion.

We previously demonstrated that KLF3 regulates differentiation gene expression by promoting the localization of CBP at active enhancers proximal to differentiation genes. As both LDTFs and epigenomic writers such as CBP have been shown to be necessary for BRD4 localization at active enhancer regions and subsequently differentiation gene expression, we

sought to compare KLF3 and BRD4 genomic localization and investigate whether KLF3 is necessary for BRD4 localization at active regions. We discovered substantial genomic correlation and co-localization of KLF3 and BRD4. Furthermore, knocking down KLF3 can impact BRD4 localization during differentiation. KLF3 knockdown reduced BRD4 binding at active enhancers near a variety of differentiation genes. Interestingly, many of these events co-occurred with reductions in CBP binding, further supporting the relationship between KLF3, CBP, and BRD4. Together, these data demonstrate that BRD4 is a novel regulator of epidermal differentiation, and that it is likely acting downstream of epidermal LDTFs like KLF3, as well as the epigenomic writer CBP.

Chapter 2 Supplemental Figures

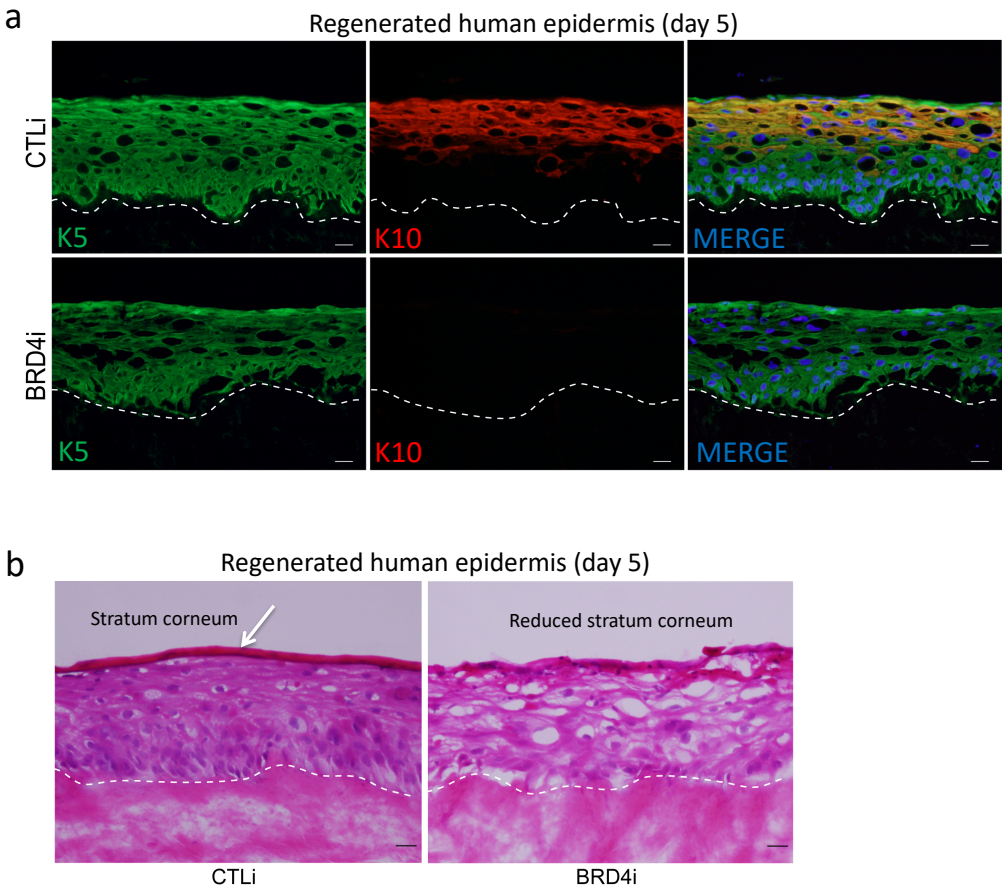

Supplementary Figure 2.1. BRD4 is necessary to promote epidermal differentiation. (A) Immunofluorescent staining of K5 (green) and K10 (red) in CTLi and BRD4i day 5 regenerated human epidermis. Merged image includes Hoechst staining of nuclei. n=3. White scale bar = 20μm. (B) Hematoxylin and eosin staining of CTLi and BRD4i day 5 regenerated human epidermis. n=3, white scale bar = 20μm.

Supplementary Figure 2.2. BRD4 is bound to active enhancers and promoters.
(A) ChIP qPCR showing BRD4 pulldown and an IgG negative control at differentiation gene proximal sites in keratinocytes differentiated for 3 days. Enrichment is represented as a percent of input. n=2. Statistics: t-test, *$p < 0.05$. (B) Mean density profile displaying histone mark ChIP-Seq profiles (H3K27ac: red, H3K4me: green, H3K27me3: orange, H3K9me3: purple) centered around BRD4 peaks (blue). The 17,569 BRD4 peaks were used as the reference coordinates and the profiles are displayed +/- 5kb from the BRD4 peak centers. (C) Heatmap plot of Pearson correlation coefficients between replicate BRD4 ChIP-Seq data sets and histone ChIP-Seq data sets (RPKM normalized). (D) Percent distribution of the 11,832 regions where BRD4 peaks overlap with both H3K27ac and H3K4me. These 11,832 regions with colocalized BRD4/H3K27ac/H3K4me were annotated using HOMER and all regions not mapped to promoters were considered enhancers. (E) Venn diagram showing the number of genes (756) decreased in the BRD4 knockdown that also have a proximal BRD4 bound active (H3K27ac/H3K4me+) enhancer, and the associated GO term enrichments for the 756 genes. (F) Venn diagram showing the number of genes (200) decreased in the BRD4 knockdown that also have a BRD4 bound active (H3K27ac/H3K4me+) promoter, and the associated GO term enrichments for the 200 genes. (G) UCSC genome browser track displaying BRD4 (blue), KLF4 (red), ZNF750 (pink), H3K27ac (maroon), and H3K4me (green) ChIP-Seq profiles near *DSC1* and *DSG1*. (H) UCSC genome browser track displaying BRD4 (blue), KLF4 (red), ZNF750 (pink), H3K27ac (maroon), and H3K4me (green) ChIP-Seq profiles near a cluster of *KRT* genes.

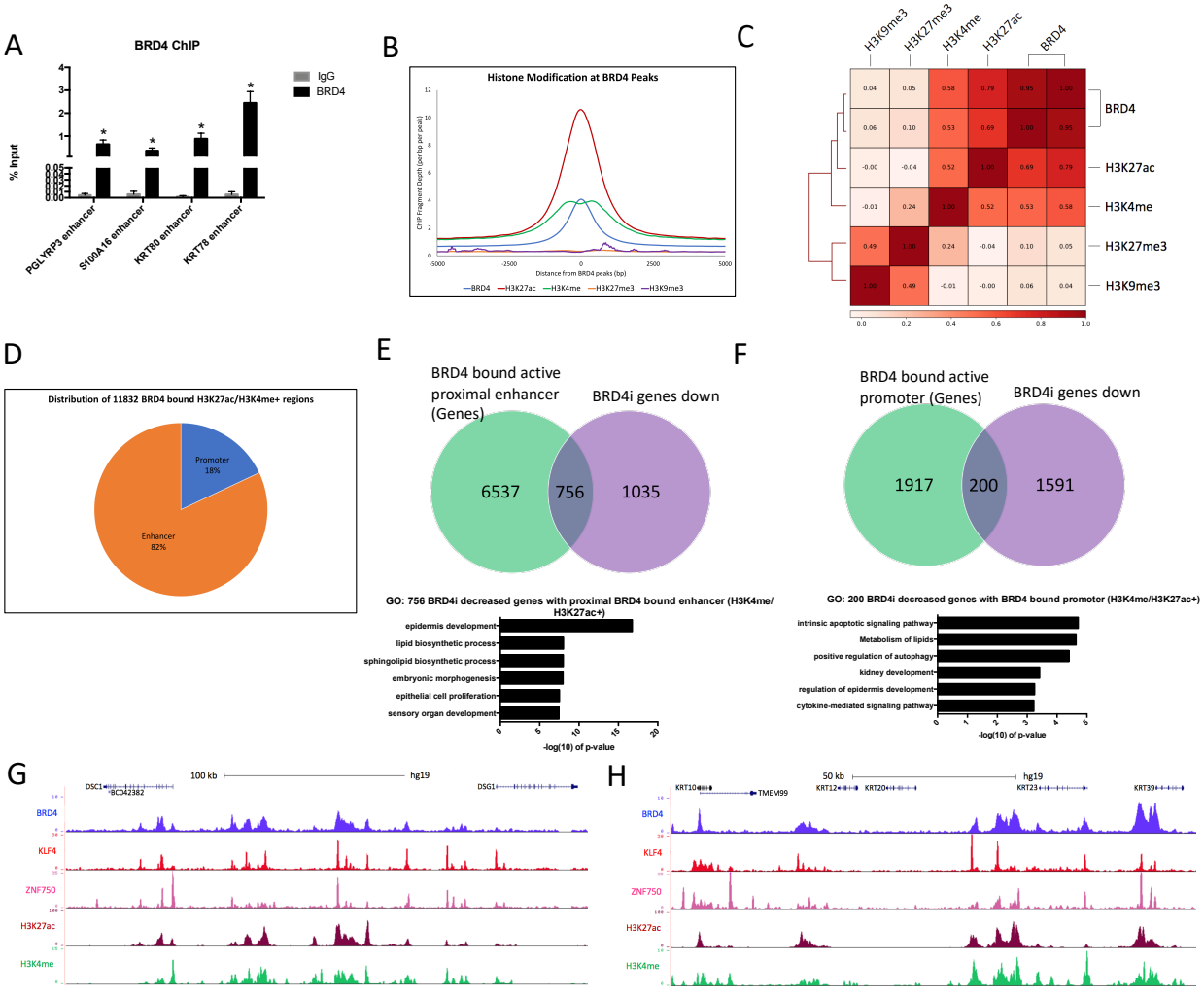
A
BRD4 ChIP
IgG
BRD4
% Input
PGLYRP3 enhancer
S100A16 enhancer
KRT80 enhancer
KRT78 enhancer
B
Histone Modification at BRD4 Peaks
ChIP Fragment Depth (per bp per peak)
Distance from BRD4 peaks (bp)
BRD4
H3K27ac
H3K4me
H3K27me3
H3K9me3
C
H3K9me3
H3K27me3
H3K4me
H3K27ac
BRD4
D
Distribution of 11832 BRD4 bound H3K27ac/H3K4me+ regions
Promoter 18%
Enhancer 82%
E
BRD4 bound active proximal enhancer (Genes)
BRD4i genes down
6537
756
1035
GO: 756 BRD4i decreased genes with proximal BRD4 bound enhancer (H3K4me/H3K27ac+)
epidermis development
lipid biosynthetic process
sphingolipid biosynthetic process
embryonic morphogenesis
epithelial cell proliferation
sensory organ development
-log(10) of p-value
F
BRD4 bound active promoter (Genes)
BRD4i genes down
1917
200
1591
GO: 200 BRD4i decreased genes with BRD4 bound promoter (H3K4me/H3K27ac+)
intrinsic apoptotic signaling pathway
Metabolism of lipids
positive regulation of autophagy
kidney development
regulation of epidermis development
cytokine-mediated signaling pathway
-log(10) of p-value
G
100 kb
hg19
BRD4
KLF4
ZNF750
H3K27ac
H3K4me
H
50 kb
hg19
BRD4
KLF4
ZNF750
H3K27ac
H3K4me

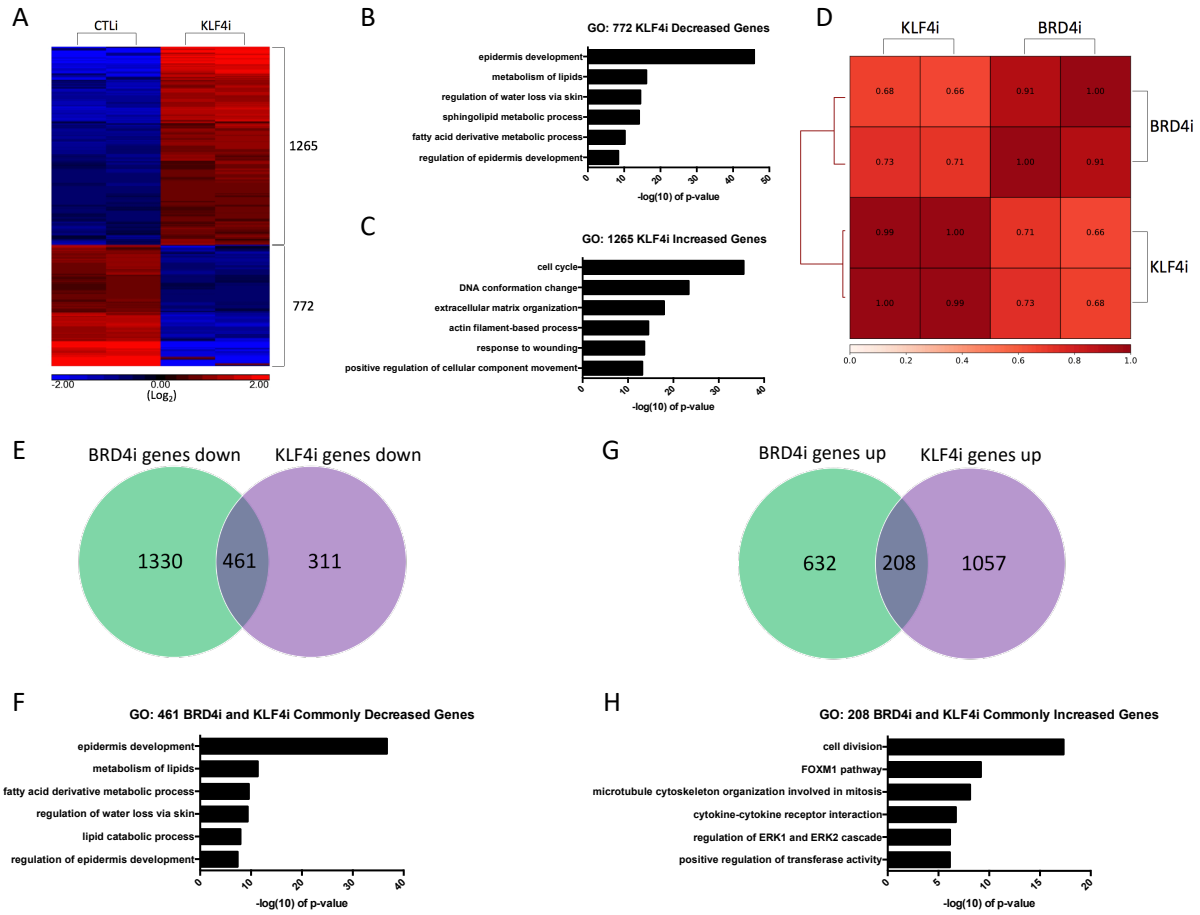

Supplementary Figure 2.3. BRD4 and KLF4 regulate a similar transcriptional program. (A) Heatmap generated for replicate (n=2) RPKM normalized RNA-Seq data from CTLi and KLF4i keratinocytes differentiated for 3 days. The expression of genes significantly increased (red) or decreased (blue) is shown. Differential expression was determined with FDR ≤ 0.05 and fold change ≥ 2 vs. CTLi. Graphs are displayed in log2 scale. (B) Gene ontology (GO) term enrichment for the 772 genes significantly decreased in KLF4 knockdown cells. (C) Gene ontology (GO) term enrichment for the 1,265 genes significantly increased in expression in KLF4 knockdown cells. (D) Heatmap plot of Pearson correlation coefficients between replicate BRD4i RNA-Seq data sets and replicate KLF4i RNA-Seq data sets (RPKM normalized). (E-F) Venn diagram showing the number of genes (461) decreased in both the BRD4 and KLF4 knockdowns and the associated GO term enrichments for the 461 genes. (G-H) Venn diagram showing the number of genes (208) increased in both the BRD4 and KLF4 knockdowns and the associated GO term enrichments for the 208 genes.

A

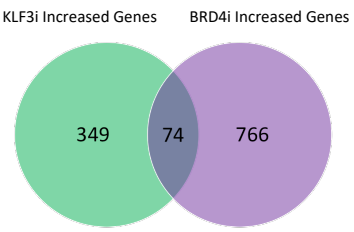

B

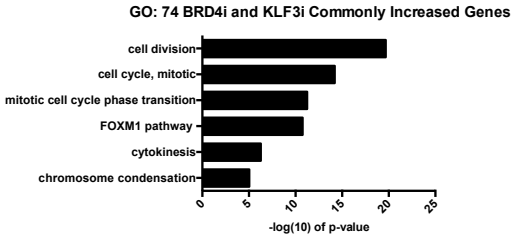

C

ChIP	Total Peaks	Shared Peaks with KLF3	% of peaks
BRD4	17569	10468	59.58

D

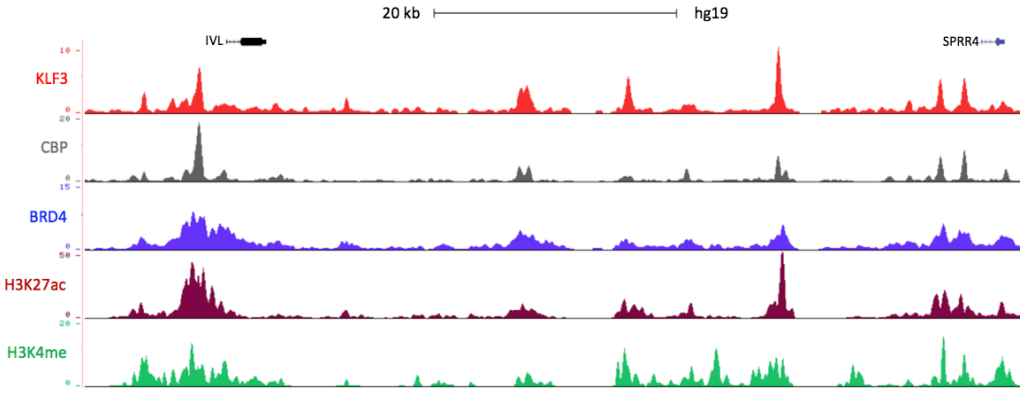

Supplementary Figure 2.4. BRD4 and KLF3 share transcriptional programs and genomic localization.
(A-B) Venn diagram showing the number of genes (74) increased in both the BRD4 and KLF3 knockdowns and the associated GO term enrichments for the 74 genes. (C) Table displaying the peak overlap between KLF3 and BRD4. The total BRD4 bound peak numbers identified by HOMER are shown with the number and percentage of overlap with KLF3 peaks. (D) UCSC genome browser tracks displaying KLF3 (red), CBP (gray), and BRD4 (blue) ChIP Seq profiles near the differentiation genes IVL and SPRR4. H3K27ac (maroon) and H3K4me (green) are included to represent open and active chromatin.

Supplemental Figure 2.5. KLF3 knockdown alters BRD4 localization during epidermal differentiation.
(A) Western blot of BRD4 protein levels in CTLi and KLF3i keratinocytes (day 3 differentiation) with B-Actin as a loading control. n=3 (B) Summary of significant BRD4 ChIP signal enrichment events in day 3 differentiated keratinocytes knocked down for KLF3. The orange circle represents the total number of regions in the genome that gain BRD4 binding upon KLF3 knockdown. The green circle represents the number of regions that gain BRD4 binding that occur at a KLF3 peak upon KLF3 depletion. The blue circle represents the regions that gain BRD4 binding which also contain KLF3, H3K4me, and H3K27ac binding upon KLF3 knockdown. BRD4 ChIP Seq was performed in replicates in CTLi and KLF3i cells. Significant signal changes were identified by Diffreps. (C) Gene ontology (GO) term enrichment for the 243 genes with KLF3i associated depletion of both CBP and BRD4. (D) UCSC genome browser tracks displaying CBP and BRD4 binding (CBP ChIP Seq profiles) from CTLi and KLF3i cells, near IVL. KLF3 (red), H3K27ac (maroon), and H3K4me (green) profiles are also shown.

A

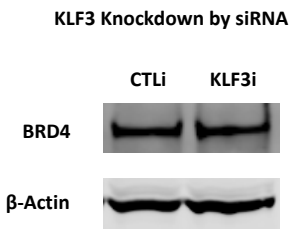
KLF3 Knockdown by siRNA
CTLi
KLF3i
BRD4
β-Actin

C

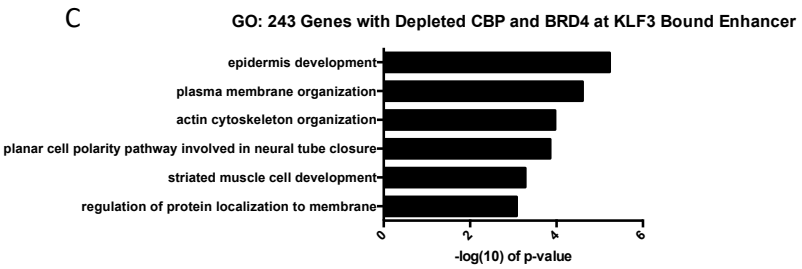
GO: 243 Genes with Depleted CBP and BRD4 at KLF3 Bound Enhancer
epidermis development
plasma membrane organization
actin cytoskeleton organization
planar cell polarity pathway involved in neural tube closure
striated muscle cell development
regulation of protein localization to membrane
0
2
4
6
-log(10) of p-value

B

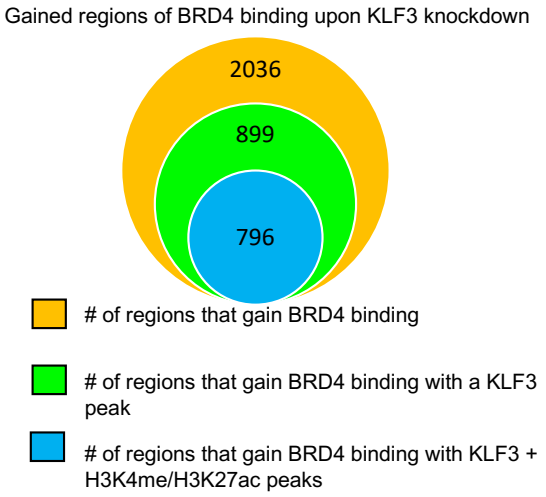
Gained regions of BRD4 binding upon KLF3 knockdown
2036
899
796
# of regions that gain BRD4 binding
# of regions that gain BRD4 binding with a KLF3 peak
# of regions that gain BRD4 binding with KLF3 + H3K4me/H3K27ac peaks

D

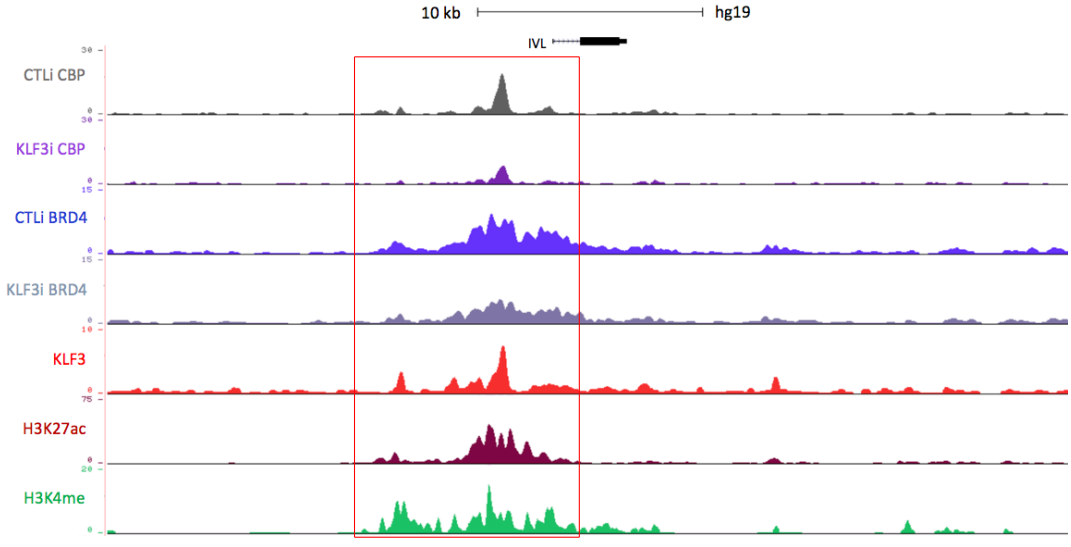
10 kb
hg19
IVL
CTLi CBP
KLF3i CBP
CTLi BRD4
KLF3i BRD4
KLF3
H3K27ac
H3K4me

Methods

Cell Culture

Primary human epidermal keratinocytes (derived from neonatal foreskin) were cultured in EpiLife medium (ThermoFisher MEPI500CA). This media was supplemented with Penicillin/streptomycin (HyClone SV30010) and human keratinocyte growth supplement (HKGS, ThermoFisher S0015). Keratinocytes were differentiated by seeding to full confluence and subsequently adding 1.2 mM calcium for 3 days as previously described [13].

Gene knockdown

siRNAs were placed into EpiLife media with the transfection reagent Lipofectamine RNAiMAX (25ul for 10cm plate transfection, 50 ul for 15cm plate transfection) (ThermoFisher 13778) and incubated for 5 minutes. This siRNA media was then diluted 1:10 and added to sub-confluent keratinocytes, with the siRNA at a final concentration of 10nM. The keratinocytes were then incubated in this media for a minimum of 18 hours to carry out siRNA knockdown. The siRNAs used in this study are as follows: Control siRNA (Ambion Silencer Select negative control 4390844), BRD4 siRNA1 (Dharmacon D-004937-05), BRD4 siRNA 2 (Dharmacon D-004937-04), KLF4 siRNA (Dharmacon:custom sequence), KLF3 siRNA (Ambion Silencer Select s229899), CBP siRNA (Dharmacon D-003477-21), P300 siRNA (Dharmacon D-003486-02). siRNA sequences can be found in the supplemental materials.

Regenerated human epidermis

Human dermis obtained from the New York Firefighters skin bank was devitalized, cut, and placed upon a cassette. The bottom of the dermis was coated in matrigel and the cassette was placed in KGM media, with the bottom of the dermis contacting the media and the top at the air interface. One million keratinocytes were then seeded on the top of the dermis and allowed to regenerate and stratify for five days. The constructs were then harvested for RNA or embedded in OCT for sectioning and staining. Additional details for regenerating human epidermis have been previously described [24,41,43].

Immunofluorescent staining

Sectioned tissue derived from regenerated human epidermis was fixed with 10% formalin solution (Sigma HT5012) for 12 minutes. Sections were blocked (PBS, 2% bovine serum albumin, 2.5% normal goat serum, and 0.3% triton X-100) for 30 minutes. Primary antibodies were then added to blocking buffer and put onto sections for 1 hour. The following antibodies were used at the following concentrations: FLG at 1:200 (Abcam ab3137), LOR at 1:400 (Abcam ab198994), KRT10 at 1:400 (ThermoFisher MS-611-P0), and KRT5 at 1:500 (Biolegend PRB-160P). Secondary antibodies were used at 1:500 for 30 minutes and included Alexa Fluor 555 goat anti-mouse IgG (ThermoFisher: A21424) and Alexa Fluor 488 donkey anti-rabbit IgG (ThermoFisher: A21206). Hoechst 33342 (ThermoFisher H3570) was used at 1:1000 to stain nuclei.

H&E staining

Sectioned tissue derived from regenerated human epidermis was fixed with 10% formalin solution (Sigma HT5012) for 12 minutes. Sections were then dipped in 0.25% Triton-X-100 in PBS for 5 minutes. Haemotoxylin (Vector H-3401) staining was performed for 8 minutes, rinsed in water, and then dipped in acid alcohol (1% HCL in 70% ethanol). After subsequent rinsing, the sections were dipped in 0.2% ammonia water for 1 minute, rinsed again, and then dipped in 95% ethanol. Eosin (Richard-Allan Scientific 71304) staining was performed for 30 seconds followed by 95% ethanol rinsing for 1 minute. Sections were then put into 100% ethanol for 4 minutes followed by 2 minutes in Xylene.

RNA extraction and analysis by RT-qPCR

The GeneJET RNA purification kit (Thermo Scientific K0732) was used to extract RNA from cultured keratinocytes. RNA concentration for each sample was measured by nanodrop and 1μg of RNA was used for generating cDNA. This cDNA was generated using the Maxima cDNA synthesis kit (Thermo Fisher: K1642). qPCR was performed using this cDNA on the Roche 480 Light Cycler. The house-keeping genes L32 or GAPDH were used for normalization of signal. Primer sequences for all genes tested are listed in the supplementary materials.

Western blotting

IP samples or 20-80ug of cell lysates were loaded into 4-12% Bis-Tris (ThermoFisher NW04122BOX) or 3-8% Tris-acetate (ThermoFisher EA03752BOX) and transferred to PVDF

membranes. Membranes were blocked in 5% BSA in TBS. Membranes were exposed to primary antibodies in blocking buffer overnight at 4 degrees. The following primary antibodies were used: KLF3 at 1:1000 (Sigma HPA049512), CBP at 1:1000 (Cell Signaling D6C5 #7389). The loading controls Beta-Actin (Santa Cruz sc-47778) and Beta-Tubulin (Santa Cruz sc-9104) were used at 1:5000. The secondary antibodies used were donkey anti-rabbit IRDye 680RD (Li-Cor 926-68073) and donkey anti-mouse IRDye 800CW (Li-Cor 926-32212) at 1:5000.

RNA sequencing and bioinformatic analysis

RNA isolated from day 3 differentiated keratinocytes was used for sequencing. Samples were sequenced by the Institute of Genomic Medicine core facility at UCSD on the Illumina Hi Seq 4000. Reads were aligned to the hg19 genome build using STAR with default settings. Identification of differential gene expression and downstream analysis was carried out using Partek Genomic Suite (Partek Incorporated, http://www. partek.com/partek-genomics-suite). Differential expression between control and knockdown samples was analyzed using ANOVA. Genes with fewer than ten reads among all samples were filtered out before analysis to avoid genes with low expression. Differentially expressed genes were selected by > 2-fold change (+/-) compared to controls and a significant p-value with FDR (< 0.05). Heatmaps representing RNA sequencing data were generated in Partek Genomic Suite. GO terms for selected gene lists were generated using Metascape [65]. DeepTools was used to RPKM normalize sequencing files and generate Pearson correlations and the representative heatmaps of those values [66,67].

ChIP sequencing and bioinformatic analysis

For each pulldown, 20 million keratinocytes were differentiated for 3 days and subsequently crosslinked. These cells were crosslinked using 2mM DSG (disuccinimidyl glutarate, Thermo Fisher 20593) and 1% formaldehyde (ThermoFisher 28908). Cells were placed in Farnham lysis buffer (5 mM PIPES pH 8.0, 85 mM KCl, 0.5% IGEPAL CA-630) and sheared with a syringe. The cells were then pelleted and resuspended in SDS-Lysis Buffer (1% SDS, 10 mM EDTA, 50 mM Tris, pH 8.0) and sonicated in a water bath sonicator. Sonicated lysate was then centrifuged, and the supernatant was diluted 1:10 in low ionic strength ChIP dilution buffer (50mM NaCl, 10mM HEPES, pH 7.4, 1% IGEPAL CA-630, 10% Glycerol) and used for ChIP. 5ug of BRD4 antibody (Bethyl A301-985A), 5ug of KLF3 antibody (Sigma HPA049512), 20ul of CBP antibody (Cell Signaling D6C5 #7389), or 5ug of control rabbit IgG (Millipore 12-370) was used for each respective pulldown. Antibody/lysate incubation was carried out at 4 degrees overnight. 50ul of Protein-G dynabeads were added to each solution of antibody/lysate the following day and incubated for 4 hours at 4 degrees. The beads were then washed twice with low ionic strength buffer, once with high salt wash buffer (500 mM NaCl, 0.1% SDS, 1% IGEPAL CA-630, 2 mM EDTA, 20 mM Tris, pH 8.0), once with LiCl wash (0.25 M LiCl, 1% IGEPAL CA-630, 1% Sodium Deoxycholate, 1 mM EDTA 10 mM Tris-Hcl, pH 8.0), and twice with TE (10 mM Tris-Cl, pH 7.5, 1 mM EDTA). Samples were then eluted at 65 degrees in elution buffer (0.09 M $NaHCO_3$, 1% SDS, 0.1 M $NaHCO_3$) and de-crosslinking mixture (0.2 M NaCl, 0.1M EDTA,0.4 M Tris-HCl, pH6.8, 0.4 mg/ml proteinase K) and treated with RNAse A to prevent RNA contamination during sequencing [43,51]. Samples were sequenced by the Institute of

Genomic Medicine core facility at UCSD on the Illumina Hi Seq 4000. Sequenced reads were trimmed and aligned to the genome build hg19 using BowTie 2 [68]. Duplicate and low-quality reads were removed. To identify significant peaks, HOMER's findPeaks was used with default statistical settings (p-value < 0.0001, FDR < 0.001, 4x enrichment vs. input) and the following options: for BRD4: style=region, size=150, minDist=500; for KLF4, ZNF750, MAF, MAFB, and GRHL3: style=factor, minDist 200; for H3K27ac and H3K4me: style=region, size=1000, minDist=2500[69]. Input sample was used as background in peak calling. Genomic localization was annotated using HOMER's annotatePeaks (Refseq hg19 transcription start sites)[69]. HOMER was also used to identify motifs (findMotifsGenome), create UCSC tracks (makeUCSCfile) to be visualized on the UCSC genome browser, and generate normalized mean density plots (annotatePeaks). mergePeaks was used to identify directly overlapping (d=given) peaks between samples. DeepTools was used to RPKM normalize sequencing files and generate Pearson correlations and the representative heatmaps of these values[66,67]. GO terms for selected gene lists were generated using Metascape [65].

Co-immunoprecipitation

Differentiated keratinocytes were harvested in IP lysis buffer (25 mM Tris-HCl pH 7.4, 150 mM NaCl, 1 mM EDTA, 1% NP-40 and 5% glycerol) and sheared with a syringe. 5ug of KLF3 antibody (Sigma HPA049512) or control rabbit IgG (Millipore 12-370) was conjugated to 50ul of Protein G dynabeads (Life Technologies 10004D) for 30 minutes at room temperature. Lysis buffer was diluted to 1ml per sample and was added to the antibody conjugated beads and

incubated overnight at 4 degrees. The following day the beads were washed with IP lysis buffer and boiled in RIPA buffer (25 mM Tris-HCl (pH 7.6), 150 mM NaCl, 1% NP-40, 1% sodium deoxycholate, 0.1% SDS) supplemented with NuPAGE LDS Sample Buffer (Life Technologies: NP0008) to elute. Samples were then loaded for western blotting.

Statistics

Statistical analyses were performed using GraphPad Prism. Histogram data are presented as the mean ± SD and the significance of differences between samples was determined by student's t tests.

Acknowledgments

Chapter 2 is based on material recently accepted for publication: Jackson Jones, Yifang Chen, Manisha Tiwari, Jingting Li, Ji Ling, and George L. Sen. BRD4 is necessary for differentiation downstream of epidermal lineage determining transcription factors. *In Press: Journal of Investigative Dermatology.* 2020. I am the primary author and researcher for this manuscript. The co-authors listed above either supervised or provided support for the research and have given permission for the inclusion of the work in this dissertation.

Conflicts of Interest

The authors declare that they have no conflicts of interest.

REFERENCES

1 Gonzales, K. A. U. & Fuchs, E. Skin and Its Regenerative Powers: An Alliance between Stem Cells and Their Niche. *Dev Cell* **43**, 387-401, doi:10.1016/j.devcel.2017.10.001 (2017).

2 Bikle, D. D., Xie, Z. & Tu, C. L. Calcium regulation of keratinocyte differentiation. *Expert Rev Endocrinol Metab* **7**, 461-472, doi:10.1586/eem.12.34 (2012).

3 Ge, Y. & Fuchs, E. Stretching the limits: from homeostasis to stem cell plasticity in wound healing and cancer. *Nat Rev Genet* **19**, 311-325, doi:10.1038/nrg.2018.9 (2018).

4 Kypriotou, M., Huber, M. & Hohl, D. The human epidermal differentiation complex: cornified envelope precursors, S100 proteins and the 'fused genes' family. *Exp Dermatol* **21**, 643-649, doi:10.1111/j.1600-0625.2012.01472.x (2012).

5 Lopez-Pajares, V., Yan, K., Zarnegar, B. J., Jameson, K. L. & Khavari, P. A. Genetic pathways in disorders of epidermal differentiation. *Trends Genet* **29**, 31-40, doi:10.1016/j.tig.2012.10.005 (2013).

6 Pearson, R., Fleetwood, J., Eaton, S., Crossley, M. & Bao, S. Kruppel-like transcription factors: a functional family. *Int J Biochem Cell Biol* **40**, 1996-2001, doi:10.1016/j.biocel.2007.07.018 (2008).

7 Pearson, R. C., Funnell, A. P. & Crossley, M. The mammalian zinc finger transcription factor Kruppel-like factor 3 (KLF3/BKLF). *IUBMB Life* **63**, 86-93, doi:10.1002/iub.422 (2011).

8 Sur, I., Rozell, B., Jaks, V., Bergstrom, A. & Toftgard, R. Epidermal and craniofacial defects in mice overexpressing Klf5 in the basal layer of the epidermis. *J Cell Sci* **119**, 3593-3601, doi:10.1242/jcs.03070 (2006).

9 Takahashi, K. & Yamanaka, S. Induction of pluripotent stem cells from mouse embryonic and adult fibroblast cultures by defined factors. *Cell* **126**, 663-676, doi:10.1016/j.cell.2006.07.024 (2006).

10 Segre, J. A., Bauer, C. & Fuchs, E. Klf4 is a transcription factor required for establishing the barrier function of the skin. *Nat Genet* **22**, 356-360, doi:10.1038/11926 (1999).

11 Jaubert, J., Cheng, J. & Segre, J. A. Ectopic expression of kruppel like factor 4 (Klf4) accelerates formation of the epidermal permeability barrier. *Development* **130**, 2767-2777, doi:10.1242/dev.00477 (2003).

12 Patel, S., Xi, Z. F., Seo, E. Y., McGaughey, D. & Segre, J. A. Klf4 and corticosteroids activate an overlapping set of transcriptional targets to accelerate in utero epidermal barrier acquisition. *Proc Natl Acad Sci U S A* **103**, 18668-18673, doi:10.1073/pnas.0608658103 (2006).

13 Sen, G. L., Boxer, L. D., Webster, D. E., Bussat, R. T., Qu, K., Zarnegar, B. J., Johnston, D., Siprashvili, Z. & Khavari, P. A. ZNF750 is a p63 target gene that induces KLF4 to drive terminal epidermal differentiation. *Dev Cell* **22**, 669-677, doi:10.1016/j.devcel.2011.12.001 (2012).

14 Boxer, L. D., Barajas, B., Tao, S., Zhang, J. & Khavari, P. A. ZNF750 interacts with KLF4 and RCOR1, KDM1A, and CTBP1/2 chromatin regulators to repress epidermal progenitor genes and induce differentiation genes. *Genes Dev* **28**, 2013-2026, doi:10.1101/gad.246579.114 (2014).

15 Turner, J. & Crossley, M. Cloning and characterization of mCtBP2, a co-repressor that associates with basic Kruppel-like factor and other mammalian transcriptional regulators. *EMBO J* **17**, 5129-5140, doi:10.1093/emboj/17.17.5129 (1998).

16 Perdomo, J., Verger, A., Turner, J. & Crossley, M. Role for SUMO modification in facilitating transcriptional repression by BKLF. *Mol Cell Biol* **25**, 1549-1559, doi:10.1128/MCB.25.4.1549-1559.2005 (2005).

17 Sue, N., Jack, B. H., Eaton, S. A., Pearson, R. C., Funnell, A. P., Turner, J., Czolij, R., Denyer, G., Bao, S., Molero-Navajas, J. C., Perkins, A., Fujiwara, Y., Orkin, S. H., Bell-Anderson, K. & Crossley, M. Targeted disruption of the basic Kruppel-like factor gene (Klf3) reveals a role in adipogenesis. *Mol Cell Biol* **28**, 3967-3978, doi:10.1128/MCB.01942-07 (2008).

18 Linhart, H. G., Ishimura-Oka, K., DeMayo, F., Kibe, T., Repka, D., Poindexter, B., Bick, R. J. & Darlington, G. J. C/EBPalpha is required for differentiation of white, but not brown, adipose tissue. *Proc Natl Acad Sci U S A* **98**, 12532-12537, doi:10.1073/pnas.211416898 (2001).

19 Eaton, S. A., Funnell, A. P., Sue, N., Nicholas, H., Pearson, R. C. & Crossley, M. A network of Kruppel-like Factors (Klfs). Klf8 is repressed by Klf3 and activated by Klf1 in vivo. *J Biol Chem* **283**, 26937-26947, doi:10.1074/jbc.M804831200 (2008).

20 Turchinovich, G., Vu, T. T., Frommer, F., Kranich, J., Schmid, S., Alles, M., Loubert, J. B., Goulet, J. P., Zimber-Strobl, U., Schneider, P., Bachl, J., Pearson, R., Crossley, M., Agenes, F. & Kirberg, J. Programming of marginal zone B-cell fate by basic Kruppel-like factor (BKLF/KLF3). *Blood* **117**, 3780-3792, doi:10.1182/blood-2010-09-308742 (2011).

21 Funnell, A. P., Maloney, C. A., Thompson, L. J., Keys, J., Tallack, M., Perkins, A. C. & Crossley, M. Erythroid Kruppel-like factor directly activates the basic Kruppel-like factor gene in erythroid cells. *Mol Cell Biol* **27**, 2777-2790, doi:10.1128/MCB.01658-06 (2007).

22 Funnell, A. P., Norton, L. J., Mak, K. S., Burdach, J., Artuz, C. M., Twine, N. A., Wilkins, M. R., Power, C. A., Hung, T. T., Perdomo, J., Koh, P., Bell-Anderson, K. S., Orkin, S. H., Fraser, S. T., Perkins, A. C., Pearson, R. C. & Crossley, M. The CACCC-binding protein KLF3/BKLF represses a subset of KLF1/EKLF target genes and is required for proper erythroid maturation in vivo. *Mol Cell Biol* **32**, 3281-3292, doi:10.1128/MCB.00173-12 (2012).

23 Himeda, C. L., Ranish, J. A., Pearson, R. C., Crossley, M. & Hauschka, S. D. KLF3 regulates muscle-specific gene expression and synergizes with serum response factor on KLF binding sites. *Mol Cell Biol* **30**, 3430-3443, doi:10.1128/MCB.00302-10 (2010).

24 Mistry, D. S., Chen, Y. & Sen, G. L. Progenitor function in self-renewing human epidermis is maintained by the exosome. *Cell Stem Cell* **11**, 127-135, doi:10.1016/j.stem.2012.04.022 (2012).

25 Chen, Y., Mistry, D. S. & Sen, G. L. Highly rapid and efficient conversion of human fibroblasts to keratinocyte-like cells. *J Invest Dermatol* **134**, 335-344, doi:10.1038/jid.2013.327 (2014).

26 Lopez-Pajares, V., Qu, K., Zhang, J., Webster, D. E., Barajas, B. C., Siprashvili, Z., Zarnegar, B. J., Boxer, L. D., Rios, E. J., Tao, S., Kretz, M. & Khavari, P. A. A LncRNA-MAF:MAFB Transcription Factor Network Regulates Epidermal Differentiation. *Dev Cell* **32**, 693-706, doi:10.1016/j.devcel.2015.01.028 (2015).

27 Hopkin, A. S., Gordon, W., Klein, R. H., Espitia, F., Daily, K., Zeller, M., Baldi, P. & Andersen, B. GRHL3/GET1 and trithorax group members collaborate to activate the epidermal progenitor differentiation program. *PLoS Genet* **8**, e1002829, doi:10.1371/journal.pgen.1002829 (2012).

28 Ting, S. B., Caddy, J., Hislop, N., Wilanowski, T., Auden, A., Zhao, L. L., Ellis, S., Kaur, P., Uchida, Y., Holleran, W. M., Elias, P. M., Cunningham, J. M. & Jane, S. M. A homolog of Drosophila grainy head is essential for epidermal integrity in mice. *Science* **308**, 411-413, doi:10.1126/science.1107511 (2005).

29 Lopez, R. G., Garcia-Silva, S., Moore, S. J., Bereshchenko, O., Martinez-Cruz, A. B., Ermakova, O., Kurz, E., Paramio, J. M. & Nerlov, C. C/EBPalpha and beta couple interfollicular keratinocyte proliferation arrest to commitment and terminal differentiation. *Nat Cell Biol* **11**, 1181-1190, doi:10.1038/ncb1960 (2009).

30 Smallwood, A. & Ren, B. Genome organization and long-range regulation of gene expression by enhancers. *Curr Opin Cell Biol* **25**, 387-394, doi:10.1016/j.ceb.2013.02.005 (2013).

31 Heintzman, N. D., Stuart, R. K., Hon, G., Fu, Y., Ching, C. W., Hawkins, R. D., Barrera, L. O., Van Calcar, S., Qu, C., Ching, K. A., Wang, W., Weng, Z., Green, R. D., Crawford, G. E. & Ren, B. Distinct and predictive chromatin signatures of transcriptional promoters and enhancers in the human genome. *Nat Genet* **39**, 311-318, doi:10.1038/ng1966 (2007).

32 Creyghton, M. P., Cheng, A. W., Welstead, G. G., Kooistra, T., Carey, B. W., Steine, E. J., Hanna, J., Lodato, M. A., Frampton, G. M., Sharp, P. A., Boyer, L. A., Young, R. A. & Jaenisch, R. Histone H3K27ac separates active from poised enhancers and predicts developmental state. *Proc Natl Acad Sci U S A* **107**, 21931-21936, doi:10.1073/pnas.1016071107 (2010).

33 Rada-Iglesias, A., Bajpai, R., Swigut, T., Brugmann, S. A., Flynn, R. A. & Wysocka, J. A unique chromatin signature uncovers early developmental enhancers in humans. *Nature* **470**, 279-283, doi:10.1038/nature09692 (2011).

34 Visel, A., Blow, M. J., Li, Z., Zhang, T., Akiyama, J. A., Holt, A., Plajzer-Frick, I., Shoukry, M., Wright, C., Chen, F., Afzal, V., Ren, B., Rubin, E. M. & Pennacchio, L. A. ChIP-seq accurately predicts tissue-specific activity of enhancers. *Nature* **457**, 854-858, doi:10.1038/nature07730 (2009).

35 Wang, Z., Zang, C., Cui, K., Schones, D. E., Barski, A., Peng, W. & Zhao, K. Genome-wide mapping of HATs and HDACs reveals distinct functions in active and inactive genes. *Cell* **138**, 1019-1031, doi:10.1016/j.cell.2009.06.049 (2009).

36 Ramos, Y. F., Hestand, M. S., Verlaan, M., Krabbendam, E., Ariyurek, Y., van Galen, M., van Dam, H., van Ommen, G. J., den Dunnen, J. T., Zantema, A. & t Hoen, P. A. Genome-wide assessment of differential roles for p300 and CBP in transcription regulation. *Nucleic Acids Res* **38**, 5396-5408, doi:10.1093/nar/gkq184 (2010).

37 Roth, S. Y., Denu, J. M. & Allis, C. D. Histone acetyltransferases. *Annual review of biochemistry* **70**, 81-120, doi:10.1146/annurev.biochem.70.1.81 (2001).

38 Holmqvist, P. H. & Mannervik, M. Genomic occupancy of the transcriptional co-activators p300 and CBP. *Transcription* **4**, 18-23, doi:10.4161/trns.22601 (2013).

39 Rebel, V. I., Kung, A. L., Tanner, E. A., Yang, H., Bronson, R. T. & Livingston, D. M. Distinct roles for CREB-binding protein and p300 in hematopoietic stem cell self-renewal. *Proc Natl Acad Sci U S A* **99**, 14789-14794, doi:10.1073/pnas.232568499 (2002).

40 Rubin, A. J., Barajas, B. C., Furlan-Magaril, M., Lopez-Pajares, V., Mumbach, M. R., Howard, I., Kim, D. S., Boxer, L. D., Cairns, J., Spivakov, M., Wingett, S. W., Shi, M., Zhao, Z., Greenleaf, W. J., Kundaje, A., Snyder, M., Chang, H. Y., Fraser, P. & Khavari, P. A. Lineage-specific dynamic and pre-established enhancer-promoter contacts cooperate in terminal differentiation. *Nat Genet* **49**, 1522-1528, doi:10.1038/ng.3935 (2017).

41 Li, J. & Sen, G. L. Generation of Genetically Modified Organotypic Skin Cultures Using Devitalized Human Dermis. *J Vis Exp*, e53280, doi:10.3791/53280 (2015).

42 Li, J., Chen, Y., Xu, X., Jones, J., Tiwari, M., Ling, J., Wang, Y., Harismendy, O. & Sen, G. L. HNRNPK maintains epidermal progenitor function through transcription of proliferation genes and degrading differentiation promoting mRNAs. *Nat Commun* **10**, 4198, doi:10.1038/s41467-019-12238-x (2019).

43 Noutsou, M., Li, J., Ling, J., Jones, J., Wang, Y., Chen, Y. & Sen, G. L. The Cohesin Complex Is Necessary for Epidermal Progenitor Cell Function through Maintenance of Self-Renewal Genes. *Cell Rep* **20**, 3005-3013, doi:10.1016/j.celrep.2017.09.003 (2017).

44 Mariotto, A., Pavlova, O., Park, H. S., Huber, M. & Hohl, D. HOPX: The Unusual Homeodomain-Containing Protein. *J Invest Dermatol* **136**, 905-911, doi:10.1016/j.jid.2016.01.032 (2016).

45 Koseki, R., Morii, W., Noguchi, E., Ishikawa, M., Yang, L., Yamamoto-Hanada, K., Narita, M., Saito, H. & Ohya, Y. Effect of filaggrin loss-of-function mutations on atopic dermatitis in young age: a longitudinal birth cohort study. *J Hum Genet* **64**, 911-917, doi:10.1038/s10038-019-0628-y (2019).

46 Ezhkova, E., Pasolli, H. A., Parker, J. S., Stokes, N., Su, I. H., Hannon, G., Tarakhovsky, A. & Fuchs, E. Ezh2 orchestrates gene expression for the stepwise differentiation of tissue-specific stem cells. *Cell* **136**, 1122-1135, doi:S0092-8674(09)00006-3 [pii] 10.1016/j.cell.2008.12.043 (2009).

47 Gerstein, M. B., Kundaje, A., Hariharan, M., Landt, S. G., Yan, K. K., Cheng, C., Mu, X. J., Khurana, E., Rozowsky, J., Alexander, R., Min, R., Alves, P., Abyzov, A., Addleman, N., Bhardwaj, N., Boyle, A. P., Cayting, P., Charos, A., Chen, D. Z., Cheng, Y., Clarke, D., Eastman, C., Euskirchen, G., Frietze, S., Fu, Y., Gertz, J., Grubert, F., Harmanci, A., Jain, P., Kasowski, M., Lacroute, P., Leng, J., Lian, J., Monahan, H., O'Geen, H., Ouyang, Z., Partridge, E. C., Patacsil, D., Pauli, F., Raha, D., Ramirez, L., Reddy, T. E., Reed, B., Shi, M., Slifer, T., Wang, J., Wu, L., Yang, X., Yip, K. Y., Zilberman-Schapira, G., Batzoglou, S., Sidow, A., Farnham, P. J., Myers, R. M., Weissman, S. M. & Snyder, M. Architecture of the human regulatory network derived from ENCODE data. *Nature* **489**, 91-100, doi:10.1038/nature11245 (2012).

48 Calo, E. & Wysocka, J. Modification of enhancer chromatin: what, how, and why? *Mol Cell* **49**, 825-837, doi:10.1016/j.molcel.2013.01.038 (2013).

49 Klein, R. H., Lin, Z., Hopkin, A. S., Gordon, W., Tsoi, L. C., Liang, Y., Gudjonsson, J. E. & Andersen, B. GRHL3 binding and enhancers rearrange as epidermal keratinocytes transition between functional states. *PLoS Genet* **13**, e1006745, doi:10.1371/journal.pgen.1006745 (2017).

50 Shen, L., Shao, N. Y., Liu, X., Maze, I., Feng, J. & Nestler, E. J. diffReps: detecting differential chromatin modification sites from ChIP-seq data with biological replicates. *PLoS One* **8**, e65598, doi:10.1371/journal.pone.0065598 (2013).

51 Mistry, D. S., Chen, Y., Wang, Y., Zhang, K. & Sen, G. L. SNAI2 controls the undifferentiated state of human epidermal progenitor cells. *Stem Cells* **32**, 3209-3218, doi:10.1002/stem.1809 (2014).

52 Ilsley, M. D., Gillinder, K. R., Magor, G. W., Huang, S., Bailey, T. L., Crossley, M. & Perkins, A. C. Kruppel-like factors compete for promoters and enhancers to fine-tune transcription. *Nucleic Acids Res* **45**, 6572-6588, doi:10.1093/nar/gkx441 (2017).

53 Funnell, A. P., Mak, K. S., Twine, N. A., Pelka, G. J., Norton, L. J., Radziewic, T., Power, M., Wilkins, M. R., Bell-Anderson, K. S., Fraser, S. T., Perkins, A. C., Tam, P. P., Pearson, R. C. & Crossley, M. Generation of mice deficient in both KLF3/BKLF and KLF8 reveals a genetic interaction and a role for these factors in embryonic globin gene silencing. *Mol Cell Biol* **33**, 2976-2987, doi:10.1128/MCB.00074-13 (2013).

54 Burdach, J., Funnell, A. P., Mak, K. S., Artuz, C. M., Wienert, B., Lim, W. F., Tan, L. Y., Pearson, R. C. & Crossley, M. Regions outside the DNA-binding domain are critical for proper in vivo specificity of an archetypal zinc finger transcription factor. *Nucleic Acids Res* **42**, 276-289, doi:10.1093/nar/gkt895 (2014).

55 Funnell, A. P., Vernimmen, D., Lim, W. F., Mak, K. S., Wienert, B., Martyn, G. E., Artuz, C. M., Burdach, J., Quinlan, K. G., Higgs, D. R., Whitelaw, E., Pearson, R. C. & Crossley, M. Differential regulation of the alpha-globin locus by Kruppel-like Factor 3 in erythroid and non-erythroid cells. *BMC Mol Biol* **15**, 8, doi:10.1186/1471-2199-15-8 (2014).

56 Mak, K. S., Burdach, J., Norton, L. J., Pearson, R. C., Crossley, M. & Funnell, A. P. Repression of chimeric transcripts emanating from endogenous retrotransposons by a sequence-specific transcription factor. *Genome Biol* **15**, R58, doi:10.1186/gb-2014-15-4-r58 (2014).

57 Crossley, M., Whitelaw, E., Perkins, A., Williams, G., Fujiwara, Y. & Orkin, S. H. Isolation and characterization of the cDNA encoding BKLF/TEF-2, a major CACCC-box-binding protein in erythroid cells and selected other cells. *Mol Cell Biol* **16**, 1695-1705, doi:10.1128/mcb.16.4.1695 (1996).

58 Turner, J., Nicholas, H., Bishop, D., Matthews, J. M. & Crossley, M. The LIM protein FHL3 binds basic Kruppel-like factor/Kruppel-like factor 3 and its co-repressor C-terminal-binding protein 2. *J Biol Chem* **278**, 12786-12795, doi:10.1074/jbc.M300587200 (2003).

59 Dewi, V., Kwok, A., Lee, S., Lee, M. M., Tan, Y. M., Nicholas, H. R., Isono, K., Wienert, B., Mak, K. S., Knights, A. J., Quinlan, K. G., Cordwell, S. J., Funnell, A. P., Pearson, R. C. & Crossley, M. Phosphorylation of Kruppel-like factor 3 (KLF3/BKLF) and C-terminal binding protein 2 (CtBP2) by homeodomain-interacting protein kinase 2 (HIPK2) modulates KLF3 DNA binding and activity. *J Biol Chem* **290**, 8591-8605, doi:10.1074/jbc.M115.638338 (2015).

60 Raisner, R., Kharbanda, S., Jin, L., Jeng, E., Chan, E., Merchant, M., Haverty, P. M., Bainer, R., Cheung, T., Arnott, D., Flynn, E. M., Romero, F. A., Magnuson, S. & Gascoigne, K. E. Enhancer Activity Requires CBP/P300 Bromodomain-Dependent Histone H3K27 Acetylation. *Cell Rep* **24**, 1722-1729, doi:10.1016/j.celrep.2018.07.041 (2018).

61 Fang, F., Xu, Y., Chew, K. K., Chen, X., Ng, H. H. & Matsudaira, P. Coactivators p300 and CBP maintain the identity of mouse embryonic stem cells by mediating long-range chromatin structure. *Stem Cells* **32**, 1805-1816, doi:10.1002/stem.1705 (2014).

62 Yao, T. P., Oh, S. P., Fuchs, M., Zhou, N. D., Ch'ng, L. E., Newsome, D., Bronson, R. T., Li, E., Livingston, D. M. & Eckner, R. Gene dosage-dependent embryonic development and proliferation defects in mice lacking the transcriptional integrator p300. *Cell* **93**, 361-372, doi:10.1016/s0092-8674(00)81165-4 (1998).

63 Tanaka, Y., Naruse, I., Hongo, T., Xu, M., Nakahata, T., Maekawa, T. & Ishii, S. Extensive brain hemorrhage and embryonic lethality in a mouse null mutant of CREB-binding protein. *Mech Dev* **95**, 133-145, doi:10.1016/s0925-4773(00)00360-9 (2000).

64 Bedford, D. C., Kasper, L. H., Fukuyama, T. & Brindle, P. K. Target gene context influences the transcriptional requirement for the KAT3 family of CBP and p300 histone acetyltransferases. *Epigenetics* **5**, 9-15, doi:10.4161/epi.5.1.10449 (2010).

65 Zhou, Y., Zhou, B., Pache, L., Chang, M., Khodabakhshi, A. H., Tanaseichuk, O., Benner, C. & Chanda, S. K. Metascape provides a biologist-oriented resource for the analysis of systems-level datasets. *Nature communications* **10**, 1523, doi:10.1038/s41467-019-09234-6 (2019).

66 Ramirez, F., Ryan, D. P., Gruning, B., Bhardwaj, V., Kilpert, F., Richter, A. S., Heyne, S., Dundar, F. & Manke, T. deepTools2: a next generation web server for deep-sequencing data analysis. *Nucleic Acids Res* **44**, W160-165, doi:10.1093/nar/gkw257 (2016).

67 Ramirez, F., Dundar, F., Diehl, S., Gruning, B. A. & Manke, T. deepTools: a flexible platform for exploring deep-sequencing data. *Nucleic Acids Res* **42**, W187-191, doi:10.1093/nar/gku365 (2014).

68 Langmead, B. & Salzberg, S. L. Fast gapped-read alignment with Bowtie 2. *Nat Methods* **9**, 357-359, doi:10.1038/nmeth.1923 (2012).

69 Heinz, S., Benner, C., Spann, N., Bertolino, E., Lin, Y. C., Laslo, P., Cheng, J. X., Murre, C., Singh, H. & Glass, C. K. Simple combinations of lineage-determining transcription factors prime cis-regulatory elements required for macrophage and B cell identities. *Mol Cell* **38**, 576-589, doi:10.1016/j.molcel.2010.05.004 (2010).

70 Lee, J. E., Park, Y. K., Park, S., Jang, Y., Waring, N., Dey, A., Ozato, K., Lai, B., Peng, W. & Ge, K. Brd4 binds to active enhancers to control cell identity gene induction in adipogenesis and myogenesis. *Nat Commun* **8**, 2217, doi:10.1038/s41467-017-02403-5 (2017).

71 Roe, J. S., Mercan, F., Rivera, K., Pappin, D. J. & Vakoc, C. R. BET Bromodomain Inhibition Suppresses the Function of Hematopoietic Transcription Factors in Acute Myeloid Leukemia. *Mol Cell* **58**, 1028-1039, doi:10.1016/j.molcel.2015.04.011 (2015).

72 Donati, B., Lorenzini, E. & Ciarrocchi, A. BRD4 and Cancer: going beyond transcriptional regulation. *Mol Cancer* **17**, 164, doi:10.1186/s12943-018-0915-9 (2018).

73 Consortium, E. P. An integrated encyclopedia of DNA elements in the human genome. *Nature* **489**, 57-74, doi:10.1038/nature11247 (2012).